SWIFT HEAVY ION IRRADIATION OF POLYESTER AND POLYOLEFIN POLYMERIC FILM FOR GAS SEPARATION APPLICATION

By

Olushola Rotimi ADENIYI

B. Tech. (Hons) FUT Akure, MSc (UWC)

A thesis submitted in fulfilment of the requirements for degree of Doctor of Philosophy in the Department of Chemistry, University of the Western Cape

Supervisor: **Prof. L. F. Petrik**

Co-supervisors: **Prof. A. N. Nechaev**
Prof. V. V. Teplyakov

November, 2015

ABSTRACT

The combination of ion track technology and chemical etching as a tool to enhance polymer gas properties such as permeability and selectivity is regarded as an avenue to establish technology commercialization and enhance applicability. Traditionally, permeability and selectivity of polymers have been major challenges especially for gas applications. However, it is important to understand the intrinsic polymer properties in order to be able to predict or identify their possible ion-polymer interactions thus facilitate the reorientation of existing polymer structural configurations. This in turn can enhance the gas permeability and selectivity properties of the polymers. Therefore, the choice of polymer is an important prerequisite.

Polyethylene terephthalate (PET) belongs to the polyester group of polymers and has been extensively studied within the context of post-synthesis modification techniques using swift heavy ion irradiation and chemical treatment which is generally referred to as *'track-etching'*. The use of track-etched polymers in the form of symmetrical membranes structures to investigate gas permeability and selectivity properties has proved successful. However, the previous studies on track-etched polymers films have been mainly focused on the preparation of symmetrical membrane structure, especially in the case of polyesters such as PET polymer films. Also, polyolefins such as polymethyl pentene (PMP) have not been investigated using swift heavy ions and chemical etching procedures. In addition, the use of *'shielded'* material on PET and PMP polymer films prior to swift heavy ion irradiation and chemical etching to prepare asymmetrical membrane structure have not been investigated. The gas permeability and selectivity of the asymmetrical membrane prepared from swift heavy ion irradiated etched *'shielded'* PET and PMP polymer films have not been determined. These highlighted limitations will be addressed in this study.

ABSTRACT

The overall objective of this study was to prepare asymmetric polymeric membranes with porous surface on dense layer from two classes of polymers; (PET and PMP) in order to improve their gas permeability and selectivity properties. The research approach in this study was to use a simple and novel method to prepare an asymmetric PET and PMP polymer membrane with porous surface and dense layer by mechanical attachment of *'shielded'* material on the polymer film before swift heavy ion irradiation. This irradiation approach allowed for the control of swift heavy ion penetration depth into the PET and PMP polymer film during irradiation. The procedure used in this study is briefly described. Commercial PET and PMP polymer films were mechanically *'shielded'* with aluminium and PET foils respectively. The *'shielded'* PET polymer films were then irradiated with swift heavy ions of Xe source while *'shielded'* PMP polymer films were irradiated with swift heavy ions Kr. The ion energy and fluence of Xe ions was 1.3 MeV and 10^6 respectively while the Kr ion energy was 3.57 MeV and ion fluence of 10^9. After swift heavy ion irradiation of *'shielded'* PET and PMP polymer films, the attached *'shielded'* materials were removed from PET and PMP polymer film and the irradiated PET and PMP polymer films were chemically etched in sodium hydroxide (NaOH) and acidified chromium trioxide (H_2SO_4 + CrO_3) respectively. The chemical etching conditions of swift heavy ion irradiated *'shielded'* PET was performed with 1 M NaOH at 80 ˚C under various etching times of 3, 6, 9 and 12 minutes. As for the swift heavy ion irradiated *'shielded'* PMP polymer film, the chemical etching was performed with 7 M H_2SO_4 + 3 M CrO_3 solution, etching temperature was varied between 40 ˚C and 80 ˚C while the etching time was between 40 minutes to 150 minutes.

The SEM (surface and cross-section micrograph) morphology results of the swift heavy ion irradiated *'shielded'* etched PET and PMP films showed that asymmetric membranes with a single-sided porous surface and dense layer was prepared and remained unchanged even after 12 minutes of etching with 1 M NaOH solution as in the case of PET and 2 hours 30 minutes of etching with 7 M H_2SO_4 + 3 M CrO_3 as observed for PMP polymer film. Also, the swift heavy ion irradiated *'shielded'*

ABSTRACT

etched PET polymer film showed the presence of pores on the polymer film surface within 3 minutes of etching. After 12 minutes chemical etching with 1 M NaOH solution, the dense layer of swift heavy ion irradiated *'shielded'* etched PET polymer film experienced significant reduction in thickness of about 40 % of the original thickness of as-received PET polymer film. The surface morphology of swift heavy ion irradiated *'shielded'* etched PET polymer film by SEM analysis revealed finely distributed pores with spherical shapes for the swift heavy ion irradiated *'shielded'* etched PET polymer film within 6 minutes of etching with 1 M NaOH solution. Also, after 9 minutes and 12 minutes of etching with 1 M NaOH solution of the swift heavy ion irradiated *'shielded'* etched PET polymer film, the pore walls experienced complete collapse with intense surface roughness. Interestingly, the 12 minutes etched swift heavy ion *'shielded'* irradiated PET did not lose its asymmetrical membrane structure despite the collapse of the pore walls. In the case of swift heavy ion irradiated *'shielded'* etched PMP polymer film, SEM morphology analysis showed that the pores retained their shape with the presence of defined pores without intense surface roughness even after extended etching with 7 M H_2SO_4 + 3 M CrO_3 for 2 hours 30 minutes. Also, the pores of swift heavy ion irradiated *'shielded'* etched PMP polymer films were observed to be mono dispersed and not agglomerated or overlapped. The SEM cross-section morphology of the swift heavy ion irradiated *'shielded'* etched PMP polymer film showed radially oriented pores with increased pore diameters in the PMP polymer film which indicated that etching was radial instead of lateral, and no through pores were observed showing that the dense asymmetrical structure was retained. The SEM results revealed that the pore morphology i.e. size and shape could be accurately controlled during chemical etching of swift heavy ion *'shielded'* irradiated PET and PMP polymer films.

The XRD results of swift heavy ion irradiated *'shielded'* etched PET revealed a single diffraction peak for various times of chemical etching in 1 M NaOH solution at 3, 6, 9 and 12 minutes. The diffraction peak of swift heavy ion irradiated *'shielded'* etched PET was observed to reduce in intensity and marginally shifted

ABSTRACT

to lower angles from 25.95˚ 2 theta to 25.89˚ 2 theta and also became broad in shape. It was considered that the continuous broadening of diffraction peaks due to an increase in etching times could be attributed to disorderliness of the ordered region within the polymer matrix and thus decreases in crystallinity of the swift heavy ion irradiated *'shielded'* etched PET polymer film. The XRD analysis of swift heavy ion irradiated *'shielded'* etched PMP polymer films indicated the presence of the diffraction peak at 9.75˚ 2 theta with decrease in intensity while the diffraction peaks located at 13.34˚, 16.42˚, 18.54˚ and 21.46˚ 2 theta disappeared after chemical etching in acidified chromium trioxide ($H_2SO_4 + CrO_3$) after 2 hours 30 minutes.

The TGA thermal profile analysis of swift heavy ion irradiated *'shielded'* etched PET did not show the evolution of volatile species or moisture at lower temperatures even after 12 minutes of etching in 1 M NaOH solution in comparison with commercial PET polymer film. Also, it was observed that the swift heavy ion irradiated *layered'* etched PET polymer film started to undergo degradation at a higher temperature than untreated PET which resulted in an approximate increase of 50 ˚C in comparison with the commercial PET polymer film. The TGA results of swift heavy ion irradiated *'shielded'* etched PMP polymer film revealed an improvement of about 50 ˚C in thermal stability before thermal degradation even after etching in acidified chromium trioxide for 2 hours 30 minutes at 80 ˚C.

Spectroscopy (IR) analysis of the swift heavy ion irradiated *'shielded'* etched PET and PMP polymer films showed the presence of characteristic functional groups associated with either PET or PMP structures. The variations of irradiation and chemical etching conditions revealed that the swift heavy ion *'shielded'* irradiated etched PET polymer film experienced continuous degradation of available functional groups as a function of etching time and also with complete disappearance of some functional groups such as 1105 cm^{-1} and 1129 cm^{-1} compared with the as-received PET polymer film which are both associated with the para-substituted position of benzene rings. In the case of swift heavy ion

ABSTRACT

irradiated *'shielded'* etched PMP polymer film, spectroscopic (IR) analysis showed significant variations in the susceptibility of associated functional groups within the PMP polymer film with selective attack and emergence of some specific functional groups such as at 1478 cm^{-1}, 1810 cm^{-1} and 2115 cm^{-1} which were assigned to methylene, CH_3 (asymmetry deformation), CH_3 and CH_2 respectively Also, the IR results for swift heavy ion irradiated *'shielded'* etched PMP polymer showed that unsaturated olefinic groups were the dominant functional groups that were being attacked by during etching with acidified chromium trioxide (H_2SO_4+CrO_3) which is an aggressive chemical etchant.

The gas permeability analysis of swift heavy ion irradiated *'shielded'* etched PET and PMP polymer films showed that the gas permeability was improved in comparison with the as-received PET and as-received PMP polymer films. The gas permeability of swift heavy ion irradiated *'shielded'* etched PET increased as a function of etching time and was found to be highest after 12 minutes of chemical etching in 1 M NaOH at 80 ˚C. In the case of swift heavy ion irradiated *'shielded'* etched PMP, the gas permeability was observed to show the highest gas permeability after 2 hours 30 minutes of etching in H_2SO_4 + CrO_3 solution. The gas permeability analysis for swift heavy ion irradiated *'shielded'* PET and PMP polymer films was tested for He, CO_2 and CH_4 and the permeability results showed that helium was most permeable compared with CO_2 and CH_4 gases. In comparison, the selectivity analysis was performed for He/CO_2 and CH_4/He and the results showed that the selectivity decreased with increasing in etching time as expected.

This study identified some important findings. Firstly, it was observed that the use of *'shielded'* material on PET and PMP polymer films prior to swift heavy ion irradiation proved successful in the creation of asymmetrical polymer membrane structure. Also, it was also observed that the chemical etching of the *'shielded'* swift heavy ion irradiated PET and PMP polymer films resulted in the presence of pores on the swift heavy ion irradiated side while the unirradiated sides of the PET and PMP polymer films were unaffected during chemical etching hence the pore depth

ABSTRACT

could be controlled. In addition, the etching experiment showed that the pores geometry can be controlled as well as the gas permeability and selectivity properties of swift heavy ion *'shielded'* irradiated etched PET and PMP polymer films.

The process of polymer bulk and surface properties modification using ion-track technology i.e. swift heavy ion irradiation and subsequent chemical treatment of the irradiated polymer serves to reveal characteristic pore profiles unique to the prevailing ion-polymer interaction and ultimately results in alteration of the polymer characteristics.

KEYWORDS

Polyethylene terephthalate

Polymethyl pentene

Swift heavy ion irradiation

Track-etch

High performance polymer

Surface modification

Membrane

Gas separation

Permeability

Selectivity

DECLARATION

DECLARATION

I declare that "**SWIFT HEAVY ION IRRADIATION OF POLYESTER AND POLYOLEFIN POLYMERIC FILM FOR GAS SEPARATION APPLICATION**" is my own work, that it has not been submitted for any degree or examination in any other university, and that all the resources I have used or quoted have been indicated and acknowledged by complete references.

Olushola Rotimi Adeniyi

November, 2015

Signature……

ACKNOWLEDGMENT

This journey will not be complete without the help, assistance and guidance of my supervisor Prof. Leslie Felicia Petrik. Thank you so much for giving me this platform to soar and reach out to my dreams, you facilitated and steered this dream. I am humbled to be your student. It has been a life-learning experience for me.

My co-supervisors; Prof. Alexander Necheav and Prof. Teplyakov, I am very grateful for the scientific assistance and your sacrifices, guidance to see to the completion of this project. Prof. Teplyakov and Dr Dasha, thank you for your assistance with gas permeability and selectivity experiments at the Laboratory for Membranes and Polymer processes, Russian Academy of Sciences (RAS) and for always being ready to assist. Prof. Apel and Dr. Yuri, I sincerely appreciate all your contributions during the irradiation experiments at the Joint Institute for Nuclear Research (JINR), Dubna and always being on hand to discuss with me. Also, the access for the use of cyclotron for swift heavy ion irradiation of polymer at the Joint Institute for Nuclear Research is sincerely appreciated.

Also my thanks go to the following people; Dr. Amarante, Neha Verma at TUDelft, Netherlands for your kind assistance in hosting me for the SAVUSA-SKILL scholarship. Dr. Noel Mkhaza and Prof. Leslie Lekala, I sincerely appreciate the opportunity you gave me to participate in the SA-JINR student practice and your constant supports. Prof. Lorna Holtman, I am grateful for allowing me to be a recipient of the SAVUSA-SKILL scholarship and Division for Post Graduate Studies (DPGS). Dr Nasiema and Peter Johnson-Smith, I am indebted to all your kind advice and encouragement.

To the Pastorate and members of Household of God Parish of Redeemed Christian Church of God (RCCG), thank you so much and God bless you all.

All the past and present Environmental and Nano-Sciences (ENS) research group *crew*, thanks you so much for the camaraderie.

ACKNOWLEDGMENT

Oluwafemi Olaofe (PhD) and *Ayaba* Olaofe, you both are wonderful and Oluwa bless you so much. Amen. Daddy and Mummy Oni, I am grateful and humbled by your show of love. Thank you so much.

To my parents; *Mama Roteeee*; I am very grateful mum for everything. Dad, I will say thank you sir. Marc and Godsgift Adeniyi you guys are awesome. Seyi and Jumoke Adeniyi (*aburo mi atata)*, Oluwa blesses you and your families. Amos Moore Adeniyi, God bless your hustles.

My lovely wife; Funmilola Foluke Adeniyi and gorgeous daughter; Oluwafifehanmi (*sisi mi*) Adeniyi, you are both my treasures and thank you for the sacrifices at the home front.

DEDICATION

This project is dedicated to God Almighty my *numero Uno*

TABLE OF CONTENTS

TABLE OF CONTENTS

ABSTRACT.....i

KEYWORDS.....iv

DECLARATION.....v

ACKNOWLEDGMENT.....viii

DEDICATION.....xiii

TABLE OF CONTENTS.....xiii

LIST OF FIGURES.....xv

LIST OF TABLES.....xx

LIST OF EQUATIONS.....xix

LIST OF ABBREVIATION.....xx

OUTPUTS.....xxi

CHAPTER ONE.....1

1 GENERAL INTRODUCTION.....1

1.1 MEMBRANE SEPARATION TECHNOLOGY AND SWIFT HEAVY IONS MODIFICATION OF POLYMERS: AN OVERVIEW.....1

1.2 POLYMERIC MEMBRANES.....4

1.3 PROBLEM STATEMENT.....6

1.4 SIGNIFICANCE OF STUDY.....6

1.5 RESEARCH QUESTIONS.....7

1.6 AIMS AND OBJECTIVES OF STUDY.....8

1.7 EXPERIMENTAL APPROACH.....8

1.8 THESIS CHAPTER LAYOUT.....9

CHAPTER TWO.....11

2 LITERATURE REVIEW.....11

TABLE OF CONTENTS

2.1 INTRODUCTION....11

2.2 POLYETHYLENE TEREPHTHALATE....12

2.3 POLYMETHYL PENTENE....13

2.4 ION TRACK TECHNOLOGY....14

2.5 ADVANCES IN SWIFT HEAVY ION IRRADIATION AND TRACK-ETCHED POLYMER MEMBRANE....15

2.6 APPLICATIONS AND LIMITATIONS OF SWIFT HEAVY IONS (SHI) 18

2.7 POLYMER PROPERTIES AND CHARGED PARTICLE INTERACTION....18

2.7.1 POLYMER SURFACE MODIFICATION, FUNCTIONALITY AND STRUCTURAL ARRANGEMENT....21

2.7.1.1 SWIFT HEAVY ION IRRADIATION 22

2.8 PRINCIPLES OF SURFACE FUNCTIONALITY BY SWIFT HEAVY ION IRRADIATION....25

2.8.1 NUCLEAR STOPPING 27

2.8.2 ELECTRONIC STOPPING 27

2.9 CHAIN SCISSION 28

2.10 STRUCTURAL CROSSLINKING 28

2.11 CHEMICAL ETCHING OF SWIFT HEAVY ION IRRADIATED POLYMER 30

2.12 POLYMER GAS PERMEABILITY AND SELECTIVITY: OVERVIEW OF GAS TRANSPORT STUDIES THROUGH POLYMERIC MEMBRANES 32

2.13 MECHANISMS FOR GAS SEPARATION IN POLYMERIC MEMBRANE PROCESSES 34

TABLE OF CONTENTS

2.14 GAS TRANSPORT MECHANISM IN POROUS MEMBRANE 35

2.14.1 KNUDSEN DIFFUSION AND POISEUILLE FLOW 35

2.14.2 MOLECULAR SIEVING 37

2.15 GAS TRANSPORT MECHANISM IN NON-POROUS MEMBRANES. 38

2.15.1 SOLUTION-DIFFUSION 39

2.16 POLYMER STRUCTURES AND THEIR GAS PERMEABILITY PROPERTIES 40

2.16.1 GLASSY POLYMERS AND THEIR GAS PERMEABILITY PROPERTIES 40

2.16.2 RUBBERY POLYMERS 40

2.17 GAP ANALYSIS AND CHAPTER SUMMARY 41

CHAPTER THREE 43

3 MATERIALS, EXPERIMENTAL PROTOCOL AND ANALYTICAL TECHNIQUES 43

3.1 INTRODUCTION 43

3.2 MATERIALS 43

3.3 EXPERIMENTAL PROTOCOLS 44

3.3.1 SWIFT HEAVY ION IRRADIATION 47

3.3.2 CHEMICAL ETCHING 53

3.3.3 CHEMICAL ETCHING CONDITIONS FOR ASPET, ASPMP AND ION IRRADIATED PET AND PMP POLYMER FILM 53

3.3.4 PREPARATION OF CHEMICAL ETCHING SOLUTIONS 55

TABLE OF CONTENTS

3.3.4.1 PREPARATION OF 1 M NaOH SOLUTION 55

3.3.4.2 PREPARATION OF 7 M H_2SO_4 +3 M CrO_3 SOLUTION 55

3.4 CHARACTERIZATION AND ANALYTICAL TECHNIQUES 55

3.4.1 SCANNING ELECTRON MICROSCOPY TECHNIQUE 56

3.4.2 X-RAY DIFFRACTION TECHNIQUE 57

3.4.3 FOURIER TRANSFORMED INFRA-RED /ATTENUATED TOTAL REFLECTION 58

3.4.4 THERMOGRAVIMETRY ANALYSIS ANALYTICAL TECHNIQUE 59

3.4.5 GAS PERMEABILITY MEASUREMENT REACTOR 60

CHAPTER FOUR 65

4 BASELINE CHARACTERIZATION OF ASPET AND ASPMP POLYMER FILMS 65

4.1 INTRODUCTION 65

4.2 CHARACTERIZATION OF ASPET (SAMPLE OA1A) POLYMER FILM 66

4.2.1 SCANNING ELECTRON MICROSCOPY (SEM) MICROGRAPH OF ASPET (SAMPLE OA1a) POLYMER FILM 66

4.2.2 X-RAY DIFFRACTION (XRD) ANALYSIS OF ASPET (SAMPLE OA1a) POLYMER FILM 68

TABLE OF CONTENTS

4.2.3 THERMOGRAVIMETRY (TGA) ANALYSIS OF ASPET (SAMPLE OA1a) POLYMER FILM.....70

4.2.4 FOURIER TRANSFORMED INFRA-RED (FTIR) SPECTROSCOPY ANALYSIS OF ASPET (SAMPLE OA1a) POLYMER FILM.....72

4.3 CHARACTERIZATION OF ASPMP (SAMPLE OA3A) POLYMER FILMS.....74

4.3.1 SCANNING ELECTRON MICROSCOPY (SEM) MICROGRAPH ANALYSIS OF ASPMP (SAMPLE OA3a) POLYMER FILM.....74

4.3.2 X-RAY DIFFRACTION (XRD) ANALYSIS OF ASPMP (SAMPLE OA3a) POLYMER FILM.....76

4.3.3 THERMOGRAVIMETRY (TGA) ANALYSIS OF ASPMP (SAMPLE OA3a) POLYMER FILM.....77

4.3.4 FTIR SPECTROSCOPY ANALYSIS OF ASPMP (SAMPLE OA3a) POLYMER FILM.....79

4.4 SUMMARY FOR BASELINE CHARACTERIZATION OF ASPET AND ASPMP POLYMER FILMS.....81

4.5 CHARACTERIZATION OF CHEMICALLY ETCHED AS-RECEIVED PET AND AS-RECEIVED PMP POLYMER FILMS.....82

4.5.1 SCANNING ELECTRON MICROSCOPY ANALYSIS OF ETCHED PET (SAMPLE OA1b) POLYMER FILM ETCHED IN NaOH SOLUTION.....83

TABLE OF CONTENTS

4.5.2 ETCHING KINETICS ANALYSIS OF PET (SAMPLE OA1b) POLYMER FILM ETCHED IN NaOH SOLUTION 85

4.5.3 FTIR SPECTROSCOPY OF (SAMPLE OA1b) PET POLYMER FILM ETCHED IN NaOH SOLUTION 86

4.6 CHARACTERIZATION OF ETCHED PMP POLYMER FILM..... 90

4.6.1 SCANNING ELECTRON MICROSCOPY ANALYSIS OF ETCHED PMP (SAMPLE OA3b) POLYMER FILM ETCHED IN ACIDIFIED CHROIMUM TRIOXIDE (H_2SO_4 + CrO_3) 90

4.6.2 ETCHING KINETICS ANALYSIS OF ETCHED PMP (SAMPLE OA3b) ETCHED IN ACIDIFIED CHROIMUM TRIOXIDE (H_2SO_4 + CrO_3).....92

4.6.3 FTIR SPECTROSCOPY OF CHEMICALLY ETCHED PMP (SAMPLE OA3b) POLYMER FILM ETCHED IN ACIDIFIED CHROIMUM TRIOXIDE (H_2SO_4 + CrO_3) 94

4.7 RESULT SUMMARY FOR ETCHED PET AND PMP POLYMER FILMS 97

4.8 CHARACTERIZATION OF SWIFT HEAVY ION IRRADIATED PET AND PMP POLYMER FILMS.....98

4.8.1 SRIM SIMULATED Xe ion IRRADIATION OF *'shielded'* PET (SAMPLE OA1c) POLYMER FILM..... 100

4.8.2 THERMOGRAVIMETRY (TGA) ANALYSIS OF SWIFT HEAVY ION OF XE IRRADIATED *'shielded'* PET (SAMPLE OA1c) POLYMER FILM..... 102

TABLE OF CONTENTS

4.8.3 FTIR SPECTROSCOPY OF SWIFT HEAVY ION OF XE IRRADIATED *'shielded'* PET (SAMPLE OA1c) POLYMER FILM 103

4.8.4 SRIM SIMULATED Kr ion IRRADIATION OF *'shielded'* AND *'direct'* PMP (sample OA3c and OA3d) POLYMER FILM..... 108

4.8.5 THERMOGRAVIMETRY (TGA) ANALYSIS OF SWIFT HEAVY KR ION IRRADIATED PMP (SAMPLES OA3c and OA3d) POLYMER FILM.....111

4.8.6 FTIR SPECTROSCOPY OF KR IONS IRRADIATED *'shielded'* PMP (SAMPLES OA3c and OA3d) POLYMER FILM 113

4.8.7 RESULT SUMMARY FOR SWIFT HEAVY ION IRRADIATED PET AND PMP POLYMER FILM 119

4.9 CHAPTER SUMMARY 119

CHAPTER FIVE 121

5 CHARACTERIZATION OF *'shielded'* SWIFT HEAVY ION IRRADIATED ETCHED POLYETHYLENE TEREPHTHALATE (PET) AND POLYMETHYL PENTENE (PMP) POLYMER FILMS 121

5.1 INTRODUCTION.....121

5.2 CHARACTERIZATION OF *'layered* SWIFT HEAVY ION IRRADIATED ETCHED PET POLYMER FILM.....122

5.3 SCANNING ELECTRON MICROSCOPY MORPHOLOGY ANALYSIS OF *'shielded'* SWIFT HEAVY ION IRRADIATED ETCHED PET POLYMER FILM 122

5.4 X-RAY DIFFRACTION ANALYSIS OF *'shielded'* SWIFT HEAVY ION IRRADIATED ETCHED PET POLYMER FILM..... 127

TABLE OF CONTENTS

5.5 FOURIER TRANSFORMED INFRA-RED (FTIR) SPECTROSCOPY ANALYSIS OF *'shielded'* SWIFT HEAVY ION IRRADIATED ETCHED PET POLYMER FILM 130

5.6 CHARACTERIZATION OF *'shielded'* and *'direct'* SWIFT HEAVY ION IRRADIATED ETCHED PMP POLYMER FILM.....
.....139

5.7 ETCHING KINETICS OF *'shielded'* SWIFT HEAVY ION IRRADIATED ETCHED PMP POLYMER FILM.....
.....139

5.8 SCANNING ELECTRON MICROSCOPY MORPHOLOGY ANALYSIS OF ETCHED UNIRRADIATED, *'shielded'* AND *'direct'* SWIFT HEAVY ION IRRADIATED ETCHED PMP POLYMER FILM
.....143

5.9 XRD ANALYSIS OF ETCHED UNIRRADIATED, *'shielded'* AND *'direct'* SWIFT HEAVY ION IRRADIATED PMP POLYMER FILM
.....148

5.10 FOURIER TRANSFORMED INFRA-RED SPECTROSCOPY ANALYSIS FOR ETCHED UNIRRADIATED, *'shielded'* and *'direct'* SWIFT HEAVY ION IRRADIATED PMP POLYMER FILM.....
.....150

5.11 RELATIVE TRANSMITTANCE ANALYSIS OF *'shielded'* AND *'direct'* SWIFT HEAVY ION IRRADIATED PMP POLYMER FILM
.....152

5.12 CHAPTER SUMMARY 153

CHAPTER SIX.....155

6 GAS PERMEABILITY AND SELECTIVITY.....155

6.1 INTRODUCTION.....155

TABLE OF CONTENTS

6.2 GAS PERMEABILITY AND SELECTIVITY ANALYSIS OF POLYETHYLENE TEREPHTHALATE (PET) 156

6.3 GAS PERMEABILITY AND SELECTIVITY STUDY OF POLYMETHYL PENTENE (PMP) 162

6.4 CHAPTER SUMMARY 168

CHAPTER SEVEN 169

7 CONCLUSION AND RECOMMENDATION 169

7.1 OVERVIEW OF FINDINGS 169

7.2 SUMMARY OF KEY FINDINGS 170

7.3 RECOMMENDATIONS 172

CHAPTER EIGHT 174

8. REFERENCES 174

LIST OF FIGURES

Figure 2-1: Structure of polyethylene terephthalate 12

Figure 2-2: Polymethylpentene (PMP) structure 13

Figure 2-3: Aspect-ratio and lateral line-width of various microtools. The technological limits are indicated in brackets 17

Figure 2-4: Etched tracks with distinct pore formations indicating the regions of swift heavy ion implantation in solids 20

Figure 2-5: The characteristic reaction sequences induced by swift heavy ion irradiation 26

Figure 2-6: Schematic of etching processes 30

Figure 2-7: Schematic of pores with various geometries that can be created by etching heavy ion tracks in polymers. (a) Cylindrical, (b) Conical, (c) Biconical (d) Funnel-shaped 31

Figure 2-8: Solution-diffusion mechanism of H_2 through a Pd-based layer.....39

Figure 3-1: Schematic flow of experiments 46

Figure 3-2: The block-schematic of gas permeability set-up 63

Figure 4-1: SEM surface morphology of ASPET (sample OA1a) polymer film ..67

Figure 4-2: XRD analysis of ASPET (sample OA1a) polymer film 68

Figure 4-3: In-situ thermal XRD analysis of ASPET 69

Figure 4-4: TGA thermal profile of ASPET (sample OA1a) polymer film 71

Figure 4-5: IR spectra of ASPET (sample OA1a) polymer film 73

Figure 4-6: SEM micrograph image of ASPMP (sample OA3a) polymer film 75

Figure 4-7: XRD analysis of ASPMP (sample OA3a) polymer film 76

LIST OF FIGURES

Figure 4-8: TGA thermal profile of ASPMP (sample OA3a) polymer film 78

Figure 4-9: IR spectra of ASPMP (sample OA3a) polymer film 79

Figure 4-10: SEM micrograph of PET (sample OA1b) polymer film etched in NaOH solution at 80 ˚C for 150 minutes 84

Figure 4-11: Kinetic analysis of etched PET (sample OA1b) polymer film in NaOH at 80 ˚C for 140 minutes 85

Figure 4-12: IR spectra of (a) ASPET (sample OA1a) and (b) PET (sample OA1b) polymer film etched in NaOH etched at 80 ˚C for 140 minutes 87

Figure 4-13: SEM micrograph of PMP (sample OA3b) polymer film etched in acidified chromium trioxide at 80 ˚C for 150 minutes 91

Figure 4-14: Chemical etching kinetic analysis of PMP (sample OA3b) polymer film 93

Figure 4-15: IR spectra of (a) ASPMP and (b) etched PMP (sample OA3b) polymer film 95

Figure 4-16: Theoretical SRIM simulated analysis for *'shielded'* swift heavy ion irradiated PET (sample OA1c) polymer film 101

Figure 4-17: Thermal profile (TGA) analysis of (a) ASPET (sample OA1a) and (b) Xe ion irradiated PET (sample OA1c) polymer film 102

Figure 4-18: IR spectra (a) ASPET (sample OA1a) and (b) swift heavy ion irradiated *'shielded'* PET(sample OA1c) polymer film 104

Figure 4-19: Probable chain scission locations (a), (b), (c), (d) and (e) in PET polymer during swift heavy ion irradiation 105

Figure 4-20: Fragments of functional groups from PET structure after swift heavy ion irradiation 106

LIST OF FIGURES

Figure 4-21: Theoretical SRIM simulated analysis of *'shielded'* swift heavy ion irradiated PMP 109

Figure 4-22: Theoretical SRIM analysis of *'direct'* swift heavy ion irradiated PMP 110

Figure 4-23: TGA analysis of (a) ASPMP polymer, (b) *'layered'* irradiated PMP (sample OA3c) and (c) *'directly'* irradiated PMP polymer film (sample OA3d) 112

Figure 4-24: IR spectra analysis of (a) ASPMP, (b) *'layered'* PMP polymer film irradiated with Kr ion irradiated (sample OA3c) and (c) PMP polymer film *'directly'* irradiated with Kr ion without layering (sample OA3d).....114

Figure 4-25: Probable chain scission locations on PMP polymer structure locations after swift heavy ion irradiation.....116

Figure 4-26: Fragments of moieties from PMP structure after swift heavy ion irradiation.....116

Figure 5-1: SEM micrograph surface morphology of (a) ASPET (OA1a), *'shielded'* swift heavy ion irradiated etched PET polymer film (b) OA2a, (c) OA2b, (d) OA2c and (e) OA2d due to various etching time and (f) SEM cross-section of sample OA2d PET polymer film.....124

Figure 5-2: X-ray diffraction analysis of (a) ASPET, (sample OA1a) and *'shielded'* swift heavy ion irradiated etched PET polymer film (b) OA2a, (c) OA2b, (d) OA2c and (e) OA2d as a function of various etching time 128

Figure 5-3: IR analysis of (a) ASPET (sample OA1a) and *'shielded'* swift heavy ion irradiated etched PET polymer film (b) OA2a, (c) OA2b, (d) OA2c and (e) OA2d as a function of various etching time. 131

LIST OF FIGURES

Figure 5-4: The relative absorbance *'shielded'* swift heavy irradiated etched PET polymer (a) OA2a, (b) OA2b, (c) OA2c and (d) OA2d as a function of etching time 138

Figure 5-5: Etching kinetics (weight loss) analysis of (a) *'shielded'* swift heavy ion irradiated etched PMP (sample OA4d) and (b) ASPMP (sample OA3b) polymer film.....140

Figure 5-6: Etching kinetics analysis of (a) etched ASPMP and (b) track-etched PMP film.....142

Figure 5-7: SEM surface micrograph (a) sample OA3b, *'shielded'* (sample OA4d) with (b) irradiated and (c) unirradiated sides, (d) and (e) *'direct'* swift heavy ion irradiated PMP (sample OA9d) 144

Figure 5-8: Cross section of SEM micrograph of *'shielded'* (sample OA4d) and *'direct'* (sample OA9d) swift heavy ion irradiated etched PMP polymer film ...146

Figure 5-9: XRD analysis (a) sample OA3b, (b) *'shielded'* (sample OA4d) (c) *'direct'* (sample OA9d) swift heavy ion irradiated PMP polymer film.....149

Figure 5-10: FTIR spectra analysis (a) sample OA3b, (b) *'shielded'* (sample OA4d) and (c) *'direct'* (sample OA9d). Figure 5.10b and 5-10c were swift heavy ion irradiated etched PMP polymer film.....150

Figure 5-11: Relative absorbance (A/A_o) analysis of selected characteristic functional groups for *'shielded'* and *'direct'* swift heavy ion irradiated etched PMP polymer films.....152

Figure 6-1: The dependence of gas permeability on etching time *'shielded'* ion irradiated PET films.....159

LIST OF FIGURES

Figure 6-2: The dependence of ideal gas selectivity on etching time *'shielded'* Xe ion irradiated PET polymer films 161

Figure 6-3: The dependence of gas permeability on ASPMP and *'shielded'* swift heavy Kr ion irradiated etched PMP films.....164

Figure 6-4: The dependence of ideal gas selectivity on ASPMP and *'shielded'* swift heavy Kr ion irradiated etched PMP films.....167

LIST OF TABLES

Table 2-1: Generic types of polymers that undergo either crosslinking or scission 29

Table 3-1: Polymer films 43

Table 3-2: Chemical reagents 44

Table 3-3: Sample codes, ion irradiation and chemical etching experimental descriptions for ASPET and ASPMP polymer films 48

Table 3-4: SEM instrument set-up condition 56

Table 3-5: XRD (Bruker AXS D8) instrument set-up conditions 57

Table 3-6: FTIR/ATR instrument set-up conditions 58

Table 3-7: TGA instrument set-up conditions 59

Table 4-1: Selected functional groups in the PET polymer film and their corresponding wavenumbers 73

Table 4-2: Selected functional groups in PMP polymer film and their corresponding wavenumbers 80

Table 4-3: Comparison of selected functional groups in ASPET and etched PET polymer film 88

Table 4-4: Comparison of selected functional groups in ASPMP (sample OA3a) and etched PMP (sample OA3b) polymer film 96

Table 4-5: Selected functional groups in PET polymer film and their corresponding wavenumbers 107

Table 4-6: Comparison of selected functional groups for samples OA3a, OA3c and OA3d PMP polymer film 117

LIST OF TABLES

Table 5-1: Comparison of selected functional group and wavenumber present in PET for ASPET and *'shielded'* swift heavy ion irradiated etched PET polymer film and their corresponding wavenumbers 133

Table 5-2: Selected functional groups in *'shielded'* and *'directly' irradiated* PMP polymer film and their corresponding wavenumbers 151

Table 6-1: Gas permeability analysis of ASPET (sample OA1a) and *'shielded'* irradiated PET (sample OA1c) polymer films 156

Table 6-2: Ideal gas selectivity of ASPET (sample OA1a) and *'shielded'* irradiated PET (sample OA1c) polymer films 158

Table 6-3: Gas permeability analysis of swift heavy Kr ion irradiated PMP films '*layered*' with PET polymer foil.....163

Table 6-4: Ideal gas selectivity of ASPMP and track-etched PMP polymer film 166

LIST OF EQUATIONS

Equation 2-1: Calculation of Ion dose 23

Equation 2-2: Energy absorbed by irradiated material 23

Equation 2-3: Bethe's equation for calculating electronic stopping power of irradiated material 24

Equation 2-4: Ion dose absorbed by polymer 24

Equation 2-5: Calculating gas flux across porous membrane by Knudsen diffusion mechanism 36

Equation 2-6: Determination of gas flux in porous membrane using Poiseuille flow 37

Equation 2-7: Calculating gas flux across porous membrane when ratio of free mean path (λ) and membrane pore radius (r) is less than 1.....37

Equation 3-1: Henry's law of solubility 60

Equation 3-2: Calculating gas flux across membrane 61

Equation 3-3: Calculating gas flux of membrane under different vapour pressures 61

Equation 3-4: Calculating permeability using diffusion and solubility coefficient 61

Equation 3-5: Calculating the permeability of single gases 62

Equation 3-6: Calculating permeability coefficient.....62

Equation 3-7: Calculating ideal selectivity of gases.....62

LIST OF ABBREVIATION

ASPMP	As-received (commercial) polymethylpentene
ASPET	As-received (commercial) polyethylene terephthalate
PET	Polyethylene terephthalate
PMP	Polymethylpentene
SEM	Scanning electron microscopy
TEM	Transmission electron microscopy
XRD	X-ray diffraction
AFM	Atomic force microscopy
TGA/DSC	Thermogravimtery analysis/differential scanning calorimetry
FTIR/ATR	Fourier Transformed Infra-red /Attenuated total reflection
PSA	Pressure swing adsorption
CD	Cryogenic distillation
SHI	Swift heavy ion
ECMO	Extracorporeal membrane oxygenation
SRIM	Stopping and Range of Ions in Matter
RT	Room temperature

OUTPUTS

1. **Title:** Ion track approach for the improvement of polymethyl pentene-1 gas separation membrane permeability *(Accepted abstract) in Russian Academy of Sciences International Conference on Ion transport in organic and inorganic membranes* (June 2014)

   Authors: Yuri Kochnev, Alex Necheav, **Olushola Rotimi Adeniyi** and Darya Syrtsova

2. **Title:** Gas separation properties of poly-4-methyl pentene-1 after ion track treatment. *(Accepted abstract) Euro Membrane 2015 (6^{th}-10^{th} September 2015)*

   Authors: D. A. Syrtsova, Yu. K. Kochnev, A. N. Necheav, **O. R. Adeniyi**, L. Petrik and V.V. Teplyakov

3. **Title: Swift heavy irradiation of polyester and polyolefins polymeric films for gas separation application.** *Oral presentation at the Joint Institute for Nuclear Research* (JINR), 4^{th} South Africa-JINR symposium. Few to Many Body Systems: Models and Methods and Applications. Dubna 2015. 21^{st}- 25^{th} September,

   Author: O. Adeniyi

Manuscripts under preparation

1. Physico-chemical properties of swift heavy ion irradiated PMP polymer film

OUTPUTS

2. IR and thermal analysis of swift heavy ion irradiated *'shielded'* PET and PMP polymer films
3. Gas permeability and selectivity studies of track-etched polyester and polyolefin

CHAPTER 1

CHAPTER ONE

1 GENERAL INTRODUCTION

This chapter provides background details on polymers, their use as membrane and application in gas permeability and selectivity. Also, this chapter describes the use of swift heavy ion (SHI) irradiation and chemical etching as track-etch post-synthesis approaches for polymer modification. The chapter layout includes problem statement, significance of study and the research questions that will be considered in this study. This chapter also contains the aims and objectives of this study and the experimental approach are presented.

1.1 MEMBRANE SEPARATION TECHNOLOGY AND SWIFT HEAVY IONS MODIFICATION OF POLYMERS: AN OVERVIEW

In recent years, there is an increase in the use of membrane technology, especially polymeric membranes, as a means to improve gas transport i.e. selectivity and permeability properties (Perry *et al.,* 2006; Baker 2002). This is because polymer membranes have been identified as viable alternatives to other existing and advanced separation techniques such as pressure swing absorption (PSA), cryogenic distillation (CD) and adsorption due to its competitive advantage such as economics and simplicity. Also, polymer membranes are still emerging while the advanced separation techniques have been applied at industrial scale for gas separation such as hydrogen enrichment (Perry *et al.,* 2006; Baker 2002). Membranes exist in the form of a thin film or flat sheet of natural or synthetic materials and must be permeable to liquid or gaseous species and selectively allow the passage of specific species across it. These two fundamental characteristics i.e. permeability and selectivity properties are being continuously explored in the study of polymer membranes. Generally, polymer membranes, just like other membrane materials, can be synthesised, modified or configured through the introduction of

CHAPTER 1

distinct physico-chemical properties for specific applications such as gas separation (Muller 1996). The modifications often involve pre-synthesis procedures such as the introduction of specific functional groups that have the ability to confer preferential characteristics such as fractional free volume on the polymer matrix. Also, other methods that have been employed in polymer modification are the use of post-synthesis approaches such as irradiation by swift heavy ions and chemical etching. These two (2) treatments can be used to tailor polymer into single or dual configuration resulting in a symmetrical (porous) or asymmetrical (semi-porous) polymer structure. The symmetrical polymer membrane structure is achieved with through pores across the polymer film while the asymmetrical structure of polymer membrane is accomplished with a porous surface on a dense layer region. The effects of post-synthesis modification i.e. swift heavy ion irradiation and chemical etching of polymer have been reported to alter polymer surface or bulk properties in comparison with the properties of the starting polymer material (Muller 1996). Swift heavy ion (SHI) is one of the examples of the post-synthesis membrane modification techniques. The recent advances and continuous use of SHI as a tool in the fabrication of polymer membranes highlights the importance of this technique. The successful applications of ion irradiated polymers have resulted in the need to explore '*new*' polymers with relatively unknown intrinsic properties after exposure to ion irradiation (Apel, 2001).

SHI is an example of ion beam technology and is used in ion track technology to irradiate solid materials. SHI are energetically charged particles with high density. The irradiation of materials by SHI is often aimed at modifying surface or bulk properties of the irradiated materials (Clough 2001; Ravanche, 2007). An ion is considered swift if its velocity is faster than the Bohr velocity value i.e. 0.22 cm/ns (Fink, 2004). Other types of ion beams include; light ions, highly focused microscopic beams and high intensity pulses. In general, x-rays beams, e-beams and ion beams are specifically used as irradiation sources on different materials. The interaction of ions with materials results in creating non-visible deformed

CHAPTER 1

regions called '*tracks*'. The three main parameters of SHI are ion type, dose, and fluence. In principle, the impinging SHI transfers energy when in contact with target materials via electronic cascading. This interaction between SHI and polymers results in the creation of two (2) types of tracks i.e. halo and core and the tracks can be chemically revealed using mild or aggressive media treatments often via a process called *'track-etching'* (Delgado *et al*., 2009). One of the emerging applications of track-etched membranes obtained from polymers is in gas permeability and selectivity. The study of track-etched polymer membranes continues because of the emergence of new polymer materials with improved properties and potential range of applications. Consequently, the use of SHI on polymers requires a basic understanding of the polymer compositions; and the relative effects of the beam parameters such as ion dose and fluence, ion velocity, electronic stopping power (energy loss) and other associated irradiation conditions such as temperature, and environment (vacuum or air) (Ravanche *et al*., 2007; Delgado *et al*., 2009). These ion irradiation parameters can be carefully manipulated to initiate change in the chemical (chain scission and crosslinking, emergence of multiple bonds), thermal (degradation), optical, electrical and surface properties (hydrophobicity or hydrophilicity) of the irradiated materials (Delgado *et al*., 2009). For instance, crosslinking or multiple bonds can be initiated at high ion fluence due to the increase in *overlapping* of ion tracks which can be confirmed during chemical etching (Delgado *et al*., 2009).

In the near future, it is anticipated that membranes will compete favourably with other consolidated separation technologies. This is because membrane technology has shown feasible economics as an alternative separation method, as well as technical and environmental sustainability advantages (Lin *et al.,* 2006). The application of polymeric membranes for gas permeability and selectivity is not a new approach. However, this application continues to evolve due to the progress in the synthesis of new polymers, co-polymers and homo-polymers in order to improve on polymers gas selectivity and permeability properties (Lin *et al*., 2006;

CHAPTER 1

Baker, 2006; Bernardo *et al.,* 2009). On the industrial scale, some of the applications of membranes include water desalination, microelectronics, filtration of beverages and separation and concentration of various suspensions (Apel, 2001; Bernardo *et al.,* 2009). There are several challenges that must be adequately addressed in order to achieve a successful application and optimal performance of polymer based gas separation membranes in industrial processes. These include a balanced trade-off between permeability and selectivity properties, enhanced thermal stability and improved mechanical strength after several cycles (Abedini and Nezhadmoghadam, 2010). Another important condition for gas separation membranes is to achieve resistance to surface poisoning by gases such as CO, CO_2, and H_2S (Freeman, 1999; Lin *et al.,* 2006; Bernardo *et al.,* 2009). In general, the applicability of polymeric membranes depends on their gas separation properties. However, the polymer of interest must be tailored towards achieving improved gas selectivity and permeability by adopting robust techniques to modify the polymer structural configurations (Bernardo *et al.,* 2009).

1.2 POLYMERIC MEMBRANES

Polymeric membranes are organic types of membranes that have been synthesised from various monomers. These types of membranes are characterized by different structural arrangements depending on the chemically reacting monomers. As a result, the compositions of these monomers confer unique physical, chemical, electrical, thermal and mechanical properties on the resulting polymers (Muller, 1996). Some polymers have been classified as high performance polymers and they include polymers such as polyethylene terephthalate (PET), polyimide (PI), polymethyl pentene (PMP). These polymers are known to exhibit selective gas permeability properties as a result of their structural, physical and chemical characteristics (Billigham and Walker, 1975; Koros and Fleming, 1993; Apel, 2003; Ramos *et al.*, 2003; Li *et al.*, 2004; Awasthi, *et al.,* 2010). To date, PMP is one of the most gas permeable polymers known. Generally, polymeric membranes have

shown commercial feasibility, thus extensive studies are being conducted to understand and improve on their intrinsic gas separation properties. For instance, modification of polymeric materials can make it symmetrical or asymmetrical membrane structure i.e. porous on dense layer. This is due to the unique properties of the polymeric materials such as sensitivity to radiation, homogeneity of tracks formation, uniformity of pore geometry (size, shape and depth), purity, availability and economics i.e. affordability and most importantly the possibility to synthesise these polymeric materials compared to natural materials (Fink, 2004; Reimar Spohr 1990). Also, the gas transport properties i.e. permeability and selectivity occur by various mechanisms such as Knudsen diffusion, solution-diffusion, molecular sieves, capillary condensation, surface diffusion among others (Nenoff *et al.*, 2006; Perry *et al.*, 2006). Most importantly, polymer separation properties and transport mechanisms depend on their class (linear and aromatic), type (glassy and rubbery), alignment of atomic species (crystallinity or amorphous), chain orientation (backbone and side) and morphology (Bernardo *et al.*, 2009; WSRC, 2008; Perry *et al.*, 2006; Muller 1996). Interestingly, glassy polymers are used for gas separation membranes due to their high selectivity and excellent mechanical properties (Low *et al.*, 2010; Bernardo *et al.*, 2009) and ability to generate pure gas in a gas mixture stream (Nenoff *et al.*, 2006; Perry *et al.*, 2006). The gas selectivity of glassy polymers depends on fractional free volume (FFV) due to atomic and molecular packing density either between or within the chains (Nagel, 2000), surface functionality, structural rigidity and moldability of the polymer film (Bernardo *et al.*, 2009). These properties can be incorporated into a polymer structure either by pre or post-synthesis approaches such as physical and chemical treatments or thermal annealing. The treatment processes induce chain scission, molecular rearrangement, atoms crosslinked along the backbone or side chain of the resulting polymers (Cleland *et al.*, 2003). The polymers that are investigated in this study belong to the polyester (polyethylene terephthalate) and polyolefin (polymethyl pentene) category. The choice of these polymers is because they belong to the

CHAPTER 1

glassy type of polymers and are considered as the appropriate polymer membrane to separate light gases such as hydrogen (Nenoff *et al.*, 2006).

1.3 PROBLEM STATEMENT

One of the key challenges associated with polymer membranes is how to improve their gas permeability and selectivity properties. In order to improve gas permeability and selectivity, the thickness of the polymer film is critical to improving these properties. It is therefore important to tailor polymer film into a membrane structure to achieve this purpose. The polymers can be tailored into asymmetrical membranes i.e. porous surface on dense layer by the track-etch approach. However, in order to use track-etching method to develop asymmetrical polymer membranes, ion irradiation of polymer must be carefully manipulated especially the control ion penetration depth into the irradiated polymer film. To address this issue, the use of *'shielded'* material on polymer during irradiation stage is considered to be a suitable approach in the fabrication of asymmetrical polymer membranes in this study.

1.4 SIGNIFICANCE OF STUDY

The use of polymer membranes for gas separation and purification is a promising technology that offers competitive economic value, simplicity and compatibility, versatility and ease of operation (Acharya, 2006). This study will explore the use of post-synthesis modification approaches to fabricate asymmetry polymer membrane with porous surface on dense layer. This is because post-synthesis modification of polymer membranes has been identified as a route that can be explored to improve polymer gas permeability and selectivity properties. The use of post-synthesis modification will be accomplished by SHI irradiation and chemical treatments i.e. *track-etching*. Also, the polymers; polyethylene terephthalate (PET), and polymethyl pentene, (PMP) that were investigated in this

study are commercially available hence this study will provide a unique platform to increase their applicability as well as generate better understanding of their physico-chemical, mechanical and thermal properties. Although membranes are limited in their applications due to limited industrial appeal, gas diffusion kinetic ambiguity, low purity level and relatively new technology (Lu *et al.*, 2007). This study intended to investigate the intrinsic properties of polymers films in relation to SHI irradiation and study their gas selectivity and permeability characteristics. It is anticipated that this study will serve as a platform to understand the possibilities in the use of asymmetrical polymer membrane structures in gas separation applications.

1.5 RESEARCH QUESTIONS

The following research question will be considered in this study:

a. What is the influence of *'shielded'* material on SHI irradiated PET and PMP polymers film?

b. What is the influence of SHI on the physico-chemical properties of PET and PMP polymers film?

c. How does variation of SHI energy affect PMP and PET physico-chemical properties?

d. What are the effects of SHI and chemical etching conditions on gas permeability properties of PMP and PET?

e. How effective is the gas permeability and selectivity of ion irradiated and track-etched polymers?

CHAPTER 1

1.6 AIMS AND OBJECTIVES OF STUDY

The aim of this study was to investigate and understand the intrinsic properties of the selected polymers, determine the effects of *'shielded'* material irradiation on the physico-chemical, thermal and gas permeability properties of the ion irradiated polymers. Also, the chemical etching of the irradiated polymers i.e. track-etching was investigated and its effects on surface functionalization and other relevant properties of the polymers will be reported.

The objectives of this study included the following:

a. To conduct baseline characterizations of polymers in order to determine their intrinsic chemical, thermal and mechanical and gas permeability properties

b. To determine the effects of SHI with *'shielded'* irradiation on PET and PMP gas permeability and selectivity properties

c. To understand the prevailing characteristics of SHI and etching conditions on PMP and PET properties

1.7 EXPERIMENTAL APPROACH

The experimental protocol used in this study was developed to create asymmetrical polymer membranes by using the *'shielded'* material approach. The asymmetrical polymer membrane was developed by mechanically covering one of the surfaces of PET or PMP polymers to be irradiated with *'shielded'* materials that are of less thickness than the PET and PMP polymers film. Thereafter, the swift heavy ion *'shielded'* irradiated PET and PMP polymers were chemically etched i.e. *track-etched*. In using the swift heavy ion irradiation for the selected polymers i.e. PET and PMP, irradiation parameters such as ion fluence, dose, ion energy and ion type

were considered after theoretical simulation by SRIM software. The chemical etching conditions that were investigated included; time of etching, temperature of etching and types and concentration of etchants. The as-received PET and PMP, swift heavy ion irradiated and track-etched PET and PMP polymers were thoroughly investigated to determine their physical, chemical, thermal and gas permeability properties. The polymer materials for this study were commercially purchased; PMP (Goodfellow, UK) and PET (Joint Institute for Nuclear Research, Dubna). The characterization techniques that were considered in this study include; infrared (IR) to investigate functionality of polymer before and after SHI irradiation and chemical etching, thermo-gravimetric analysis (TGA) for thermal properties, surface morphology by scanning electron microscopy (SEM), and crystallinity profile will be studied by X-ray diffraction (XRD) technique and gas hydrogen gas permeability and permselectivity analysis.

1.8 THESIS CHAPTER LAYOUT

Chapter One: This chapter provides concise information in form of a general introduction and overall concept of the study. Also, the chapter highlights the summary of hydrogen energy and polymeric membranes for gas separation, presents the problem statement, research questions, aims and objectives of study and the experimental approach.

Chapter Two: A compendium of relevant literature is covered and presented in this chapter. Each section in this chapter addresses specific areas related to the study in a chronological order.

Chapter Three: In chapter three, the experimental layout is presented. The experimental approach includes; varied parameters, methodology, experimental conditions as well as characterization techniques used to analyse samples.

CHAPTER 1

Chapter Four: This chapter presents the characterization results of as-received (commercial) PET and PMP polymer films. The characterizations include IR, SEM, TGA and XRD.

Chapter Five: The results and discussion of SHI irradiated polymer and track-etched polymer are presented in this chapter. The characterization included in this chapter includes etching kinetics study, IR, SEM, TGA.

Chapter Six: In this chapter, the gas permeability and selectivity properties are investigated and results are presented.

Chapter Seven: This chapter contains the conclusion and recommendations from the overall investigations and available experimental data from this study.

Chapter Eight: The chapter is a compendium of consulted resources i.e. references used in this study.

CHAPTER 2

CHAPTER TWO

2 LITERATURE REVIEW

This chapter will discuss the general concept of ion track technology and chemical etching properties of two polymers i.e. polyethylene terephthalate (PET) and polymethyl pentene (PMP) that have been selected for this study. Also, the use of SHI and chemical etching techniques to modify materials such as polymer films will be discussed. This chapter also discusses the various mechanisms that have been identified during the interaction between swift heavy ions and polymer films. In addition, this chapter will describe the applications of symmetrical membranes structure as well as the various gas transport mechanisms associated with symmetrical and asymmetrical polymer structure.

2.1 INTRODUCTION

Polymers are known to possess unique structural and atomic configurations which can be modified using single or multiple treatment methods such as swift heavy ions or chemical etching. The atomic compositions and structural orientations of polymers can be directly responsible for the generation of specific functional groups especially during swift heavy ion irradiation and chemical etching. The generated species within the polymer can be from either the backbone structure or side chain attachment of the polymer. The subsequent sections will address two different class of polymers considered in this study and how swift heavy ion irradiation affects their properties. They are polyethylene terephthalate (PET) which belongs to polyester class and polymethyl pentene (PMP) which is a polyolefin. Although polyamides and polycarbonates are not investigated in this study, some salient information is provided based on previous studies especially on the swift heavy ion irradiation studies on these types of polymers.

CHAPTER 2

2.2 POLYETHYLENE TEREPHTHALATE

Polyethylene terephthalate (PET) is a linear chain polyester (Figure 2-1) with unique thermal, chemical and physical properties (Awasthi, *et al.*, 2010). PET is synthesised via the chemical reaction of ethylene glycol with either terephthalic acid or dimethyl terephthalate. The reaction process of PET occurs by four successive chemical routes namely; trans or direct esterification, pre-polymerization, including the melt and solid state polycondensation. As a high performance polymer, PET attracts considerable scientific interest due to its versatile applications in aerospace, space satellite, radiotherapy and other high technology composites industries (Apel, 2003).

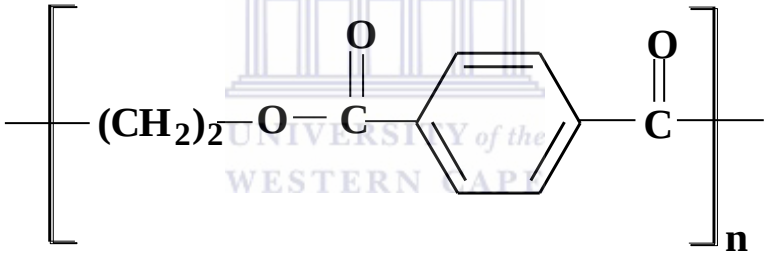

Figure 2-1: Structure of polyethylene terephthalate

PET polymer (Figure 2-1) has been reported to undergo changes in surface, structural, chemical, optical and thermal modifications due to ion irradiation (Singh *et al.*, 2006). This response to surface modification makes PET one of the most appropriate polymers that can be used to determine polymer behaviour under different surface modification procedures due to polymer-ion irradiation interactions in experimental conditions (Abdesselam, 2011). The expansive applications of PET polymers have resulted in the study of their intrinsic properties using a variety of techniques. One of these techniques includes the use of heavy ion irradiation to investigate their properties. For instance, Awasthi *et al.*, 2010 determined the effects of irradiation on PET with oxygen ions. The study reported

CHAPTER 2

considerable change in optical, mechanical, chemical and structural properties of PET as a function of ion fluence. In another related study, Abdesselam *et al.*, 2011 reported the evolution of gaseous species such as hydrogen, carbon and oxygen as a function of ion fluence due to alpha particle irradiation on PET. It was stated that hydrogen, oxygen and carbon contents in PET are released at a steady but continuous rate due to increase in ion fluence.

2.3 POLYMETHYL PENTENE

Polymethylpentene (PMP) with trade name TPX belongs to the thermoplastic polyolefin polymer group and is one of the most gas permeable polymers with characteristic dual amorphous-crystalline properties. PMP has two tertiary carbon atoms per repeating units and these carbon atoms are each located on the side chain and backbone respectively (EL-Naggar *et al.*, 1990) with some unique characteristics.

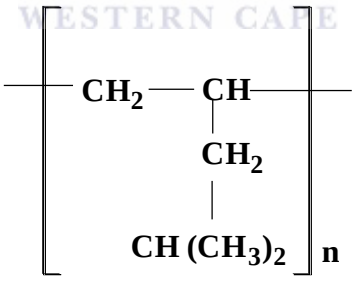

Figure 2-2: Polymethylpentene (PMP) structure

The characteristics of PMP include; high optical transparency, high crystalline and melting point (250°C), low density (0.83; for any known commercial thermoplastic), good electrical properties, and heat resistance properties (Billigham and Walker, 1975). These intrinsic properties have been responsible for the application of PMP as lens materials for infrared windows, membrane materials, and food packaging. According to previous studies, PMP has been reported to show

CHAPTER 2

unique susceptibility to irradiation using γ-irradiation and electron beams due to the structural configuration i.e. the presence and location of tertiary carbon atoms (Billigham and Walker, 1975; EL-Naggar *et al*., 1990). The residual effects of swift heavy ion irradiation on PMP have been reportedly reinforced by the location of these two tertiary carbon atoms (EL-Naggar, 1990). PMP has been widely used in medical sciences as extracorporeal membrane oxygenation (ECMO) which is a life support oxygenator. Also, it is used as an alternative to solid silicone membrane oxygenator due to its non- harmful nature to the human body as well as biocompatibility properties (Peek *et al*., 2002).

2.4 ION TRACK TECHNOLOGY

Ion tracks (IT) were first discovered in the late 1950s by Young through the fission-fragment irradiation of LiF. The commercial potentials of IT as well as its industrial applications have been extensively described by Reimar Spohr (1990) and Hellborg *et al*., 2009. Generally, ion tracks are stable remnants of swift heavy ions after interaction or impingement on solids (Fink, 2004) and such solids can be organics and inorganics materials. Energetic ions are known as charged atoms with kinetic energy and they interact with electrons or nuclei of materials via Coulombs forces. Due to interaction between the energetic ion and electrons of materials, energy transfer occurs followed by atomic excitation via scattering or dislocation of individual or aggregation of atoms within a material (Hellborg *et al*., 2009). In principle and from available experimental data, the patterning of porous (micro and nano) membranes with highly uniform geometry and precisely determined structures is one of the promising examples of industrial application in material-chemistry, electronics, biomedical and physics, in the use of ion tracks in polymers (Yoshida *et al*., 1993; Yoshida *et al*., 1997; Apel *et al.*, 1997a; Apel *et al.*, 1997b; Apel *et al.*, 2000; Bohm *et al.*, 2000; Apel 2003). Therefore, ion track technology has resulted in the fabrication of track membrane (TM) materials such that both organic and inorganic materials can be modified by this technology. Track

CHAPTER 2

membranes (TMs) materials were first made by irradiation of organic material polymer sheets and inorganic materials such as micas, and glasses with fragments from the fission of heavy nuclei such as californium or uranium (nuclear track etch method) (Baccaro, and Chen, 2005). However, this technique presents limitations due to the contamination of the foil with radioactive products hence "*cooling*" of the irradiated material is required before use which often takes a few months. In the case of swift heavy ion, the ions are usually of high energy on the order of several MeV from accelerators (Baccaro, and Chen, 2005; Fleischer *et al*., 1975). The heavy ion beams offer competitive advantages over the fission of heavy nuclei in the following ways.

a. Absence of induced radioactivity in the irradiated material (ion energy is below the Coulomb barrier)
b. Uniformity of etching properties of tracks
c. Intense ion penetration in the material due to higher energy of particles
d. Higher density (>10^9 cm^{-2} for smaller pores) track arrays
e. Easy control of the ion impact angle on materials and production of arrays of parallel tracks.

2.5 ADVANCES IN SWIFT HEAVY ION IRRADIATION AND TRACK-ETCHED POLYMER MEMBRANE

Swift heavy ions are energetic ions used for polymer irradiation and are produced from ion implanters or ion accelerators. Other methods for production of these energetic ions include cyclotrons, synchrotrons, radioactive samples or nuclear reactors. The sources of the energetic ions could be hot-filament hollow-cathode or sputter ion. Consequently, the energetic ions produced from these devices differ in energy range, travel pattern of ion beam and ion beam current (Fink, 2004). The availability and otherwise R&D use of cyclotron facilities has been succinctly covered by Apel, (2003). Also, the applications and commercial viability of these

CHAPTER 2

facilities was extensively reported. Despite the enormous potentials capability in the use of cyclotron facilities as SHI irradiation option, their commercialization remains a huge challenge. This is partly due to the cost implications and also the limited industrial appeal (Fink, 2004). The early study of ion-track technology was restricted to inorganic crystalline materials such as mica and MoS_2. However, recent advances (state-of-the-art) in SHI have led to the discovery of SHI potentials in materials (polymers, glass) with superior track formation compared with other irradiation approaches as presented in Figure. 2.3. The continuous advancement and potentials of SHI as tool for the fabrication of ion track material emphasises the importance of extensive studies and use of polymers as materials for several applications such as space research, mineralogy, medicine, geology, oil and uranium prospecting and more recently optoelectronics and gas separation applications (Fink, 2004). The use of ion-track technology on polymers for gas permeability and selectivity is an emerging frontier aimed at using a combination of materials and technology for innovative and robust gas separation applications. In this case, the conventional phenomenon are applied i.e. the polymers serves as ion detector while chemical etching of the ion irradiated polymers are tailored to fabricate a specific pore profile (Apel, 2003; Fink, 2004). Prior to the introduction of accelerator based ion track technology for the manufacture of micro filter membranes, nuclear fission fragment was the preferred technology. However, since the advent of ion track technology, the nuclear fission technique has been discontinued due to the overwhelming advantages of accelerated ion track technology. These advantages have been well outlined by Apel (1995). Polymers experience latent damage during irradiation due to impregnation of accelerated energetic ions into the polymer structure leading to physical deformity as well as several chemical modifications via various reaction processes such as chain scission, crosslinking etc within the polymer chain (Lee, 1999; Calcagno *et al.*, 1992). The penetrating ion experience energy loss due to the interactions with the atoms or electrons of the target material. This energy loss per unit path length is

CHAPTER 2

called stopping power and denoted as $\frac{dE}{dx}$. Polymer surfaces are often exposed to different ions (low, medium and heavy ions) under various conditions (Jung *et al.*, 2012; Mathakari *et al.*, 2009; Briggs and Hearn, 1986) hence; the impinging ion dislodges the loosely packed atoms in the polymer due to their weak associated bonds. Some of the important parameters during polymer irradiation include ion dose and fluence (Calcagno *et al.*, 1992).

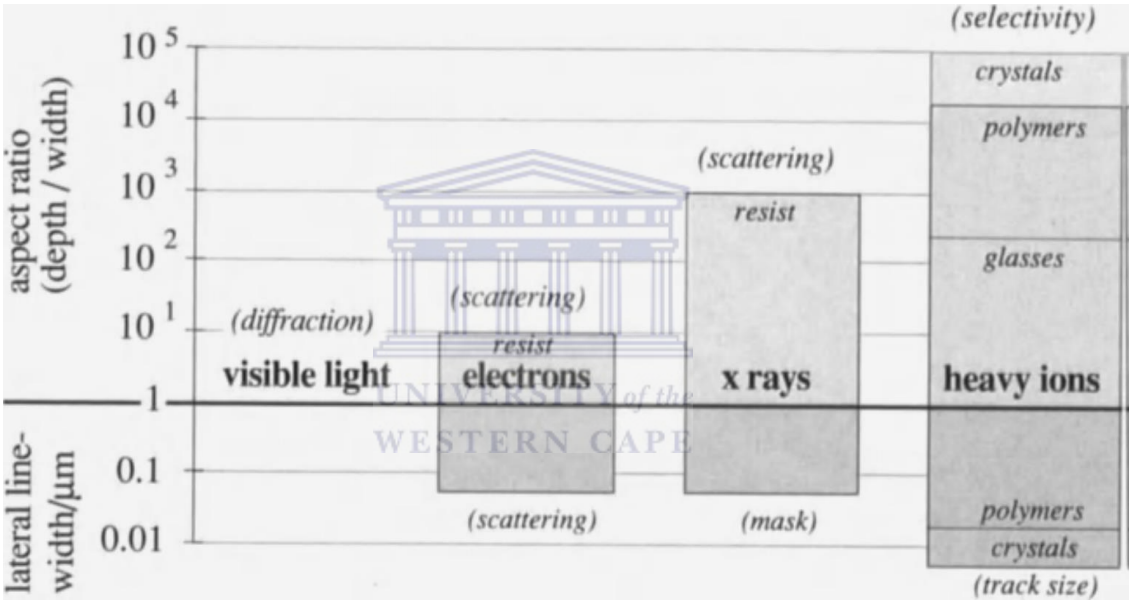

Figure 2-3: Aspect-ratio and lateral line-width of various microtools. The technological limits are indicated in brackets

In Figure 2-3, the various ion irradiation methods are highlighted as well as the limitations associated with these irradiation methods. In the case of heavy ions column in Figure 2-3, it could be observed that the aspect ratio and lateral line were highest but limited by selectivity for the aspect ratio while the lateral line is limited by track-size. Also, the heavy ions can be applied on various materials such as glasses, polymers and crystals.

CHAPTER 2

2.6 APPLICATIONS AND LIMITATIONS OF SWIFT HEAVY IONS (SHI)

Ion track technology is a versatile approach that can be used for material engineering due to radiation effects after exposure to swift heavy ions (SHI). One of the fundamental applications of this technique is the possibility of altering polymers physical, chemical, mechanical and thermal properties (Zaporojtchenko *et al*., 2003; Fink, 2004; Wohl *et al*., 2005, Mathakari *et al*., 2009). Several polymeric materials such as polycarbonate, polyacetate, cellulose etc (Delgado *et al*., 2009), polyimide (Mathakari *et al*., 2009), ultra-high molecular weight polyethylene (UHMWPE) (Chappa *et al*., 2006) are being investigated so as to improve on the existing applications (Apel 2003). Also, the use of accelerator based research in material sciences and engineering to modify polymeric materials has become imperative. Although accelerator based scientific research is expensive, there is a need to create avenues to make it economically more viable. The SHI possess ions with a dose range of Mev and GeV per nucleons which have been used to synthesize, characterize and modify materials (Avasthi, 2009). Also it is important to identify commercialization possibilities of the SHI technique especially in the area of TE polymer membrane for gas separation. The overall implication of these limitations is that there is a need for extensive research in material synthesis on one hand and ion track modification approach on the other hand, hence the combination of material sciences and modification technology.

2.7 POLYMER PROPERTIES AND CHARGED PARTICLE INTERACTION

Polymers are known to exhibit intricate physical, chemical, thermal and mechanical properties due to the structural configuration of the molecular moieties i.e. repeating chemical units. Effectively, the repeated chemical units define the existing chemical bond networks, bond strength, orientation and susceptibility of chemical attacks on

CHAPTER 2

these bonds during post-synthesis modification processes such as use of ion track and chemical treatment procedures (Fink, 2004**)**. Fundamentally, the two major structural changes observed in swift heavy ion irradiated polymers are crystallinity i.e. degree of alignment of polymer chains within certain regions, while the second change is associated with the build-up of local density fluctuations which often result in the release of volatile atoms or molecules via bond breakage and thermal diffusion due to fractional free volume of polymer films. Generally, the energy transfer and bonding energy present in the target material determines the effective prevailing phenomenon of chemical crosslinking, chain scission or molecular rearrangement (Fink, 2004). Heavy ion irradiation of the polymer is one of the modern technologies used to modify polymeric materials and also probe the interaction of polymer with ion irradiation (Jung *et al.,* 2012; Kormunda *et al.,* 2012; Chen *et al.,* 2009; Mathakari *et al.,* 2009; Kudo 2009; Rivaton and Arnold 2008; Qureshi *et al.,* 2007; Verdianz *et al.,* 2006b; Verdianz *et al.,* 2006; Chmielewski *et al.,* 2005; Quamara *et al.,* 2004; Chmielewski *et al.,* 2004; Hama *et al.,* 2003; Guenther *et al.,* 2002; Seguchi *et al.,* 1999; Lee 1999). The interaction between the ions (mostly protons) released by the heavy ions source, polymers atoms have been studied for decades and several theories have been postulated to explain this phenomenon (Mark, 2007). Some of the important factors that determine the degree of interactions between polymers and swift heavy ion irradiation include; chemical structure of polymer (i.e. crystallinity, aromaticity, nature of attaching pendants and presence of unsaturation) inter-atomic bond strength, environmental conditions (i.e. generated radical species from irradiated polymer and their stability when exposed to other competing species) (Mark, 2007). Generally, the swift heavy ion irradiation technique results in the reorientation of the polymer structure in the form of chain scission (inter and intra), cross-linking and release of radicals. The systematic alteration of polymeric properties can be inferred from the pattern of ion tracks formation as presented in Figure. 2-4.

CHAPTER 2

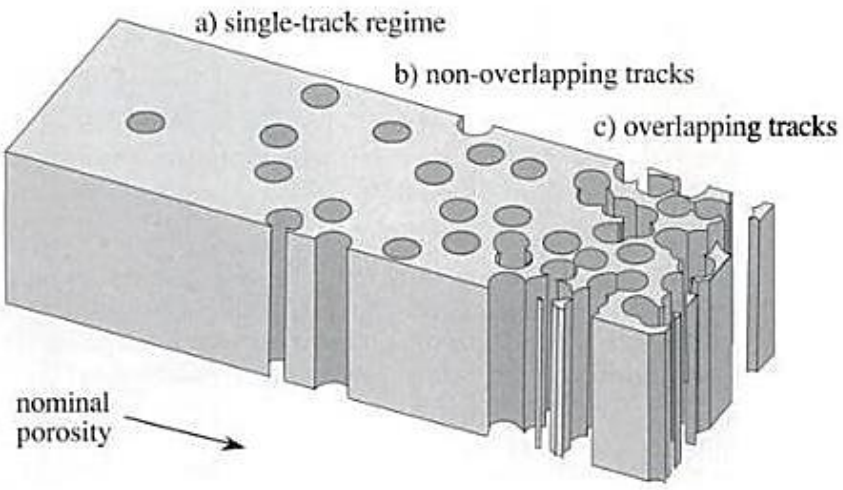

Figure 2-4: Etched tracks with distinct pore formations indicating the regions of swift heavy ion implantation in solids

The various characteristics tracks i.e. single, less discrete and overlapping tracks in solids after swift heavy ion irradiations are shown in Figure 2-4. In single (isolated) track formation, the change in properties is restricted to localized region of ion interaction with the respective solid. For a less discrete track such as non-overlapping tracks, the effective alteration of properties experienced by the target is orientated towards a globalized and dispersive change in properties. The third type of track present in solids is referred to as overlapping tracks. They are formed due to the agglomeration or concentration of swift heavy ion density in a region. In this scenario, the bulk properties of the target are compromised with complete transformation, replacement or dissolution. As a result, the original properties are compromised with the conferment of new properties due to the swift heavy ion modification effects (Reimar Spohr 1990).

CHAPTER 2

2.7.1 POLYMER SURFACE MODIFICATION, FUNCTIONALITY AND STRUCTURAL ARRANGEMENT

Surface modification of polymers using procedures such as swift heavy ion irradiation has been identified as a major pathway to alter polymer physico-chemical, crystallinity, mechanical and thermal properties (Mathakari *et al*., 2009; Mark, 2007). The exposure of the latent damaged tracks in polymer after swift heavy ion irradiation is facilitated by using appropriate chemical solvents (alkaline, peroxides or acids) as post-treatment conditions to assist in the fabrication of defined pore geometry with dispersed or uniform distribution through the polymer surface (Shtanko *et al.,* 2000; Apel, 2001a; Apel, 2001b). Consequently, the choice of any selected surface treatment technique of polymer is determined by cost, coverage uniformity, environmental friendliness and ultimately the final application of the polymer film (Goddard *et al*., 2007; Pandiyaraj, *et al.,* 2009). The essence of polymer functionality alterations via bulk or surface properties is to adopt a versatile technique via irradiation in order to introduce or induce highly reactive species within the polymer side chains and backbone structures. This approach often results in the selective alterations of polymer physico-chemical properties as well as chemical preference for '*attacking*' species. As a result, multiple surface treatments have been identified as suitable and robust approach in the fabrication of different but ordered sieving channels (pores) on surfaces of the latent track (*damaged*) polymer using chemical etchants (Apel, 2001). The etching technique emphasises the suitability of polymer films as viable candidates for membrane applications. Another benefit of using the irradiation-etching technique is the enhancement of polymer surface roughness which can serve as a mechanical interlocking site for metal adhesion on polymer surface (Siperko and Thomas, 1989). Besides, polymer chains (both the side chain or pendants and backbone structures) can be altered such that the fragility of these chains (backbone and side) can have a direct effect on polymer gas selectivity and permeability properties (Kulshrestha *et al.,* 2005; Abedini and Nezhadmoghadam, 2010). Basic

understanding of these techniques has been employed to deposit metal films on polymer surfaces (Jung *et al.*, 2012; Park *et al.*, 2008; Gershevitz *et al.*, 2006; Akamatsu *et al.*, 2003; Marin and Serruys, 1995; Baglin, 1992). Therefore, understanding polymer structural configurations can serve as leverage in order to pre-determine an appropriate and effective surface functionality technique towards the polymer final application (Chmielewski *et al.*, 2005; Chmielewski *et al.*, 2004; Calcagno *et al.*, 1992). This is because polymer structural configuration such as aromaticity, presence of side chains, type of side chain species, bonds status and backbone structures determine their physical and chemical orientation. Hence, the exposure of these polymers to irradiation dose and aggressive chemicals etching can lead to controlled degradation pathways with a compromise between the polymer bulk and surface properties i.e. functionality and structural adjustment. One of the physical characteristic of the track-etching process is the formation of pores and the emergence of new polymer functionalities (Chmielewski *et al.*, 2004; Briggs and Hearn, 1986).

2.7.1.1 SWIFT HEAVY ION IRRADIATION

Swift heavy ion irradiation is one of the prominent material engineering processes that have been employed in polymer surface treatments (Apel, 2001; Clough, 2001) and in the modification of polymer properties for specific applications under various environmental conditions (Mark, 2007). It is a technique that has proven to be suitable in the enhancement of polymer applicability such as surface properties (hydrophilicity, hydrophobicity, adhesion, topography etc.) as well as for other research and development purposes (Jung *et al.*, 2012; Wohl *et al.*, 2010; Gray *et al.*, 2005; Briggs and Hearn, 1986). Several studies have shown the use of swift heavy ion irradiation techniques as an effective tool in polymer modification thus emphasising the versatility of this method (Jung *et al.*, 2012; Mathakari *et al.*, 2009; Briggs and Hearn, 1986). Polymer structure such as the presence of straight chain or bulky side chains, single or double cyclic aromatics often determine the

modification pathway for the respective polymers (Lee, 1999; Calcagno *et al.*, 1992). Depending on the dominating processes during irradiation, molecular rearrangement, chain scission or crosslinking of the irradiated surface can occur via electronic or nuclear phenomenon (Zaporojtchenko *et al.*, 2003; Lee, 1999; Calcagno *et al.*, 1992) resulting in the irreversible modification of polymer physico-chemical, electrical conductivity, optical and surface properties (Ensinger, 2007; Calcagno *et al.*, 1992). Some of the advantages of irradiation over other known surface modification techniques include; defined ion fluence, accurate lateral space resolution especially in film texturing. This technique also makes it possible to vary the modification depth via choice of ion beam energy thereby leading to alteration of polymer properties within the surface region in a controlled way (Zaporojtchenko *et al.*, 2003).

$$\text{Ion dose} = \frac{(fluence)\ x\ (energy)}{(density)\ x\ (thickness)}$$

Equation 2-1: Calculation of Ion dose

The energy absorbed by a given material under irradiation by high-energy charged particle is represented by (*D*)

$$D = (S/\rho)Q$$

Equation 2-2: Energy absorbed by irradiated material

S = electronic stopping power, of the material for incident ions

ρ= density of material

Q= ion fluence

CHAPTER 2

S can be calculated from Bethe's equation which is given as:

$$S = \frac{dE}{dx} = \frac{4\pi z^2 e^4}{m_o NZ}\left[In\left(\frac{2m_o v^2}{< I >\left(1-\beta^2\right)} \right) - \beta^2 \right]$$

Equation 2-3: Bethe's equation for calculating electronic stopping power of irradiated material

ze represents charge on the particle; v is its velocity (cm/s). N and Z are the number of atoms per cubic centimetre and mean atomic number of the target material respectively. m_o represents mass of electron (a.m.u.) while $\boldsymbol{\beta^2}$ is v/c (c is the velocity of light), and <I> is the mean excitation energy of the medium (eV). The mean excitation energy <I> of each polymer was calculated from the excitation energy of each element constituting the polymer using an additivity rule.

In the case of polymers, the absorbed dose is related as:

$$D_e = D_o\left(\frac{S_e \ of \ polymer}{S_e \ of \ CTA} \right)$$

Equation 2-4: Ion dose absorbed by polymer

D_o is the measured dose by CTA film dosimeter

S_e is the stopping power for electrons

S_e can be calculated by Seltzer and Beger method (Sasuga *et al.*, 1991)

CHAPTER 2

2.8 PRINCIPLES OF SURFACE FUNCTIONALITY BY SWIFT HEAVY ION IRRADIATION

SHI damage on materials such as polymers occur due to the energy loss, transfer or projectiles to the polymer molecular, atomic or susceptible functional species leading to ionization or excitation. One of the resultant effects of ion-polymer interaction is the absorption of energy by polyatomic molecules resulting in bond cleavage hence generation of unsaturated fragments referred to as free radicals. However, it is difficult to accurately predict the preferential bonds within the polymer structures (main or side chains) that will be attacked during polymer-ion interaction such as in SHI irradiation of polymers. It is possible to alter the surface properties of polymers without compromising the bulk properties (Chapiro, 1988; Calcagno, 1992; Fink, 2004). In sections 2.9 and 2.10 the two prominent phenomenon i.e. chain scission and structural crosslinking in polymers due to ion irradiation are discussed. According to Lee (1999), the efficiency of crosslinking or chain scission does not depend on polymer structure alone but also on the source of radiation, ion specie and energy. Balanzat *et al.,* 1995 reported the method of identifying isolated monomers and the physico-chemical modifications that each of these monomers undergo during heavy ion irradiation. The penetration of heavy ion into polymers results in the loss of energy by two fundamental processes namely; nuclear and electronic stopping. These two processes have been shown to have direct effects on chemical, physical, optical, mechanical and thermal properties of polymers. The nuclear and electronic stopping will be discussed in the following sections i.e. 2.8.1 and 2.8.2.

CHAPTER 2

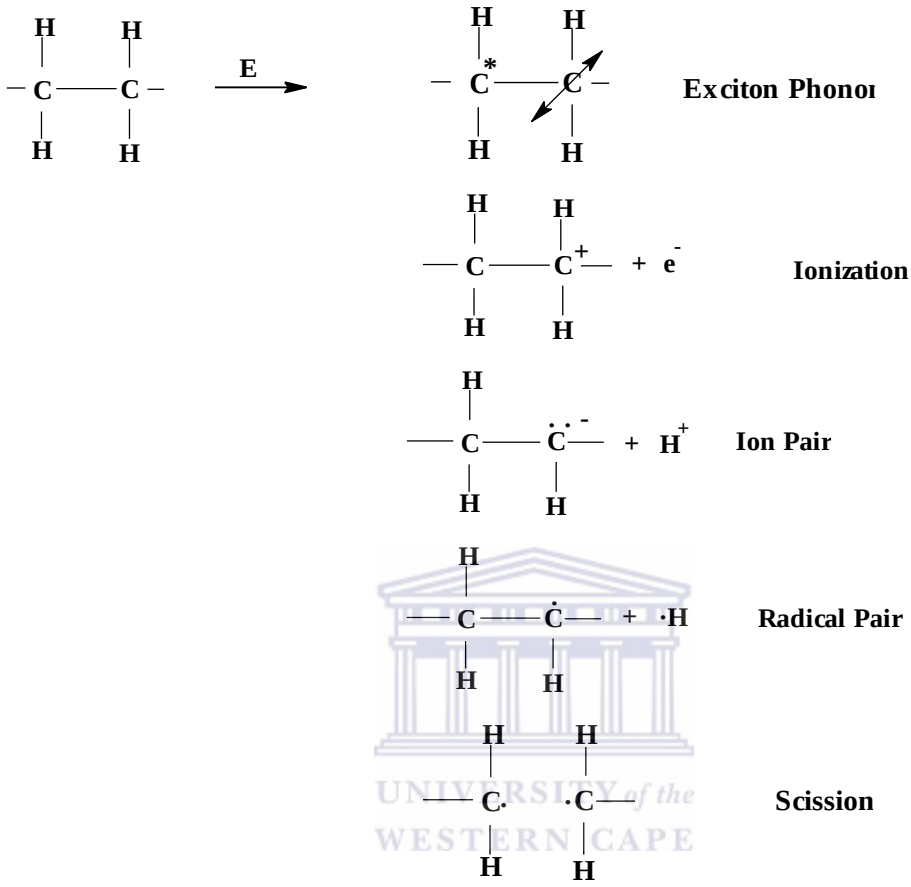

Figure 2-5: The characteristic reaction sequences induced by swift heavy ion irradiation in polymer

The reaction sequence of experienced by polymer materials after swift heavy ion irradiation is presented in Figure 2-5. The impact of swift heavy ion initiates series of reactions including excitation phonon, ionization, ion pair, radical pair and scission. In addition, the atomic composition of polymer determines the probable locations of swift heavy ion irradiation attack and ultimately the generation of the reaction sequence presented in Figure 2-5. It could be seen in Figure 2-5 that swift heavy ion irradiation attacked on a polymer structure causes the irradiated polymer undergoes deprotonation, alkylation, availability of free radicals and chain scission along the back bone structure. Also, the stability and preferential location of attack can be predicted depending on the polymer structure.

2.8.1 NUCLEAR STOPPING

In nuclear stopping, energy is lost due to collision between energetic ion and target nuclei. Consequently, the resulting energy loss leads to atomic displacement and phonons within the polymer materials. Phonons are energy dissipated in form of atomic vibrations by irradiated materials. This atomic displacement occurs when the colliding particle imparts an energy which is greater than the specific displacement threshold energy (E_d) to a target atom. Some of the factors that facilitate nuclear stopping include; inter-atomic binding energy, ion velocity and charge of the two colliding atoms. One of the high points of nuclear stopping is when an ion slows down to approximately Bohr velocity which is also the orbital electron velocity. At this velocity, the maximum nuclear energy loss occurs near the end of the ion track in the case of high energetic ions (Lee, 1999).

2.8.2 ELECTRONIC STOPPING

Electronic stopping occurs due to the charge state of irradiation ion specie and its velocity. The energetic ions experience 'stripping' of their orbital electrons as they travel through target materials. The 'stripping' of these orbital electrons vary and directly depend upon the velocity (V_{ion}) of the energetic ions. Electromagnetic interaction between the positively charged ion and target electrons have been considered to be responsible for electronic energy loss. This energy loss is as a result of glancing and knock-on collisions. These collisions transfer energy in two ways vis-à-vis electronic excitation and ionization. The excited electrons (plasmons) subsequently lose energy after being thermalized. Theoretical predictions and experimental data have shown that each of these collisions shares equal electronic energy loss and this phenomenon is called the *equipartition principle* (Lee, 1999).

CHAPTER 2

Although nuclear and electronic stopping are two different phenomenon and they affect polymer physicochemical properties. Nuclear stopping has been reported to favour chain scission while electronic stopping is responsible for crosslinking (Lee, 1999). In this regard, crosslinking and chain scission reaction mechanisms will be considered in the subsequent section.

2.9 CHAIN SCISSION

Chain scission observed in polymer during irradiation is often due to the impact of ion interaction with polymer differs. The degree of chain scission within polymer structures depends on the selected ion and surrounding environment i.e. vacuum or air (Kudo *et al.*, 2009). Consequently, several parameters have been considered as well as polymeric structural configuration in order to understand the underlying mechanism that favours or influences chain scission in irradiated polymers. Some of these parameters include; ion dose and ion fluence (Chapiro, 1988; Mathakari *et al*., 2009).

Kudo *et al.*, 2009 reported the use of selected ion beams and studied their effects on polyimide spectroscopic and optical properties. Interestingly, the choice of ions selected in their study ranged from low to high energetic ions. The IR study reported degradation of imide rings leading to cyclization and condensation in the case of polyimide irradiated with high energetic ions compared with the irradiation using low energetic ions. As expected, the IR spectroscopic studies showed the degradation of carbonyl, ether and imide groups as a function of ion type and dose.

2.10 STRUCTURAL CROSSLINKING

Unlike chain scission, structural crosslinking due to irradiation in polymers continues to be of paramount interest because of its overall effects on polymer physical, chemical, mechanical, optical properties especially from an industrial

point of view (Sasuga *et al.,* 1991; Lee, 1999). Crosslinking in polymers has been reported to occur as a result of the presence of chemically reactive species within the polymer chain structures. These reactive species can be unsaturated bonds or associated radicals which are capable of undergoing successive chemical reactions (Kashiwabara *et al.,* 1991). As discussed by Kudoh *et al.,* (1996), crosslinking directly relates to polymer mechanical properties but seldom becomes the dominating mechanism during polymer irradiation. In the study conducted by Sasuga *et al.,* (1991), aliphatic and aromatic polymers structures were investigated to determine their mechanical properties after proton and electron ion irradiation. The study revealed that aromatic polymers are more favourably disposed to structural crosslinking compared to the aliphatic polymers and their mechanical properties is dependent on ion dose.

Table 2-1: Generic types of polymers that undergo either crosslinking or scission during swift heavy ion irradiation

Prone to crosslinking	Prone to scission
Polyacrylates	Polyisobutylene
Polyvinylchloride	Poly a-methylstyrene
Polysiloxanes	Polymethacrylates
Polyamides	Polymethacrylamides
Polystyrene	Poly (vinylidene chloride)
Polyacrylamides	Polytetrafluoroethylene (PTFE)
Polyethylene copolymers (EVA, EEA, EMA, EBA)	Polytrifluorochloroethylene
Unsaturated elastomers	Polypropylene ether
Ethylene propylene elastomers	Cellulose and derivatives
Polyacrolein	Polymethylmethacrylate (PMMA)
Polyethylene	
Poly ethylene terephthalate (PET)	Polymethyl pentene

CHAPTER 2

Table 2.1 represents the different types of polymers and their preferential reaction during swift heavy ion irradiation. From Table 2-1 above, the type of polymers that after due to irradiation cover a range of polyolefins, polyesters as well as rubbery and glassy polymers.

2.11 CHEMICAL ETCHING OF SWIFT HEAVY ION IRRADIATED POLYMER

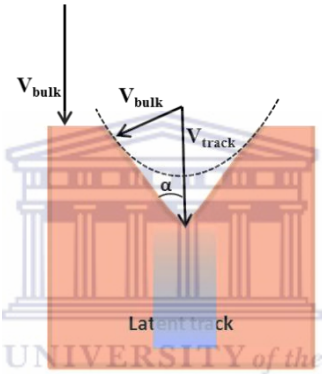

Figure 2-6: Schematic of etching processes

This use of chemical etchants is considered as a complimentary ion track technique to probe the radiation effects in polymers and is considered as the pore-shape and pore-size determining step as presented in Figure 2.6. Beside the pore activation of irradiated polymer substrates, chemical etching can serve as intermediate in the attachment of specific functionality, as anchor site for extended attachment of metals, non-metals etc during further treatment such as electroless plating where specific metals are attached on polymers due to ion exchange (Goddard *et al.*, 2007). Chemical etching involves the use of varieties of chemical solutions such as aggressive or mild chemicals including alkaline solutions (NaOH and NaOCl) or stronger oxidisers such as acidified CrO_3 to reveal latent damaged regions of irradiated polymer film as hollow channels (Shtanko *et al.*, 2000). The composition

of chemical etchants allows for a controlled pore profile (i.e. shape, size, distribution and depth) by varying the etchant conditions (Apel, 2001). These compositions include variables such as concentration, presence of surfactants for chemical etchants while temperature and time account for etching conditions (Shtanko *et al.*, 2000; Apel, 2001). The direct consequence of the etchant's, compositions and etching conditions can result in the fabrication of nano, ultra micro or micro-filters of pore profiles with symmetrical or asymmetrical configuration during chemical etching configurations (Ensinger, 2007).

Figure 2-7: Schematic of pores with various geometries that can be created by etching heavy ion tracks in polymers. (a) Cylindrical, (b) Conical, (c) Biconical (d) Funnel-shaped

The hollow filter structures i.e. pore formation in polymers (Figure 2-7) can be made in various shapes depending on the prevailing etching rate (Figure 2-6). The pore shapes is governed by two different and established etching rate phenomena; track etch (V_T) and bulk etch (V_B) rate respectively. In principle, the ion modified regions of the polymer dissolve faster along the ion track via V_T compared to the non-irradiated bulk material V_G. The V_T/V_G etching rates is called selectivity and depends on the irradiated materials as well as etching conditions. By varying the V_T and V_G ratio, specific pore shapes can be developed or transformed from one shape to another such that $V_T > V_G$ represents the transformation of conical to cylindrical shaped pores, $\frac{V_T}{V_G} \geq 2$ depicts biconical shaped pores while $\frac{V_T}{V_G}$ results in the creation of cylindrical shaped pores (Apel, 2001).

CHAPTER 2

Generally, chemical etching is often preceded by ion track surface modification techniques and the geometry of pores is often determined by the size and structure of the damaged zone around the particle path (Zaporojtchenko *et al.,* 2003; Maria Eugenia Toimil Molares, 2001). The different pore profiles i.e. shapes are shown in Figure 2-7. Other methods that have been reported for the preparation of porous polymeric membranes include; solution casting, sintering stretching and phase separation (Abedini and Nezhadmoghadam, 2010).

2.12 POLYMER GAS PERMEABILITY AND SELECTIVITY: OVERVIEW OF GAS TRANSPORT STUDIES THROUGH POLYMERIC MEMBRANES

Generally, polymeric membranes can either be glassy or rubbery polymers with characteristic dense structures (Adhikari, *et al*., 2006). The permeability and selectivity properties of polymers are two important characteristics that describe their gas transport properties and effectively the performance of polymeric membranes in gas separation (Nagel, 2000) and vary according to their types (Stannett, 1978). Permeability (*P*) is defined as the pressure and thickness-normalized gas flux through the polymer film. This depends on the product of gas molecules that dissolve in the polymer as well as their rate of movement (flux) through the polymer matrix. Selectivity defines the preferential ratio of permeation of gas mixtures such that one gas is more permeable than another. Selectivity can be attributed to an ideal or real separation factor. The separation factor of a membrane depends on the properties of the gas–polymer system, process parameters such as upstream and downstream pressure, and composition of gas stream and polymer (Matteucci *et al*., 2006). One of the experimental limitations to determine selectivity for gas mixture is the competitiveness especially in gas mixture as the presence of a gas can regulate the transport of other gases permeating through the membrane (Matteucci *et al*., 2006). This is prominent with real selectivity measurement of gases. Several studies have shown that gas transport

CHAPTER 2

across polymers (non-porous) depend on the solution-diffusion model with experimental demonstrations indicating that porosity is not a prerequisite for gas transport (mass transfer) across polymer membranes (Matteucci *et al.*, 2006). However, the formulation of the gas transport phenomenon through polymeric membranes is aimed at addressing two key areas: (1) to develop quantitative theories (i.e. solution diffusion, Knudsen diffusion, molecular sieving) based on the thermodynamics and kinetic properties associated with the polymer-gas system, and (2) to conduct experimental studies of gas transport through various polymers (Matteucci *et al.*, 2006). The structural changes in polymers can be effected in three (3) point during processing i.e. pre-synthesis, synthesis and post-synthesis changes. In pre-synthesis changes, the changes in polymer configuration involve the reaction pathways of precursors whereas the changes induced by the introduction of specific functional groups during the synthesis can be altered by the presence of aromatic backbone structures, chain packing and distribution. As for the post-synthesis, the use of multiple surface modifications such as swift heavy ion irradiation and chemical etching approaches can initiate physical, chemical (bonding), thermal (glass transition temperatures) and mechanical changes in polymers hence also affect their gas permeability characteristics (Barbari *et al.*, 1988; Robeson, 2008). However, the limitation of polymer gas permeability and separation factor (selectivity) properties is such that at high permeability, selectivity is low and vice versa (Nagel *et al.*, 2000). Primarily, polymer gas permeability properties is characterised by the upper boundaries. These upper boundaries define the optimal performance of polymeric membranes with respect to their gas selectivity and permeability (Robeson, 2008). The pioneer study in polymer membrane application for gas separation was reported for helium recovery from natural gas (Robeson *et al.*, 1994). Afterwards, separation of pairs several pairs of gases has been investigated using various polymeric membranes. These gases include; CO_2/CH_4 which has been used in natural gas enrichment and landfills, O_2/N_2 as a source of nitrogen generation or production of medical oxygen. Others include H_2/N_2 for ammonia purge gas and H_2/hydrocarbon as hydrogen recovery from petrochemical

CHAPTER 2

refining (Nagel, *et al.,* 2000; Robeson, 2008). In recent studies, additional applications have been suggested for polymeric membranes in synthesis gas adjustment (H_2/CO), solvent vapour recovery pervaporation (alcohol/water) and CO_2/flue gas (Robeson *et al.,* 1994). Interestingly, polymer surface modification techniques have been shown to enhance polymer gas permeability and selectivity properties (Robeson, 2008). One of the well-established surface modification technologies is the track-etching of polymers films which has been used to develop polymer membranes for application in biological and industrial processes (Apel, 2001). According to Nagel, *et al*., (2000), the structural orientations of polymers often determine their gas permeability and selectivity properties. This information can be employed in the study of high performance polymers such as polyethylene terephthalate (PET) and polymethylpentene (PMP) which are being considered in this study. Also, other properties of polymer that have been identified include fractional free volume and pin holes. The pin holes observed in polymers are due to structural defects by chemical reorientation under the influence of irradiation and chemical etching (Budd, 2009; Robeson *et al.,* 1994).

2.13 MECHANISMS FOR GAS SEPARATION IN POLYMERIC MEMBRANE PROCESSES

The gas separation performance of polymers is governed by their physico-chemical characteristics which have been highlighted in section 1.1; as well as compatibility or solubility limit of the penetrant into the polymer matrix and molecular size of the penetrant species (Abedini and Nezhadmoghadam, 2010). All of these factors can determine the prevailing mechanism for gas transport across the polymeric membrane. Generally, the transport processes of species across a membrane occur via pressure gradients, concentration and temperature (Ravanchi, *et al.,* 2009). The overall determination of the probable phenomenon for polymer permeability or selectivity properties is often attributed to known models (Abedini and Nezhadmoghadam, 2010). This implies that for any given membrane, an observable

CHAPTER 2

gas transport mechanism is studied and assigned to the existing models under which such interaction is most suitably described. In polymeric membranes, diffusion depends on the concentration of the diffusant. There are several mechanisms associated with gas transport in polymeric (porous and non-porous) membrane processes. These include; molecular sieving, Knudsen diffusion and solution-diffusion models and all depend on the morphological structure of polymers i.e. porous and non-porous as well as the interacting species (Abedini and Nezhadmoghadam 2010).

2.14 GAS TRANSPORT MECHANISM IN POROUS MEMBRANE

The process of gas transport across porous membranes is reportedly governed by different separation conditions due to differences in pore sizes. These types of membranes are classified based on their pore diameters i.e. microporous, mesoporous, macroporous as these pore sizes significantly affect their selectivity and permeability capacity (Ulbricht, 2006). Membranes can also exist as organic (polymeric) or inorganic membranes. However, the main challenge associated with these types of membranes is to obtain an ordered pore profile that can adequately address the trade-off between gas selectivity and permeability properties (Ulbricht, 2006).

2.14.1 KNUDSEN DIFFUSION AND POISEUILLE FLOW

Knudsen diffusion occurs in porous membrane structure and this phenomenon strongly depends on the interfacial interaction between the pore radius (r) associated with the membrane and the available free mean path (λ) of the diffusing gas molecules (Abedini and Nezhadmoghadam, 2010). The gas diffusion through the porous substrates is dominated by interaction via collision between the gas species and pore walls while collision between gases are less predominant, thus gas

separation is accomplished due to difference in the velocity of the gases. This mechanism depends on the ratio of the square root of the corresponding molecular weights of the separated gases especially when there is less collision of gases (Checchetto *et al*., 2004). The free mean path is written mathematically in equation 9. In practice, the pore diameter is relatively smaller than the diffusing gas species (mean free path) thus the separation of two gases by Knudsen diffusion are often considered to be weight dependent. In other words, low separation factors are generally obtained for membranes with the Knudsen diffusion mechanism (Ravanchi *et al.*, 2009).

$$\lambda = \frac{3\eta(\pi RT)^{0.5}}{2P(2M)}$$

Equation 2-5: Calculating gas flux across porous membrane by Knudsen diffusion mechanism

η = gas viscosity

R is the universal gas constant

T represents temperature

M the molecular weight

P represents the pressure.

The Poiseuille phenomenon becomes dominant when the ratio of the pore radius and free mean path of gas molecules is far less than unity i.e. λ/r <<< 1. This is mathematically expressed in equation 13 (Checchetto *et al*., 2004).

$$G_{vis} = \frac{r_2 (P_1 - P_2)}{16LuRT}$$

Equation 2-6: Determination of gas flux in porous membrane using Poiseuille flow

r is the pore radius

P_1 represents the partial pressure of gas on the retentate side and P_2 is the partial pressure on the permeate side.

L is the pore length

u is the gas viscosity

R represents the universal gas constant.

In the case where the ratio of free mean path (λ) of gas molecules and membrane pore radius (r) i.e. (λ / r) is considerably less than unity, gas flux in the Knudsen or molecular sieve is mathematically expressed in equation 14 (Checchetto *et al*., 2004).

$$G_{mol} = \frac{8r (P_1 - P_2)}{3L(2\pi MRT)^{0.5}}$$

Equation 2-7: Calculating gas flux across porous membrane when ratio of free mean path (λ) and membrane pore radius (r) is less than 1

2.14.2 MOLECULAR SIEVING

Porous membranes are generally referred to as molecular sieve membranes and are known for their as an excellent membrane material for the separation of non-adsorbable or weakly adsorbable from strongly adsorbable gases. The separation

mechanism occurs via competitiveness between membrane pore diameter and the average pore size of the interacting gas. It therefore implies that the transport rate of gases through these types of membranes depends upon the effective size of the gas molecules rather than the adsorption phenomenon (Abedini and Nezhadmoghadam, 2010).

2.15 GAS TRANSPORT MECHANISM IN NON-POROUS MEMBRANES

Gas transport across non-porous or dense membranes occurs via different mechanisms such as solution-diffusion etc. The non-porous membranes are known for their high gas selectivity but low permeability (Abedini and Nezhadmoghadam, 2010). Nagel *et al*., (2000) studied the permeability and permselectivity properties of glassy and rubbery polymers using experimental results and modelling techniques. The study indicated chain flexibility, inter and intra-atomic spacing and bulky groups determine the packing density and thus the permeability properties of the respective polymers. Glassy polymers were reported to exhibit low packing density and high chain stiffness associated with high permeability while rubbery polymer have low chain stiffness due to high packing density, thus higher permeability.

CHAPTER 2

2.15.1 SOLUTION-DIFFUSION

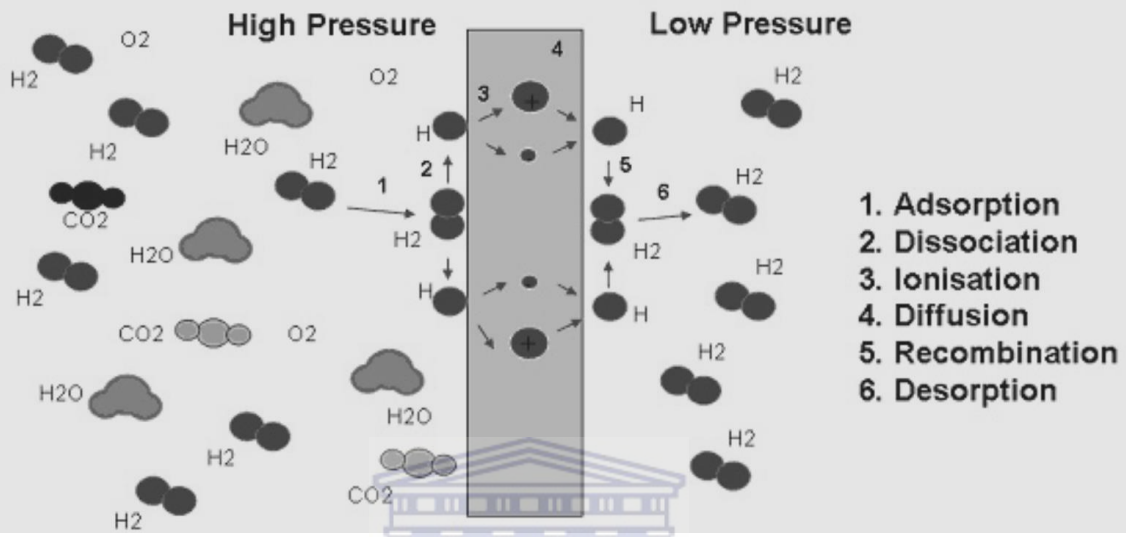

Figure 2-8: Solution-diffusion mechanism of H_2 through a Pd-based layer

The solution-diffusion concept (Figure 2-8) is a type of gas transport mechanism for non-porous polymeric or non-polymeric membranes. Unlike porous membranes, non-porous polymeric films do exhibit gas permeability properties without the presence of microscopic pore or capillaries in the polymeric film which are considered as a pre-requisite prior to polymer gas permeability application (Matteucci *et al.*, 2006). The separation mechanism in solution-diffusion is determined by the difference in the respective amount of each component gas dissolution and their corresponding diffusion through the membrane (Wijmans and Baker, 1995). One of the concepts of this phenomenon has been related to chemical affinity of gas species with polymeric structures (Matteucci *et al.*, 2006).

CHAPTER 2

2.16 POLYMER STRUCTURES AND THEIR GAS PERMEABILITY PROPERTIES

Membranes, especially polymeric based, have enjoyed global interest due to their ability to show unique gas separation properties. Depending on their backbone structure and substituted side groups (Raharjo *et al.*, 2005), polymers tends to show specific physico-chemical attributes such as segmental chain motion, allowing the creation of free volumes to promote their gas separation characteristics (Raharjo *et al.*, 2005). Other surface properties that have been reported to affect gas permeation properties of the polymer include fractional free volume (FFV). In section 1.16.1, the gas permeability properties of glassy polymers will be discussed

2.16.1 GLASSY POLYMERS AND THEIR GAS PERMEABILITY PROPERTIES

Glassy polymers are mechanically strong, rigid, glass-like polymers and are identified by their ability to operate below their glass transition temperatures (T_g). These types of polymers exhibit low chain intrasegmental mobility as well as long relaxation time. Glassy polymers demonstrate low gas permeability but high selectivity. Examples of glassy polymers include; polyacetylenes, poly [1-(trimethylsilyl)-1-propyne] (PTMSP), polyimides, polyamides, polyarylates, polycarbonates, polyethylene terephthalate (PET) (Barbari *et al*., 1988; Bastani *et al*., 2013).

2.16.2 RUBBERY POLYMERS

Rubbery polymers are soft, flexible with characteristically high intrasegmental chain mobility thus high gas permeability but low selectivity. Rubbery polymers are known to operate above their glass transition temperatures (T_g) as well as having short relaxation times. Despite their high gas permeability, rubbery polymers are

not viable option for industrial application in gas separation due to their inherent poor mechanical strength (Bastani *et al*., 2013). Although polymers have been reported to show impressive gas permeability properties, the major hurdle has been to apply these polymers in commercial separation at industrial scale. For instance, poor chemical resistance and physical aging have been identified in the case of poly (1-trimethylsilyl-1-propyne) (PTMP) which is the best known gas permeable polymer and Poly [1-phenyl-2-[p-(trimethylsilyl) phenyl] acetylene] (PTMSDPA) (Raharjo *et al.*, 2005).

2.17 GAP ANALYSIS AND CHAPTER SUMMARY

Understanding the intrinsic polymer properties and the ability to improve on polymer gas permeability and selectivity has become one of the focus points of polymer track-etching research. The gas selectivity and permeability properties of a polymer are dependent on pore created in polymer using swift heavy ion irradiation and chemical etching i.e. track-etching of polymers. The available knowledge on track-etching has been mainly focused on *'direct'* swift heavy ion irradiation of polymer which results in physical deformation with through pores. Although *'direct'* swift heavy ion irradiation of PET polymer has been extensively investigated, there were no proven similar studies on PMP polymer film. As far as could be ascertained for PMP polymer, the available literature studies have not extended to track-etched studies of PMP polymer. There is inadequate information on the track-etching modification of PMP will be one of the key focal point of this study. Consequently, this study will provide specific knowledge towards understanding the changes induced in PMP polymer film during swift heavy ion irradiation and chemical etching and how these changes affect the physical, chemical, thermal and gas permeability and selectivity properties of the track-etched PMP polymer film. The research approaches that will be systematically followed in this study will involve the use of *'shielded'* materials on the PET and PMP polymer film prior to swift heavy ion irradiation of the *'shielded'* PET and

CHAPTER 2

PMP polymer to the preparation of asymmetrical membrane structure. The chemical etching after swift heavy ion irradiation of the *'shielded'* PET and PMP is to reduce the thickness of PET and PMP polymer film and ultimately create asymmetrical membrane structure with a single sided porous surface on a dense layer.

CHAPTER 3

CHAPTER THREE

3 MATERIALS, EXPERIMENTAL PROTOCOL AND ANALYTICAL TECHNIQUES

3.1 INTRODUCTION

In this chapter, detailed experimental procedures of ion irradiation and chemical etching treatment of as-received (commercial) polyethylene terephthalate (ASPET) and as-received (commercial) polymethyl pentene (ASPMP) are presented and described. This chapter also include the experimental descriptions as well as the parameters investigated during ion irradiation and chemical etching of polymer films. Also, the materials specifications for polymer films and chemical reagents used for this study are presented. This chapter is concluded with brief explanation of the various characterization techniques and the sample preparation procedures used for the ion irradiated and chemically etched polymer films.

3.2 MATERIALS

The source and materials specifications of polymer films investigated in this study are presented in Table 3-1 and information on the various chemical reagents used are highlighted in Table 3-2.

Table 3-1: Polymer films

Polymer	Thickness (µm)	Supplier
Polymethyl pentene (ASPMP)	50	Goodfellow, United Kingdom
Polyethylene terephthalate (ASPET)	20	Joint Institute for Nuclear Research (JINR), Dubna

*AS= as-received

CHAPTER 3

In Table 3-1, the specifications and other relevant information are stated. However, for the sake of clarification, the starting materials used in this study were commercially sourced. Polymethyl pentene films were purchased from Goodfellow United Kingdom While polyethylene terephthalate polymer films were supplied by Joint Institute for Nuclear Research (JINR), Dubna, Russia. All polymer films were thoroughly cleaned, dried in air and used as received without further treatment. The chemical reagents used for the chemical etching experiments of polymer film (as-received and swift heavy ion irradiated) presented in Table 3-2. All reagents were obtained from Sigma Aldrich, South Africa and used as purchased.

Table 3-2: Chemical reagents

Name of Chemical	Source	Purity
Sodium hydroxide (NaOH)	Sigma Aldrich, South Africa	99.0 %
Sulphuric acid (H_2SO_4)	Sigma Aldrich, South Africa	98.0 %
Chromium (V1) oxide (CrO_3)	Sigma Aldrich, South Africa	99.0 %

3.3 EXPERIMENTAL PROTOCOLS

In this section, the experimental protocols are presented including the schematic summary of the experiments as shown in Figure 3-1. The stages of the experimental protocols are divided into 3 (three) parts i.e. control experiments, protocols for ion irradiation and for chemical etching. The first stage of the experimental protocols represents the control experiment for ASPET and ASPMP polymer films. The control experiment is further divided into 3 (three) parts which are direct

instrumental analysis of ASPET and ASPMP, chemical etching and the third part of the control experiment considered heavy ion irradiation of ASPET and ASPMP.

In the second stage of the experiments, the detailed descriptions of ion irradiation experiments and applied conditions are presented in section 3.3.1. The third stage of the experiments details the chemical etching experiments including the conditions of etching are explained in section 3.3.2. Also, the choice of the irradiation and chemical etching conditions are explained. The final stage of the experiments details the use of analytical techniques to investigate specific properties of the treated polymer films. The summary of the experimental approach, various parameters investigated during ion irradiation and chemical etching and characterizations techniques are presented in Figure 3-1.

CHAPTER 3

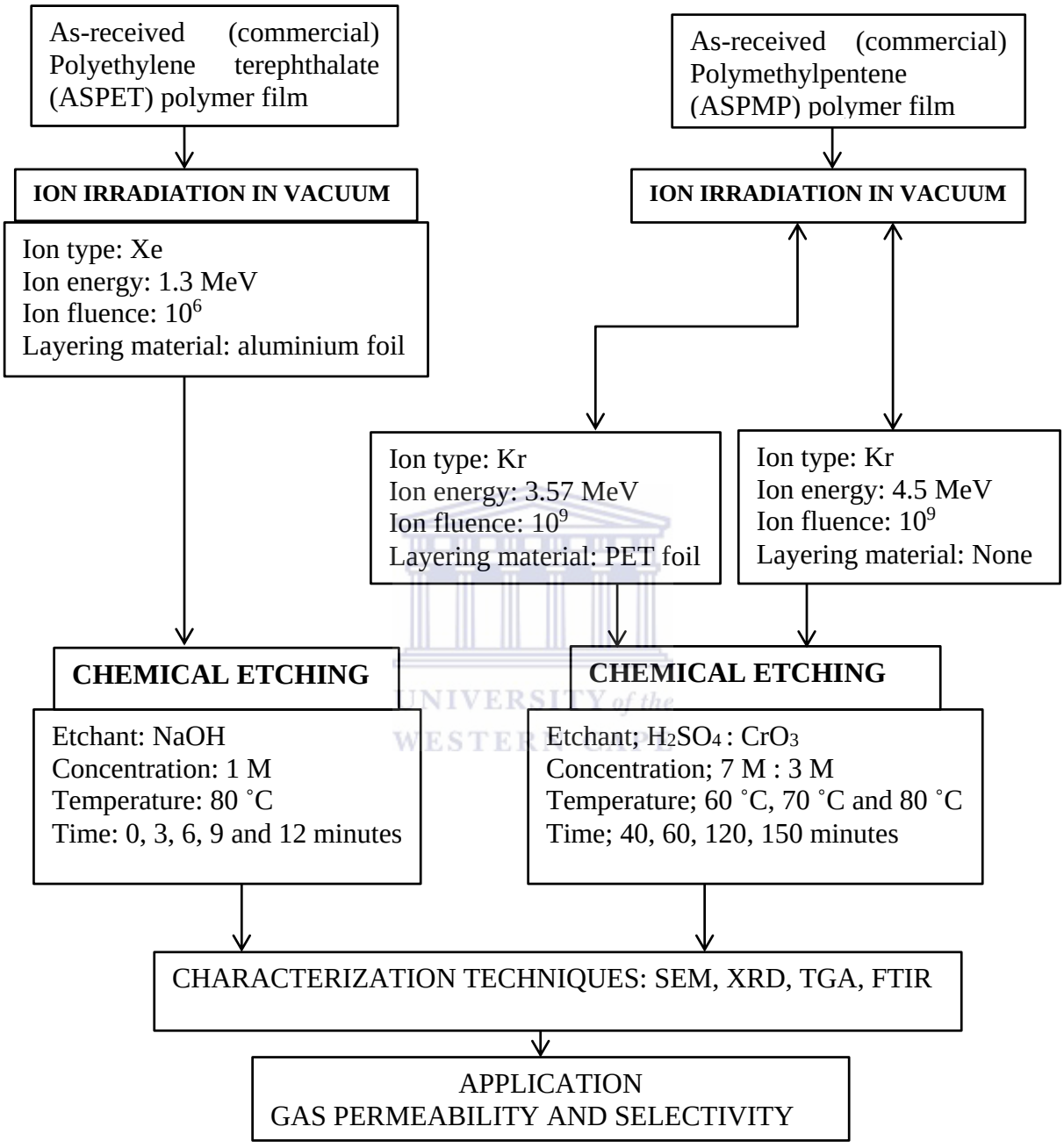

Figure 3-1: Schematic flow of experiments

The schematic summary of the research approach followed in this study including some details of the experimental conditions is presented in Figure 3-1. Commercial polymer films of polyethylene terephthalate and polymethyl pentene herein referred to as as-received (commercial) PET and PMP respectively are the starting materials.

CHAPTER 3

In this study, three (3) control experiments were performed on each of the polymer films (ASPET and ASPMP) in order to understand the effects of individual conditions which are ion irradiation and chemical etching. The first control experiment was direct characterization of ASPET and ASPMP which served as baseline results. In the second control experiment, ASPET and ASPMP polymer films were chemically etched without swift heavy ion irradiation and then characterized while the third control experiment was irradiation of ASPET and ASPMP polymer films using swift heavy ions of Xe and Kr respectively without chemical etching. All the three (3) control experiments were characterized using SEM, TGA, XRD, FTIR analytical techniques and etching kinetics study of etched polymer films where applicable especially in the second control experiment. The experimental description of the ion irradiation procedures performed on ASPET and ASPMP polymer films are presented in the next section.

3.3.1 SWIFT HEAVY ION IRRADIATION

One of the methods used to alter the physico-chemical properties of polymer films is their exposure to energetic ions. This approach has been used to treat polymers and create specific surface or bulk properties on the polymer films (Apel, 1996). In this study, two different swift heavy ions were used to irradiate ASPET and ASPMP polymer films. The swift heavy ions are xenon and krypton. The use of two different ion types and ion energies (Figure 3-1) to irradiate the polymer films was mainly due to the availability of ion types and ion energies at the U400 accelerator at Joint Institute for Nuclear Research (JINR), Dubna. However, in selecting these ion irradiation conditions i.e. ion type and energies, Stopping and Range of Ions in Matter (SRIM) software simulation (Zeigler et al., 2010) was used as theoretical model to understand the probable experimental results for both *'shielded'* and *'direct'* irradiated ASPET and ASPMP polymer films. Also, SRIM was used to calculate the effective ion stopping power of the polymer film as well as the ion energy loss within the polymer and this information was used to predict the experimental outcomes during ion irradiation of the polymer films. The concept of

CHAPTER 3

using *'shielded'* and *'direct'* ion irradiation of polymer films was to develop an asymmetrical polymer membrane with a porous surface on a dense layer which will be described in detail in this section. Also, the different irradiation conditions used for ASPET and ASPMP are presented in Table 3-3.

Table 3-3: Sample codes, ion irradiation and chemical etching experimental descriptions for ASPET and ASPMP polymer films

Sample code	Polymer Type	Irradiation condition	Etchant	Etching condition
OA1a	ASPET	Unirradiated	Unetched	None
OA1b	ASPET	Unirradiated	NaOH	Concentration: 1 M Temperature: 80 ˚C Time: 135 minutes
OA1c	ASPET	*Layered* with Al foil Ion type: Xe Ion energy: 1.3 MeV Ion fluence: 10^6	Unetched	None
OA2a	ASPET	Same ion irradiation condition as sample **OA1c**	NaOH	Concentration: 1 M Temperature: 80 ˚C Time: 3 minutes
OA2b	ASPET	Same ion irradiation condition as sample **OA1c**	NaOH	Concentration: 1 M Temperature: 80 ˚C Time: 6 minutes
OA2c	ASPET	Same ion irradiation condition as sample **OA1c**	NaOH	Concentration: 1 M Temperature: 80 ˚C Time: 9 minutes
OA2d	ASPET	Same ion irradiation condition as sample **OA1c**	NaOH	Concentration: 1 M Temperature: 80 ˚C Time: 12 minutes
OA3a	PMP	Unirradiated	Unetched	Unetched
OA3b	PMP	Unirradiated	H_2SO_4/CrO_3	Concentration: 7 M:3 M Temperature: 80 ˚C

				Time:135 minutes
OA3c	ASPMP	*Layered* with PET foil Ion: Kr Ion energy: 3.57 MeV Ion fluence: 10^9	Unetched	Unetched
OA3d	As-received PMP	*Directly* irradiated (without PET foil layer) Ion: Kr Ion energy: 4.5 MeV Ion fluence: 10^9	Unetched	Unetched
OA4a	ASPMP	*Layered* with PET foil Ion: Kr Ion energy: 3.57 MeV Ion fluence: 10^9	H_2SO_4/CrO_3	Concentration: 7 M:3 M Temperature: 60 ˚C Time: 40 minutes
OA4b	ASPMP	Same as sample OA4a	H_2SO_4/CrO_3	Concentration: 7 M:3 M Temperature: 60 ˚C Time: 60 minutes
OA4c	ASPMP	Same as sample OA4a	H_2SO_4/CrO_3	Concentration: 7 M:3 M Temperature: 60 ˚C Time: 120 minutes
OA4d	ASPMP	Same as sample OA4a	H_2SO_4/CrO_3	Concentration: 7 M:3 M Temperature: 60 ˚C Time: 150 minutes
OA5a	ASPMP	*Layered* with PET foil Ion: Kr Ion energy 3.57 MeV Ion fluence: 10^9	H_2SO_4/CrO_3	Concentration: 7 M:3 M Temperature: 70 ˚C Time: 40 minutes
OA5b	ASPMP	Same as sample OA5a	H_2SO_4/CrO_3	Concentration: 7 M:3 M Temperature: 70 ˚C Time: 60 minutes
OA5c	ASPMP	Same as sample OA5a	H_2SO_4/CrO_3	Concentration: 7 M:3 M Temperature: 70 ˚C Time: 120 minutes
OA5d	ASPMP	Same as sample OA5a	H_2SO_4/CrO_3	Concentration: 7 M:3 M Temperature: 70 ˚C

				Time: 150 minutes
OA6a	ASPMP	*Layered* with PET foil Ion: Kr Ion energy 3.57 MeV Ion fluence: 10^9	H_2SO_4/CrO_3	Concentration: 7 M:3 M Temperature: 80 ˚C Time: 40 minutes
OA6b	ASPMP	Same as sample OA6a	H_2SO_4/CrO_3	Concentration: 7 M:3 M Temperature: 80 ˚C Time: 60 minutes
OA6c	ASPMP	Same as sample OA6a	H_2SO_4/CrO_3	Concentration: 7 M:3 M Temperature: 80 ˚C Time: 120 minutes
OA6d	ASPMP	Same as sample OA6a	H_2SO_4/CrO_3	Concentration: 7 M:3 M Temperature: 80 ˚C Time: 150 minutes
OA7a	ASPMP	*Directly* irradiated (without PET foil layer) Ion: Kr Ion energy: 4.5 MeV Ion fluence: 10^9	H_2SO_4/CrO_3	Concentration: 7 M:3 M Temperature: 60 ˚C Time: 40 minutes
OA7b	ASPMP	Same as sample OA7a	H_2SO_4/CrO_3	Concentration: 7 M:3 M Temperature: 60 ˚C Time: 60 minutes
OA7c	ASPMP	Same as sample OA7a	H_2SO_4/CrO_3	Concentration: 7 M:3 M Temperature: 60 ˚C Time: 120 minutes
OA7d	ASPMP	Same as sample OA7a	H_2SO_4/CrO_3	Concentration: 7 M:3 M Temperature: 60 ˚C Time: 150 minutes
OA8a	ASPMP	*Directly* irradiated (without PET foil layer) Ion: Kr Ion energy: 4.5 MeV	H_2SO_4/CrO_3	Concentration: 7 M:3 M Temperature: 70 ˚C Time: 40 minutes

CHAPTER 3

		Ion fluence: 10^9		
OA8b	ASPMP	Same as sample OA8a	H_2SO_4/CrO_3	Concentration: 7 M:3 M Temperature: 70 ˚C Time: 60 minutes
OA8c	ASPMP	Same as sample OA8a	H_2SO_4/CrO_3	Concentration: 7 M:3 M Temperature: 70 ˚C Time: 120 minutes
OA8d	ASPMP	Same as sample OA8a	H_2SO_4/CrO_3	Concentration: 7 M:3 M Temperature: 70 ˚C Time: 150 minutes
OA9a	ASPMP	*Directly* irradiated (without PET foil layer) Ion: Kr Ion energy: 4.5 MeV Ion fluence: 10^9	H_2SO_4/CrO_3	Concentration: 7 M:3 M Temperature: 80 ˚C Time: 40 minutes
OA9b	ASPMP	Same as sample OA9a	H_2SO_4/CrO_3	Concentration: 7 M:3 M Temperature: 80 ˚C Time: 60 minutes
OA9c	ASPMP	Same as sample OA9a	H_2SO_4/CrO_3	Concentration: 7 M:3 M Temperature: 80 ˚C Time: 120 minutes
OA9d	ASPMP	Same as sample OA9a	H_2SO_4/CrO_3	Concentration: 7 M:3 M Temperature: 80 ˚C Time: 150 minutes

In Table 3-3, the ion irradiation and chemical etching conditions for ASPET and ASPMP polymer films are outlined. The ion irradiation conditions include ion types, ion incident energies, ion fluence and more importantly the use of shielded materials. The use of *'shielded'* materials is crucial during irradiation of polymer film as it helps to control ion penetration depth into the polymer due to ion energy loss within the polymer matrix. Also, by using *'shielded'* materials to cover the surface of the polymer films prior to heavy ion irradiation, the irradiated polymer

film can be tailored into an asymmetrical structure with a porous surface on a dense layer of polymer film after chemical etching. The procedures on the use of *'shielded'* material on polymer film during heavy ion irradaition experiment is explained as follows; an aluminum film (11 µm) was attached to the surface of ASPET polymer film surface using adhesive tapes on the edges of polymer films samples. Thereafter the shielded polymer film was then irradiated through the attached aluminum foil. This irradiation procedure is referred to as *'shielded'* due to the presence of aluminum foil material for ASPET (sample OA1c) in Table 3-3. After irradiation, the *'shielded'* material was detached from the irradiated polymer film. The irradiated polymer film samples were etched under various conditions (Table 3-3) and characterized. The same *'shielded'* irradiation procedure was performed for ASPMP polymer film (sample OA3c) as shown in Table 3-3. However, in the case of ASPMP, the *'shield'* material used was 12 µm PET foil. Also, Table 3.3 shows that a single ion source (Xe ion) and energy was used for ASPET polymer film (i.e. 1.3 MeV/nucleon). As for the ASPMP polymer film, Kr ion was selected but two different ion energies of the Kr ions were used. The difference in choice of ions used for irradiation ASPET and ASPMP was mainly due to availability of these ions at the time of the irradiation experiment at JINR. However, SRIM software was used to theoretically predict the energy loss, and ion penetration depth into the polymer film. The Kr ion energies used for the irradiation of ASPMP were 3.57 MeV/nucleon (sample OA3c) and 4.5 MeV/nucleon (sample OA3d). For instance, Table 3-3 showed that sample OA3c ion irradiation was performed through a *'shield'* of PET foil (12 µm thick) while sample OA3d ion irradiation was performed without the use of a shielded material i.e. *'direct'* irradiation. In addition, the *'direct'* ion irradiation experiment was performed for sample OA3d which in this case did not involve the use of any shielded materials before ion irradiation. Although the aim of this study was to create an asymmetrical membrane structure using a *'shield'* film approach, the limited prior research on ion irradiation study of PMP polymer film was a motivation to perform *'direct'* swift heavy ion irradiation on sample OA3d. The use of swift heavy ion to irradiate ASPMP polymer film has not been reported in literature except for the

polypropylene (PP) polymer film which is a polyolefin and also belongs to the same class of polymer as PMP (Apel, 1996). Also, the experimental approach used on sample OA3d was to determine if it would result in the development of symmeterical membrane structure due to complete ions penetration through the ASPMP polymer film. This is mainly because ASPET and ASPMP belong to different classes of polymers i.e. polyesters and polyolefins respectively and are known to have distinct structural configurations. Traditionally, chemical etchants are used to reveal the latent damaged regions of ion irradiated polymer films. In the next section (3.3.2), the chemical etching experiments will be described.

3.3.2 CHEMICAL ETCHING

This section describes the chemical etching experiments following from the control experiments (i.e. ASPET and ASPMP) and the swift heavy ion irradiated polymer films (Table 3-3). The details of the chemical etching experiment conditions have been presented in Figure 3-1 and Table 3-3. In addition, each of the chemical etching conditions for ASPET, ASPMP and ion irradiated polymer films will be described in the subsequent section (3.3.3).

3.3.3 CHEMICAL ETCHING CONDITIONS FOR ASPET, ASPMP AND ION IRRADIATED PET AND PMP POLYMER FILM

The chemical etching conditions investigated during the treatment of ASPET, ASPMP and ion irradiated PET and PMP polymer films will be described in this section. Table 3-3 shows that there was only one parameter that was varied at a time during the chemical etching experiments of samples ASPET and ion irradiated PET polymer film and samples have been assigned the following codes; OA2a, OA2b, OA2c and OA2d for 3, 6, 9 and 12 minutes etching time respectively (Table 3-3). The fixed parameters include etching solution, etchant concentrations and etching temperature. The chemical etching of ASPET polymer film served as control experiment which was performed at various times up to a maximum of 140 minutes.

CHAPTER 3

Sodium hydroxide (NaOH) 1 M concentration was used as the chemical etching solution and the etching temperature was kept at 80 ˚C for etched PET polymer film samples. The weight loss of ASPET sample was monitored at intervals as a function of etching time. However, the weight loss of samples OA2a, OA2b, OA2c and OA2d were not monitored because their degradation was fast during chemical etching experiment.

Similarly, the experimental summary of chemical etching conditions applied to samples ASPMP and ion irradiated PMP have been described in Table 3-3. In brief, samples OA3b, OA3c and OA3d depict the unirradiated but directly etched PMP, *'shield'* (3.57 MeV/nucleon) Kr ion irradiated PMP and *'directly'* (4.5 MeV/nucleon) irradiated PMP respectively. The procedure for *'shielded'* irradiated of PMP has been described in section 3.3.1. Also, Table 3-3 highlights the chemical etching solution for the treatment of these polymer film samples i.e. ASPMP, OA3a, OA3b, OA3c and OA3d. The swift heavy ion irradiated (i.e. *layered* and *directly*) PMP polymer films were etched in acidified chromium oxide solution: (7 M H_2SO_4 + 3 M CrO_3). The temperature of etching was varied between 60 ˚C to 80 ˚C and the duration of etching was from 40 minutes to 150 minutes (Table 3-3).

It is important to explain that the use of swift heavy ion to modify polymethyl pentene (PMP) polymer film has not been reported in literature. However, in the polyolefin class of polymers, polypropylene (PP) has reportedly been investigated by swift heavy ion irradiation and chemical etching hence the motivation for choosing these etching conditions described in Table 3-3 (Apel, 1996). The choice of etching temperature was determined from the understanding that polymers undergo structural disorderliness at regions above their glass transition temperature (T_g). All polymer film samples were characterized by SEM, TGA, XRD, FTIR and gas permeability and selectivity analysis. In the next section (3.3.4), the preparation procedures for the different chemical etching solutions are presented.

CHAPTER 3

3.3.4 PREPARATION OF CHEMICAL ETCHING SOLUTIONS

This section describes the preparation of the chemical etching solutions i.e. sodium hydroxide (NaOH) solution was used as chemical etchant for ASPET and ion irradiated PET polymer and acidified chromium trioxide (H_2SO_4 + CrO_3) used to etched ASPMP and ion irradiated PMP polymer films.

3.3.4.1 PREPARATION OF 1 M NaOH SOLUTION

4.000 g of NaOH (Sigma Aldrich) was weighed out on a balance. The weighed NaOH was transferred into a 100 mL volumetric flask, dissolved with deionised water and made up to the mark to give 1 M concentration of NaOH. A fresh solution of NaOH was prepared for each etching experiment.

3.3.4.2 PREPARATION OF 7 M H_2SO_4 +3 M CrO_3 SOLUTION

250.000 g of CrO_3 (Sigma Aldrich) was weighed out and dissolved in 1 litre volumetric flask of deionised water to make a 3 M CrO_3 concentration. 380 mL of concentrated sulphuric acid (Sigma Aldrich) was gently streamed into the initially dissolved chromium solution; deionised water was added into the mixture of acidified CrO_3 to make up to mark. The prepared solution gives 7 M sulphuric acid and 3 M CrO_3 (i.e. 7 M H_2SO_4 + 3 M CrO_3).

3.4 CHARACTERIZATION AND ANALYTICAL TECHNIQUES

In order to determine the effects of various polymer treatment conditions i.e. ion irradiation and chemical etching on ASPET and ASPMP polymer films, the use of appropriate analytical techniques is critical to understanding the specific properties of the polymer samples being investigated. Also, these analytical techniques assist in measuring the response factor from the various experiments that have been

performed. This section gives the procedures for sample preparation for the various characterization techniques. It also includes the instrumental set-up conditions.

3.4.1 SCANNING ELECTRON MICROSCOPY TECHNIQUE

Scanning electron microscope (SEM) analysis is one of the techniques used to probe the morphological features of samples. In scanning electron microscopy analysis, fast moving electrons are ejected from an electron gun, bombarded on samples and images are obtained due to the transmitted electrons. The topography of samples can be revealed using scanning electron microscopy at different magnifications to understand details of the sample surface morphology. The SEM analysis of samples was performed using the Nova NanoSEM model.

Sample preparation for scanning electron microscopy

All polymer film samples i.e. ASPET and ASPMP, and modified samples were cut into smaller pieces and mounted on aluminium stubs with the aid of double-sided carbon conductive adhesive tape. The samples were gold-coated with an Edward sputter coater and their surface and cross-sectional morphologies were characterized. The SEM instrumental conditions are presented in Table 3-4.

Table 3-4: SEM instrument set-up condition

Parameter	Condition
Working distance	(6-13 mm)
Accelerating voltage	(5-20 KeV)
Emission current	(75-80 A)

3.4.2 X-RAY DIFFRACTION TECHNIQUE

The x-ray diffraction (XRD) analytical technique is used to investigate the crystalline properties of a material. Crystalline material with atomic spacing is almost similar in magnitude as x-ray wavelengths hence capable of diffracting x-rays. The qualitative identification of crystalline materials is made from a measurement of the angles of diffraction.

Sample preparation for x-ray diffraction

For sample preparation in XRD analysis, the polymer (PET and PMP) samples were mounted on aluminium stubs by adhesive tape and the surface flattened to promote maximum x-ray exposure. The collected XRD spectra collected were matched with the JCPDS (joint committee of powder diffraction standards) file data base software. Table 3-5 presents the XRD instrumental conditions.

Table 3-5: XRD (Bruker AXS D8) instrument set-up conditions

Parameter	Condition
Detector	Sodium Iodide
Monochromator	Graphite
Generator current (mA)	40
Electron Intensity (KeV)	40
X-ray source	Cu-Kα
Radiation wavelength (λ)	1.542 Å
α1/α2	0.497
Scan range (2θ °)	5-100
Scan rate	0.05 /min

3.4.3 FOURIER TRANSFORMED INFRA-RED /ATTENUATED TOTAL REFLECTION

As in almost all spectroscopic methods, FTIR/ATR consists of a radiation source, monochromator or wavelength selection device, sample holder and a detector. The spectra analysis by Fourier transformed infra-red/attenuated total reflection (FTIR/ATR) is an infrared technique that can be used to investigate quantized molecular resonances that absorb electromagnetic energy selectively from a broadband infrared source. This analytical technique transmits infrared energy through the sample and the spectra is analysed to understand the existing bonds and associated functional groups present in a material. FTIR/ATR is a non-destructive technique. The FTIR/ATR model used was Perkin Elmer 100 series.

Sample preparation for Fourier transformed Infra-red spectroscopy

The polymer film samples were cut into small pieces and positioned in the diamond disc plate for analysis in the attenuated total reflection (ATR) mode. The spectra analysis of the sample is performed by applying pressure using the hand holder. Table 3-6 presents the instrumental condition for FTIR/ATR analysis.

Table 3-6: FTIR/ATR instrument set-up conditions

Parameter	Condition
Wave number range (cm^{-1})	4000- 380
Scan rate ()	4
Force gauge	150

3.4.4 THERMOGRAVIMETRY ANALYSIS ANALYTICAL TECHNIQUE

Thermogravimetric analysis (TGA) was used to measure the mass of a sample as a function of temperature. TGA was used to determine the thermal profile such as stability, degradation, melting point and glass transition temperature in the case of polymers. TGA analysis can be used to quantify the composition of samples, weight loss in relation to the applied temperature gradient. The model used for thermal analysis of samples was Perkin Elmer TGA 4000.

Sample preparation for thermogravimetry

The sample preparation for TGA analysis required at least 1 mg of sample placed in a platinum heating pan. The heating rate was adjusted to 5 °C/min with an initial temperature of 20 °C and the maximum temperature of 600 °C for PMP using a ramping rate of 10 °C/min from 30 °C to 600 °C for PET samples. Table 3-7 presents the instrumental condition for the TGA analysis.

Table 3-7: TGA instrument set-up conditions

Parameter	Conditions
Temperature range	PET: 10 °C/ minutes PMP: 5 °C/ minutes
Temperature range	PET polymer film: 30 °C to 600 °C PMP polymer film: 20 °C to 600 °C
Sweep gas	N_2
Gas flow	20 mL/min
Gas pressure	3.8 bar

3.4.5 GAS PERMEABILITY MEASUREMENT REACTOR

Gas permeability and selectivity studies were performed on the PET and PMP polymer films. The samples tested for their gas permeability and selectivity properties include the ASPET (sample OA1a), *'shielded'* swift heavy ion irradiated unetched PET polymer film (sample OA1c) and the *'shielded'* swift heavy ion irradiated etched PET (samples OA2a, OA2b, OA2c and OA2d) polymer films. The gas permeability of the PET polymer films was performed using the set-up in Figure 3-2.

$$P = C/S$$

Equation 3-1: Henry's law of solubility

From equation 3-1, the dissolution of a gas is based Henry's law of solubility where the concentration of gas in membrane is directly proportional to the applied gas pressure.

P= permeability coefficient
C= concentration
S= solubility coefficient

Under steady state condition i.e. constant diffusant concentration, assumed diffusion and solubility coefficient are independent of concentration; gas permeation flux can be determined by this expression.

CHAPTER 3

$$J = D.\ S.\ \frac{P_f - P_p}{l} = P\frac{\Delta p}{l}$$

Equation 3-2: Calculating gas flux across membrane

P_f and P_p = upstream and downstream pressures imposed on membrane

$\Delta p / l$ = applied pressure gradient across the membrane thickness (l)

P = gas permeability

But where surface concentration of membrane is unknown, the rate of diffusant is expressed in terms of vapour pressures ρ_1 and ρ_2 hence gas permeation flux can be calculated using

$$J = P\frac{(\rho 1 - \rho 2)}{l}$$

Equation 3-3: Calculating gas flux of membrane under different vapour pressures

P= permeability coefficient

But if *D* is constant, the relationship between *D, P* and *S* can be written thus:

$$P = D.S$$

Equation 3-4: Calculating permeability using diffusion and solubility coefficient

If the rate of diffusion is empirically determined, solubility coefficient for the diffusant is known then permeation and diffusion coefficients can be calculated from equations 3-3 and 3-4, Permeability of single gases was calculated as:

CHAPTER 3

$$Q = \frac{c'V}{Sp\ (c_i - c')}$$

Equation 3-5: Calculating the permeability of single gases

V is gas is carrier flow rate, (m^3/s)

S is membrane area, (m^2)

p is atmospheric pressure, (Pa)

c_i is penetrant concentration in upstream, (vol. %)

$c^{/}$ is penetrant concentration in downstream, (vol. %)

Permeability coefficient P is equal:

$$Q = \frac{c'V\,d}{Sp\ (c_i - c')}$$

Equation 3-6: Calculating permeability coefficient

d is dense layer thickness.

The ideal selectivity of single gases was defined as:

$$\alpha_{ij} = \frac{Q_i}{Q_j} = \frac{P_i}{P_j}$$

Equation 3-7: Calculating ideal selectivity of gases

Q_i and Q_j, P_i and P_j represent the permeability and permeability coefficients of i and j gas, respectively. The schematic of the gas permeability reactor is presented Figure 3-2.

CHAPTER 3

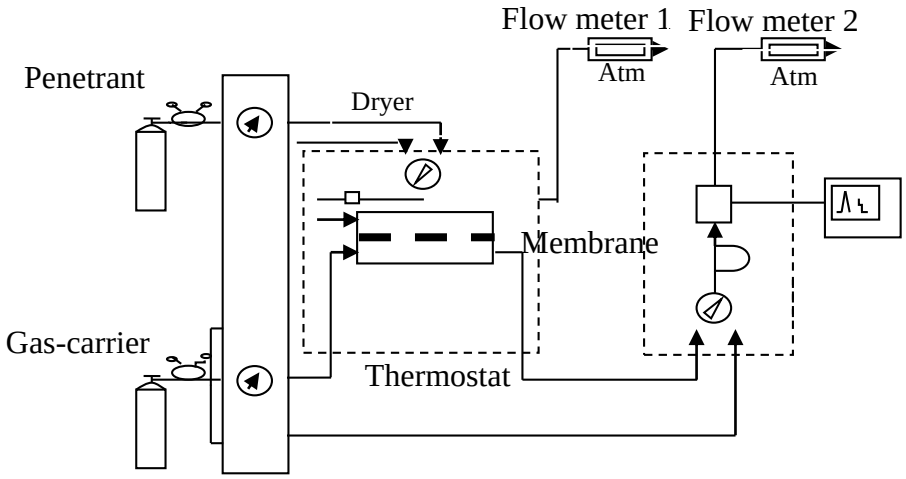

Figure 3-2: The block-schematic of gas permeability set-up

The operational procedure of the gas permeability set-up (Figure 3-2) is briefly described. To determine the permeability of gases and lower hydrocarbons, gas permeation reactor developed at TIPS RAS was used. The gas permeability unit is equipped with two thermal conductivity detectors (DT) for separate registration of the kinetics of diffusion and the stationary flow of individual or gas mixtures with subsequent computer processing. The installed thermal conductivity detector used in the gas permeability unit (Figure 3-2) allows gas permeability experiment to be performed within a temperature range of 20 ˚C and 200 ˚C gases and pressures from 1 atm to 5 atm. The gas permeability block schematic unit (Figure 3-2) comprises of gases source i.e. gas cylinder which contain the penetrant gas and carrier gas, membrane compartment (air tight), switch gas flow valves, flow meter and gas chromatography instrument. The gas sources (cylinder) are directly connected to pressure gauge in order to determine the pressure of gas that exits the gas cylinders. A gas dryer is connected to the penetrant gas line in order to remove traces of moisture from the gas during permeability measurement. The permeability unit (Figure 3-2) has two flow meters in which one was directly connected to the membrane compartment to determine the flow rate of gas while the second flow meter records the flow rate of gas in the gas chromatograph. The two flow meters

can be used to estimate steady state measurement of gases in the gas permeability unit. The polymer membrane sample is tightly secured in the diffusion cell which is in an air oven. The membrane divides the volume of the cell into two cavities i.e. tanker and receiver. Before starting the experiment via the receiver tank, the set is first calibrated by allowing the carrier gas (He or Ar) from the carrier gas cylinder to flow through the unit (Figure 3-2). This procedure is performed without the polymer membrane sample in the membrane compartment of the unit until a stable background signal on the gas chromatograph is achieved. The gas permeability measurement was performed using differential measurement methods from permeability data generated from the gas chromatographic analysis.

CHAPTER 4

CHAPTER FOUR

4 BASELINE CHARACTERIZATION OF ASPET AND ASPMP POLYMER FILMS

4.1 INTRODUCTION

This chapter is divided into two main sections; baseline characterization of as-received (commercial) PET (ASPET) and as-received (commercial) ASPMP polymer films which are samples OA1a and OA3a (Table 3-3) respectively. In the first section of this chapter, baseline characterization results of samples OA1a and OA3a (Table 3-3) polymer films will be discussed which were directly characterized. In the control experiments, as-received films of PET and PMP polymer were individually exposed to swift heavy ion irradiation or chemical etching conditions. The first control experiment was performed by chemical etching of ASPET and ASPMP polymer films i.e. samples OA1b and OA3b (Table 3-3). In the second control experiment, ASPET (sample OA1c) and ASPMP (samples OA3c and OA3d) polymer films were irradiated without chemical etching. All samples were characterized using appropriate instrumental techniques such as FTIR, SEM, XRD and TGA. The data generated from the baseline characterizations of samples OA1a and OA3a (Table 3-3) were then compared with results from samples OA1b, OA1c, OA3b, OA3c and OA3d. In both control experiments, the polymer films were characterized using FTIR, TGA, XRD and SEM while etching kinetics were performed where applicable. The results of samples OA1a and OA3a (Table 3-3) i.e. ASPET and ASPMP polymer films respectively will be presented first and discussed. Thereafter, the experimental results generated on ASPMP polymer film will be discussed.

CHAPTER 4

4.2 CHARACTERIZATION OF ASPET (SAMPLE OA1A) POLYMER FILM

The use of appropriate analytical methods in the characterization of ASPET (sample OA1a, Table 3-3) will provide valuable information and insight into the physical, chemical and thermal properties of the polymer films. This section will present and discuss the direct characterization results of OA1a. The characterization results presented in this section include SEM which was used to probe the surface morphology, TGA to determine the thermal properties such as evolution of volatile species, degradation and stability, XRD technique to understand the lattice arrangement of atoms within the polymer matrix and FTIR to determine the structural and functional groups identities of ASPET and ASPMP polymer films.

4.2.1 SCANNING ELECTRON MICROSCOPY (SEM) MICROGRAPH OF ASPET (SAMPLE OA1a) POLYMER FILM

The surface morphology analysis of sample OA1a polymer film using SEM is crucial as it helps to determine the visual features such as presence of pores, identification of defects and other physical characteristics of the polymer film. In Figure 4-1 below, the SEM micrograph result of ASPET (sample OA1a) is presented and discussed.

CHAPTER 4

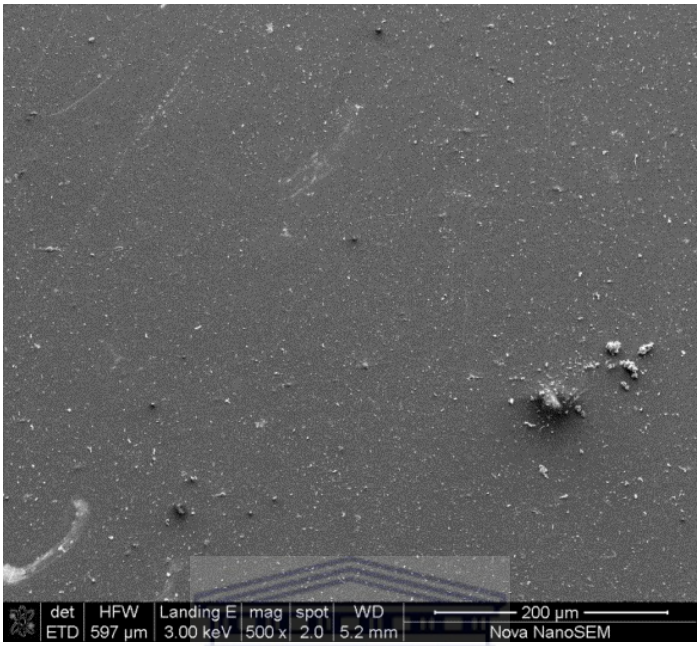

Figure 4-1: SEM surface morphology of ASPET (sample OA1a) polymer film

The SEM micrograph of sample OA1a polymer film is shown in Figure 4-1 above. The topography of the polymer film was relatively smooth without any distinct surface defects except for the presence of tiny specks. These tiny specks could be as a result of the synthesis approach of the PET film (Kitamura et al., 2009). According to Abdesselam *et al*., (2008), a similar surface topography for as-received (commercial) PET polymer film surface has been reported to exhibit undulated surface profile which was not observed for sample OA1a. It was suggested that the presence of the irregular tiny specks could be inherent surface characteristics of the polymer film or the accumulation of dust particles. The XRD analysis of sample OA1a will be presented in section 4.1.2

CHAPTER 4

4.2.2 X-RAY DIFFRACTION (XRD) ANALYSIS OF ASPET (SAMPLE OA1a) POLYMER FILM

The structure and alignment of atoms within a polymer matrix can be investigated using the XRD instrumental technique. Polyethylene terephthalate (PET) has been reported to exhibit both amorphous and crystalline phases hence it is important to determine the crystallinity properties of OA1a used in this study in order to explain the atomic alignment and inter-spacing within the polymer structures. The crystallinity investigation by XRD analysis of samples OA1a is presented in Figure 4-2.

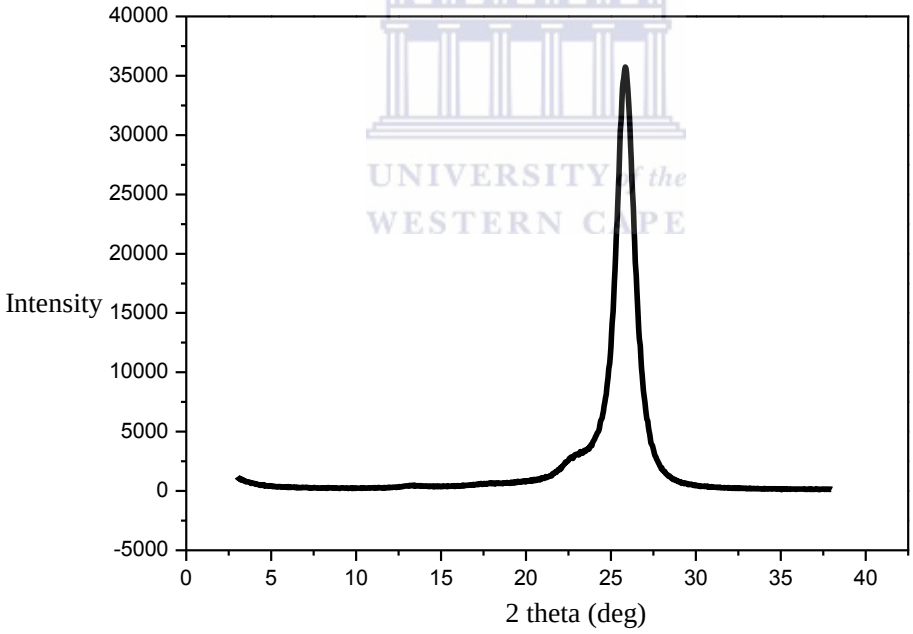

Figure 4-2: XRD analysis of ASPET (sample OA1a) polymer film

The XRD analysis of sample OA1a (Figure 4-2) showed a single and intense diffraction pattern peak located at 2θ = 26.0062°. The diffraction pattern peak at 26.002° for sample OA1a suggests a semi-crystalline polymer film as reported by Singh *et al*., (2006) and Singh *et al*., (2008) who stated a similar XRD diffraction

pattern for virgin PET film and ion irradiated PET polymer films under two types of heavy ion bombardment conditions was observed. In order to understand the crystallinity property of sample OA1a i.e. transition from semi-crystalline (Figure 4-2) to amorphous halo (Figure 4-3), in-situ thermal XRD analysis (Figure 4-3) was performed to determine if phase transition occurs within sample OA1a polymer matrix. The in-situ XRD analysis was conducted via cycle heating of sample OA1a polymer from RT (25 °C) up to 300 °C. In Figure 4-3, the in-situ XRD result of sample OA1a is presented.

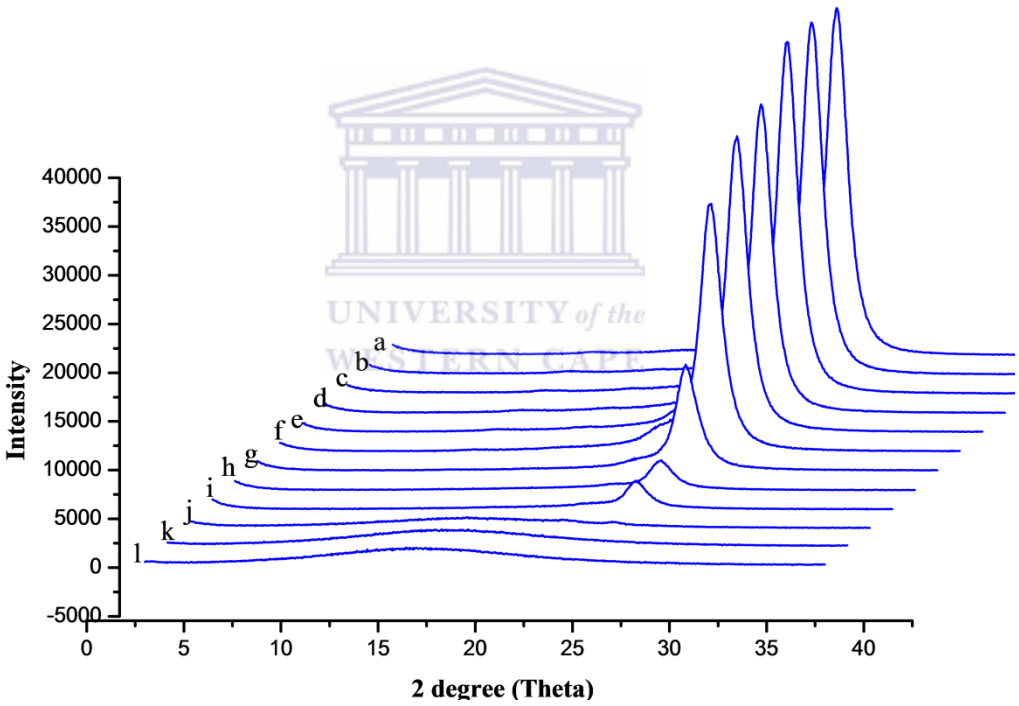

Figure 4-3: In-situ thermal XRD analysis of ASPET

It was observed that the XRD pattern and peaks of sample OA1a remained relatively stable as seen in Figure 4-3a-d but gradually decreased with broad peaks at 220 °C cycle heating (Figure 4-3g). In comparison with the XRD result in Figure 4-2, the in-situ XRD of sample OA1a polymer film showed a transformation of the PET crystalline phase from the sharp peak (Figure 4-2) to a broad peak with a shift

from 26.006° at room temperature to 16.96° at 300 °C (Figure 4-3j). This change in peak shape (i.e. sharp to broad) in polymers has been attributed to amorphous halo of polymers (Singh *et al.*, 2008). This suggests that PET molecular arrangement underwent disordering of crystal arrangement during heating which seems to have resulted in the delocalization of atoms within the polymer matrix.

In section 4.1.3, the thermal properties of sample OA1a is presented and the result is discussed.

4.2.3 THERMOGRAVIMETRY (TGA) ANALYSIS OF ASPET (SAMPLE OA1a) POLYMER FILM

Polyethylene terephthalate (PET) polymer is known to exhibit good thermal stability above 300 °C (Abdesselam *et al.*, 2008; Awasthi *et al.*, 2010). However, the thermal stability of PET could be compromised after exposure to swift heavy ion of chemical etching conditions hence a baseline characterization using TGA technique can provide a better understanding of the thermal stability of the polymer. In Figure 4-4, the TGA result i.e. thermal profile of sample OA1a is presented. The TGA measurement was performed from ambient temperature (RT) to 600 ˚C at a heating rate of 10 ˚C/minutes.

CHAPTER 4

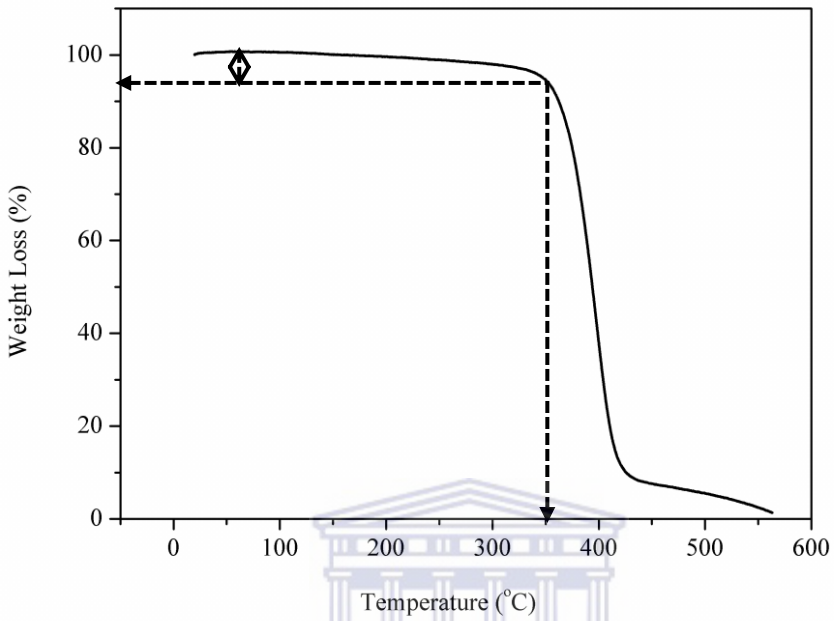

Figure 4-4: TGA thermal profile of ASPET (sample OA1a) polymer film

The TGA result of sample OA1a (Figure 4-4) polymer film can be seen to experience a gradual and unstable thermal profile from 30 ˚C up to 350 ˚C with a mass loss of approximately 3 % due to continuous evolution of volatile contents such as ethylene glycol residue which the solvent used during synthesis of PET polymer film. Also, it was observed that a single thermal degradation profile occurred for sample OA1a from 350 ˚C up to 430 °C resulting in a mass loss of approximately 98 %. The region of thermal stability (Figure 4-4) of sample OA1a polymer film agreed with the in-situ XRD analysis previously presented and discussed in Figure 4.3 which showed the transformation of sample OA1a from crystalline to amorphous halo (Singh *et al*., 2008) with a characteristic broad peak typical in polymer analysis. The in-situ XRD analysis was performed in a heat-cool cycle up to 300 °C. The relative stability in thermal properties experienced by sample OA1a could be as a result of the degree of chain linearity of the polymer backbone structure and small side chain moieties (Burgess *et al*., 2014). Also, the absence of branched chains in the PET structure (Figure 2-1) could have enhanced

the rigidity of chain packing (Toress *et al.*, 2000). This is because the main chains of PET, like most polymers, are primarily covalent bonds with less free fractional volume within the polymer matrix thus less heat absorption. This result agreed with PET thermal studies reported by Bandyopadhyay *et al.*, (2007) and Carneiro-da-Cunha *et al.*, (2010). In section 4.1.4, the IR analysis of sample OA1a will be presented.

4.2.4 FOURIER TRANSFORMED INFRA-RED (FTIR) SPECTROSCOPY ANALYSIS OF ASPET (SAMPLE OA1a) POLYMER FILM

The characteristic functional groups present in the starting materials ASPET (sample OA1a) were identified using the ATR/IR technique. The chemical bonds in the polymers i.e. intra and inter atomic bonding determine the chemical, physical, thermal or mechanical properties of the polymer material. It is therefore imperative to understand the existing functionalities associated with polyethylene terephthalate (PET) polymer film. In Figure 4-5, the IR spectra results of ASPET are shown. Also, the selected functional groups and their corresponding wavenumber from the IR spectra result of ASPET is presented in Table 4-1.

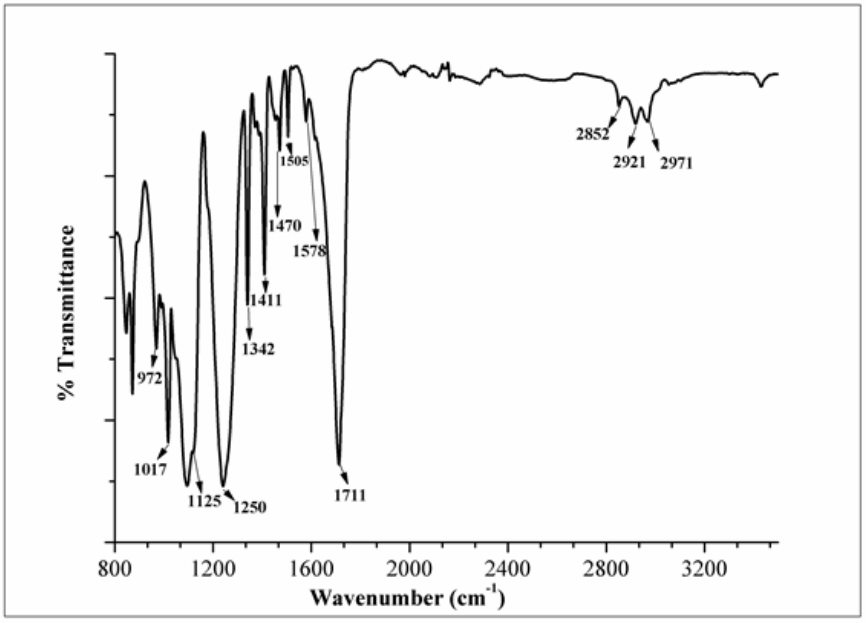

CHAPTER 4

Figure 4-5: IR spectra of ASPET (sample OA1a) polymer film

Table 4-1: Selected functional groups in the PET polymer film and their corresponding wavenumbers

Functional group	Wavenumber (cm^{-1})
CH_2 rocking	857
CH_2 bending	1250
C=O	1720
Ethylene glycol	972, 1052,1344 and1480
Aromatics	1532
Aliphatic	1344
Para-substituted aromatic	1129 and 1505
C-H $(CH)_2$	2857, 2921, 2971

The presence of characteristic functional groups with the corresponding band peak (Transmittance) intensities in a polymer can occur as weak, medium and strong band intensities. It was observed from the IR analysis of sample OA1a (Figure 4-5) that weak band intensities occurred at 973 cm^{-1} and 1470 cm^{-1} and these bands correspond to the trans ethylene glycol residues which have been reported (Singh *et al*., 2006) to be associated with PET crystallinity. Also, weak band with low intensity peaks were observed at 1125 cm^{-1} (shoulder) and 1505 cm^{-1} for the *p*-substituted benzene ring. The C-C stretch ring is represented by the band intensity at 1578 cm^{-1} and the bands located at 2852 cm^{-1}, 2921 cm^{-1} and 2971 cm^{-1} indicate the presence of C-H (CH_2) moieties (Mathakari *et al*., 2009). The medium intensity bands observed at 1017 cm^{-1} were assigned to the triple carbon bend ring (C-C-C). The IR intensity at 1095 cm^{-1} is assigned to ring C-C, C=O and ethylene glycol C-C stretch (Awasthi *et al*., 2010) while the bands with intensities at 1342 cm^{-1} and

1411 cm^{-1} are associated with the para substituted benzene ring present in PET. The strong band intensities can be seen at 1250 cm^{-1} and 1711 cm^{-1} which correspond to the presence of C-O (stretch) and C=O (stretch) both of which describe the stretch of esters respectively. In the next section (4.2), the characterization of as-received PMP (sample OA3a) will be presented and discussed.

4.3 CHARACTERIZATION OF ASPMP (SAMPLE OA3A) POLYMER FILMS

In this section, the SEM (4.2.1), XRD (4.2.2), TGA (4.2.3) and FTIR (4.2.4) results of as-received PMP polymer film (sample OA3a) is presented and discussed. Although polymethyl pentene (PMP) is a highly valuable polymer due to its excellent gas permeability properties, there are limited studies dedicated to investigating the physico-chemical properties and thermal characteristics including surface modification using swift heavy ion and chemical etching technique. This section therefore will investigate some of the properties of ASPMP and compare them with other existing studies including other polyolefin polymers such as polypropylene (PP). It is important to emphasise that even though polypropylene does not enjoy the unique gas permeability properties of PMP, both belong to the polyolefin class of polymer and more importantly are isotactically configured in their structure hence with similar physico-chemical properties. In section 4.2.1, the SEM result of sample OA3a will be presented and discussed.

4.3.1 SCANNING ELECTRON MICROSCOPY (SEM) MICROGRAPH ANALYSIS OF ASPMP (SAMPLE OA3a) POLYMER FILM

The presence of surface defects on polymer can be used to elucidate the degree of surface roughness of polymer films. The accumulation of dust particles, process of polymer manufacturing are some of the defects that could be investigated on

polymer surface. The SEM micrograph of ASPMP (sample OA3a) polymer film is presented in Figure 4-6.

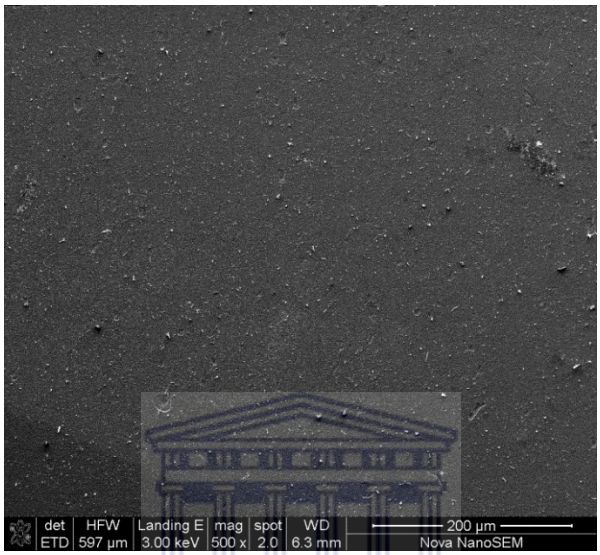

Figure 4-6: SEM micrograph image of ASPMP (sample OA3a) polymer film

The SEM morphology image of sample OA3a polymer film is shown in Figure 4-6 revealed the presence of micro defects with several patches of bulging particles on the surface of polymer film. The SEM morphology of sample OA3a did not show surface smoothness of the samples. Although there is no clear understanding of the surface defects that were observed on sample OA3a polymer film, the synthesis processes according to Johnson Mathew, (2000) has been suggested to be responsible for the high surface roughness due to the orderliness or uniformity of the defects. The degree of surface roughness could also increase the rate dust particle accumulation which is possible if the polymer film is not properly stored. In section 4.2.2, the XRD result of sample OA3a will be presented and discussed

CHAPTER 4

4.3.2 X-RAY DIFFRACTION (XRD) ANALYSIS OF ASPMP (SAMPLE OA3a) POLYMER FILM

Polymethyl pentene (PMP) is generally regarded as a semi-crystalline polymer hence the intra and interatomic spacing and distribution within the polymer matrix is essential to understand the crystallinity properties of PMP. The XRD analysis of as-received (commercial) PMP is expected to provide insight into existing crystalline orientations. In Figure 4-7 below, the XRD result of sample OA3a is presented.

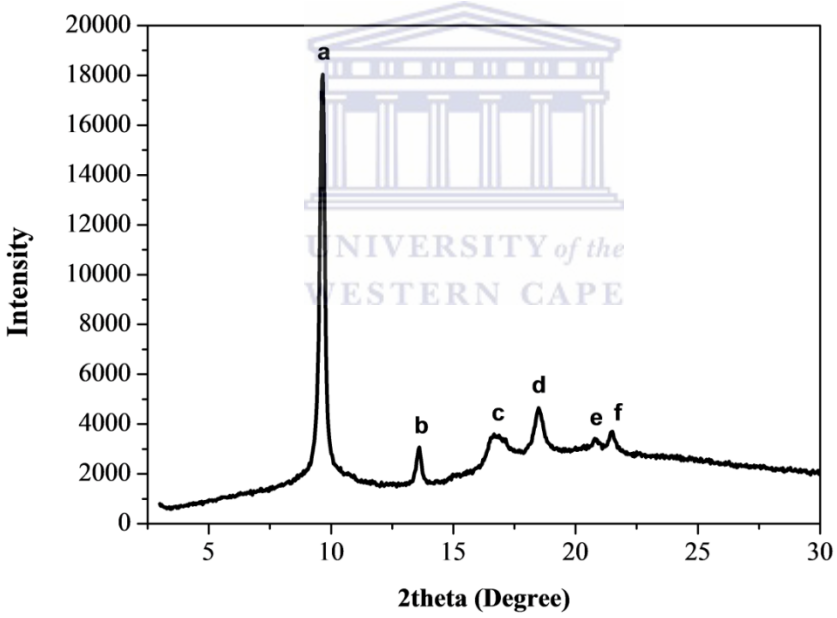

Figure 4-7: XRD analysis of ASPMP (sample OA3a) polymer film

In Figure 4-7, the XRD analysis of ASPMP (sample OA3a) showed the presence of a high intensity sharp peak at 9.8 ˚ 2 theta. Also, other peaks with relatively low intensities compared with peak at 9.8 ˚ 2 theta were observed at 13.6 ˚, 17.9 ˚, 21. 5 ˚ and 22. 3 ˚ 2 theta while a broad peak was identified at about 16.7 ˚ 2 theta (Aharoni *et al*., 1981). The shapes of the diffraction peaks at 9.8 ˚ and 13.6 ˚ 2 theta were sharp while the peaks located at 17.9 ˚ and 21.5 ˚ 2 theta were both observed

to be broad in shape. The multiple peaks present in the XRD analysis of sample OA3a (Figure 4-7) and their shapes have been reported to indicate the α-monoclinic crystalline orientation of the polymer sample and have been indexed into 110, 040, 130, 060, 200 and 220 for peaks positions a, b, c, d, e and f respectively (Aharoni *et al*., 1981).The orderly arrangement of the methyl groups along the same side of the chain in the polymer backbone structure confers on it a high degree of crystallinity due to the regular, repeating units (Karacan and Benli, 2011). In section 4.2.3, TGA analysis of sample OA3a will be presented and discussed.

4.3.3 THERMOGRAVIMETRY (TGA) ANALYSIS OF ASPMP (SAMPLE OA3a) POLYMER FILM

Thermogravimetric analysis of polymer samples can be determined as a result of their continuous degradation at increasing temperature. The response of polymer to heat depends on the polymer structural orientations i.e. chain packing and intra-atomic and interatomic bonds and the atomic composition. The thermal profile of a polymer is such that volatile species will be favourable to vaporize first while bulk species undergo further defragmentation into low molecular weight compounds at higher temperatures. In Figure 4-8, the TGA analysis of sample OA3a is presented.

CHAPTER 4

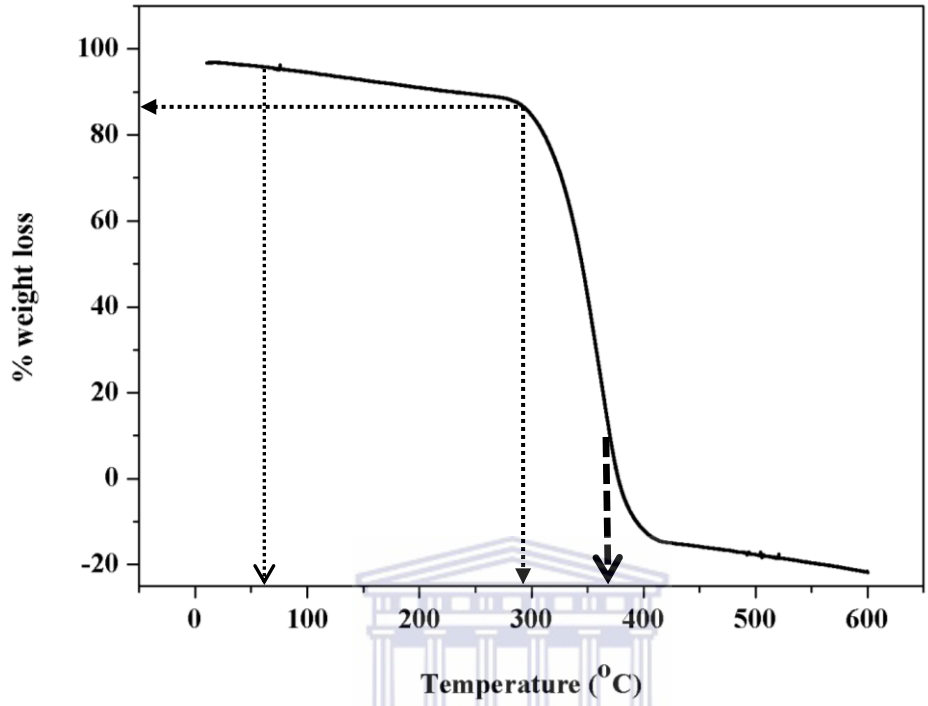

Figure 4-8: TGA thermal profile of ASPMP (sample OA3a) polymer film

The thermal analysis result of sample OA3a polymer film in (Figure 4-8) showed that sample OA3a underwent gradual but continuous degradation of the polymer film with a mass loss of 10-15 % between 30 ˚C and 300 ˚C. The amount of mass loss by sample OA3a as well as the temperature region i.e. from 30 ˚C to 300 ˚C was indicative of a gradual release of volatile species present in sample OA3a. Also, a single thermal degradation of sample OA3a in Figure 4-8 was observed with rapid thermal degradation of the sample between 300 °C and 375 ˚C with a mass loss of approximately 90 %. The continuous but gradual release of volatile species of sample OA3a as seen in Figure 4-8 could be as a result of the presence of small percentage of volatiles species or low molecular weight compounds which could easily be given off between low to medium temperature. This may be due to the composition of as-received (commercial) PMP polymer film which is mainly C-C and C-H bonds and also the presence of antioxidant fillers (Apel, 1996). In the case

of sample OA3a (ASPMP), it could be that molecular flexibility and thermal transformation via bond breakage may be initiated due to the effects of the thermal profile multiple modification approaches used in this study. In section 4.2.4, the IR result of sample OA3a will be presented.

4.3.4 FTIR SPECTROSCOPY ANALYSIS OF ASPMP (SAMPLE OA3a) POLYMER FILM

The use of IR to investigate characteristic spectra in polymers has been a reliable technique as it helps in a better understanding of polymer configuration. The IR spectra analysis occurs in the form of specific bond identities that are unique to each polymer and thus assigned accordingly. The bond identities can be present in varying intensities such as weak, medium or strong. In Figure 4-9, the IR spectra of sample OA3a are presented.

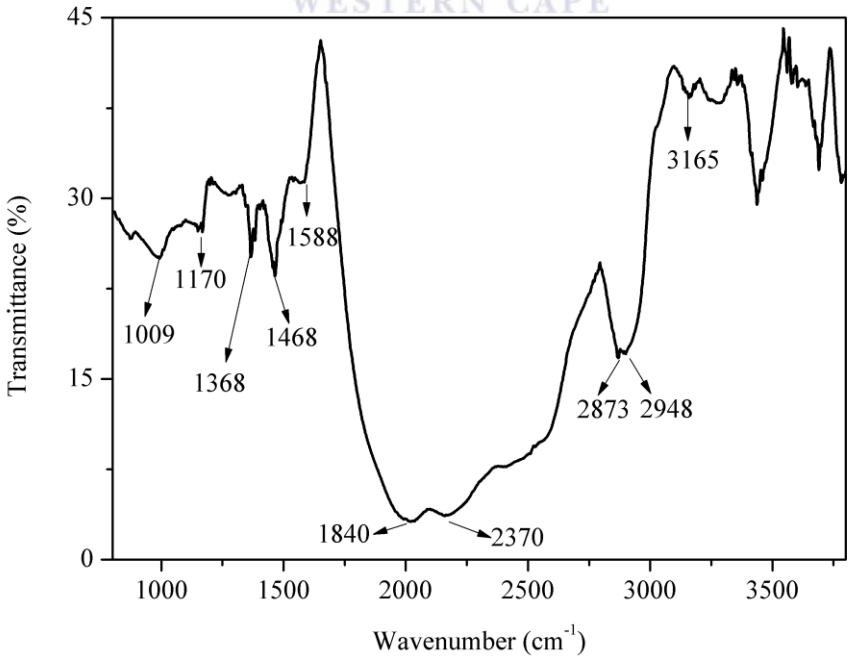

Figure 4-9: IR spectra of ASPMP (sample OA3a) polymer film

CHAPTER 4

Table 4-2: Selected functional groups in PMP polymer film and their corresponding wavenumbers

Functional group	Wavenumber (cm^{-1})
Methyl (CH_3) rocking	1009
Methyl (CH_3) wagging	1170
Asymmetry and out-of-plane methyl (CH_3)	1368, 1468
Unsaturated alkyne	1840, 2370
CH_2 symmetry vibration	2873, 2948
Methylene (CH_2) asymmetrical stretch	3165

The IR analysis result for selected functional groups for sample OA2a are presented in Table 4-2 and characteristics spectra intensities are shown in Figure 4-9. The weak band at 1009 cm^{-1} is associated with methyl (CH_3) rocking and the IR band at 1170 cm^{-1} is assigned to methyl (CH_3) wagging. The characteristic band intensity at 1468 cm^{-1} is associated with the presence of an asymmetrical vibration and out-of-plane methyl (CH_3) which is confirmed by the IR intensity at 1368 cm^{-1}. At 1588 cm^{-1}, a weak shoulder was observed and assigned to CH_2 twisting, while the weak intensities located at 2873 cm^{-1} and 2948 cm^{-1} are due to CH_2 symmetry vibration. The unsaturated alkyne functionality was identified due to the intensity at 2370 cm^{-1} and confirmed at 1840 cm^{-1} (Abedini *et al*., 2014; Samuel and Mohan 2004). The IR analysis of PMP has shown that the functional groups present in the PMP polymer structure (Fig. 2.2) were mainly due to saturated and unsaturated C-H and C-C bonds.

CHAPTER 4

4.4 SUMMARY FOR BASELINE CHARACTERIZATION OF ASPET AND ASPMP POLYMER FILMS

The investigation of the intrinsic properties of ASPET polymer film used in this study showed that sample OA1a exhibited physico-chemical and thermal properties in agreement with other previous reported studies on PET polymer film. Also, the SEM morphology showed that sample OA1a is relatively smooth without any distinct surface defects. This can be attributed to the method of synthesis or inertness of polymer film to post synthesis degradation as a result of environmental effects such as oxidation. In addition, the TGA analysis of sample OA1a indicated thermal stability profile of sample OA1a polymer up to 350 ˚C film. The XRD result showed that sample OA1a is semi-crystalline with a single intense peak at 26.0062˚ 2 theta. In the FTIR analysis, the presence of characteristics functional groups associated with PET polymer film were identified at specific wavenumber and assigned to their respective functional groups. The IR result showed the various functional groups associated with sample OA1a polymer side chain and backbone matrix. In general, the baseline characterization of ASPET polymer film has shown consistency with other results of PET polymer films that have been reported in literature.

The baseline analysis of sample OA3a polymer film using SEM surface morphology showed that sample OA3a has moderately surface roughness with patches and micro-defects present and highly distributed. The XRD analysis of sample OA3a polymer film showed the presence of multiple peaks that are associated with the α-monoclinic crystalline orientation of polyolefin polymer. The thermal profile study of sample OA3a by TGA technique showed that sample OA3a experienced continuous but gradual release of volatile species up to 300 ˚C after which a single rapid degradation was observed. IR results of sample OA3arevealed the presence of mainly unsaturated aliphatic functional groups. The major difference between the baseline characterization of sample OA1a and OA3a

CHAPTER 4

including their thermal stability profile which showed that the thermal stability of sample OA3a was lower compared with sample OA1a i.e. 350 ˚C and 300 ˚C respectively. XRD analysis of ASPET and ASPMP polymer films indicated the presence of a single peak in sample OA1a while sample OA3a showed structural ordering with multiple peaks. Also, the IR analysis of sample OA1a and sample OA3a vary significantly due to the unique atomic constituents of each polymer with respect to their side chain and back bone structures.

In the next section (4.4), the results of chemically etched as-received polyethylene terephthalate (PET) and as-received polymethyl pentene (PMP) polymer film will be presented and discussed.

4.5 CHARACTERIZATION OF CHEMICALLY ETCHED AS-RECEIVED PET AND AS-RECEIVED PMP POLYMER FILMS

In this section, a control experiment was performed by chemical etching of as-received (commercial) PET and as-received (commercial) PMP polymer films. The as-received (commercial) PET film was etched in sodium hydroxide (NaOH) solution and as-received (commercial) PMP film was etched in acidified chromium oxide (7 M H_2SO_4 + 3 M CrO_3). The etched polymer films were then characterized using SEM, FTIR and their chemical etching kinetics were studied. The difference in chemical etchant is mainly because PET and PMP polymer films belong to different classes of polymers. The chemical etching experiment is briefly described thus; as-received (commercial) PET was chemically etched in sodium hydroxide (1 M NaOH) solution at 80 °C and etching time was 140 minutes. The as-received (commercial) PMP polymer film was etched in a solution of acidified chromium trioxide (7 M H_2SO_4 + 3 M CrO_3) at 80 °C and at a similar etching time i.e. 140 minutes. This section will first present and discuss the experimental results for etched PET and thereafter the results for etched PMP polymer films. The etching of the unirradiated, etched PET and PMP polymer films served as a baseline to

better distinguish the additional changes experienced by as-received PET and as-received PMP polymer film after exposure to chemical etching conditions. In Figure 4.4.1, the SEM micrograph result of NaOH etched PET (sample OA1c) will be presented.

4.5.1 SCANNING ELECTRON MICROSCOPY ANALYSIS OF ETCHED PET (SAMPLE OA1b) POLYMER FILM ETCHED IN NaOH SOLUTION

The effects of chemical etching on the physico-chemical properties of polymer film after chemical etching can be investigated using microscopy technique such as SEM to determine the presence of surface defects or change in surface topography i.e. smoothness roughness, pores etc. The SEM surface morphology analysis of sample OA1b (PET polymer film) etched for 140 minutes at 80 ˚C in 1 M NaOH solution is presented in Figure 4-10 below.

CHAPTER 4

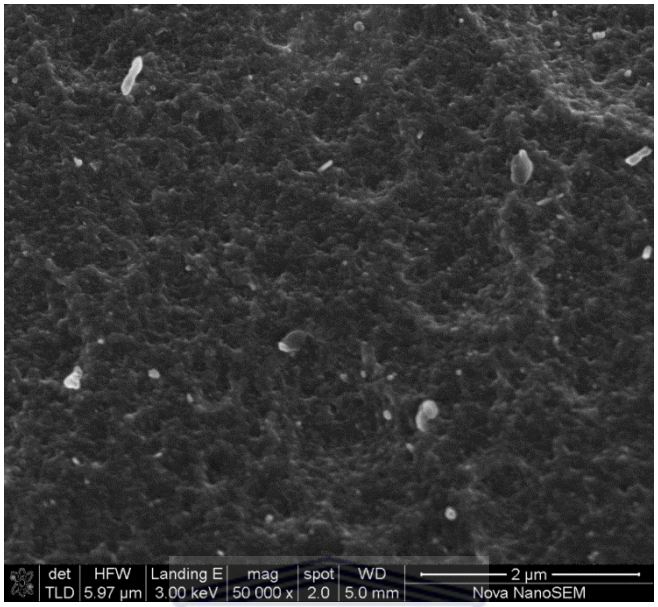

Figure 4-10: SEM micrograph of PET (sample OA1b) polymer film etched in NaOH solution at 80 ˚C for 150 minutes

The SEM micrograph image analysis of sample OA1b (Figure 4.10) showed an extensive surface defects with coarse uneven surface. Also, it was observed that there were patches of undulating regions. Sample OA1b did not show any distinct visible pores on its surface and this could suggest that the chemical etching process was restricted to the surface region of the polymer film. This may indicate that the PET polymer film surface is more susceptible to chemical attack during etching even though there no visible pores, and that the conditions of etching applied were not so extreme as to destroy sample OA1b polymer but is strong enough to attack and modify the polymer structure. In section 4.4.2, the etching kinetic study of sample OA1b is presented and discussed.

CHAPTER 4

4.5.2 ETCHING KINETICS ANALYSIS OF PET (SAMPLE OA1b) POLYMER FILM ETCHED IN NaOH SOLUTION

One of the fast methods that can be used to determine the physical deterioration of a polymer film is to monitor the weight loss of polymer film over time due to continuous chemical etching of polymer film. The benefit of this approach i.e. etching kinetics study is that it provides an insight into the probable weight loss of polymer film sample per unit time and this loss in mass can be related to many factors such as susceptibility of the polymer to etching, the presence of active sites, intra-atomic and interatomic bond strength and reactive functional groups within the polymer matrix. The chemical etching result of PET sample OA1b polymer film is presented in Figure 4.11. The chemical etching experiment of PET (sample OA1b) was replicated three (3) times.

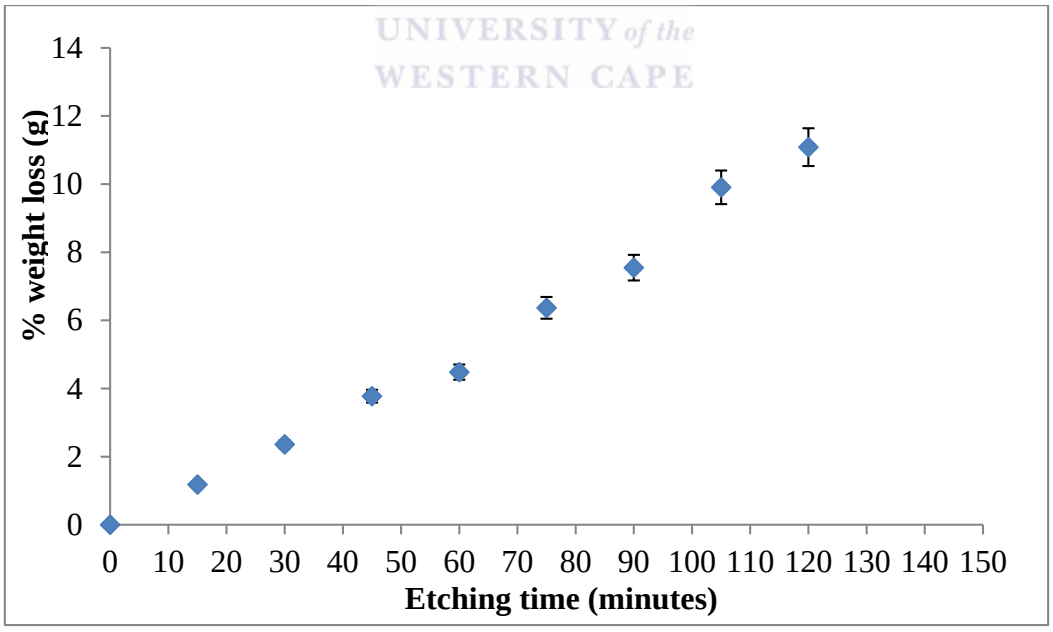

Figure 4-11: Kinetic analysis of etched PET (sample OA1b) polymer film in NaOH at 80 ˚C for 140 minutes

CHAPTER 4

The direct chemical etching kinetic analysis of sample OA1b polymer film is shown in Figure. 4-11. It was observed that sample OA1b experienced continuous weight loss throughout the etching time. The weight loss of sample OA1b and etching time showed a linear relationship. The weight loss of the etched PET polymer film was almost 5 % within the first 60 minutes and almost 12 % after 2 hours (i.e. 120 minutes) of chemical etching. The amount of mass loss experienced by sample OA1b showed the chemical etchant continued to attack the polymer film which could be due to the functional groups composition present in PET polymer structure. In addition, the ease of chemical attack on sample OA1b may be attributed to the chain linearity of PET and availability of sites which can be easily attacked. In section 4.4.3, the IR result of sample OA1b will be presented and discussed.

4.5.3 FTIR SPECTROSCOPY OF (SAMPLE OA1b) PET POLYMER FILM ETCHED IN NaOH SOLUTION

The functional groups identity of polymer films can be modified via exposure to single or multiple treatments such as chemical etching. The use of chemical etching as a modification technique can affect chemical, physical, thermal and mechanical properties of the polymers. It is based on this premise that the as-received (commercial) PET polymer was submitted to chemical etching in order to understand the possible effects such as presence or disappearance of functional group bands due to chemical attack on the polymer functionalities. These attacks may be random or specific to functional groups within the polymer matrix and this can be revealed by using the IR analytical method. The IR analysis of sample OA1b is presented in Figure 4-12.

CHAPTER 4

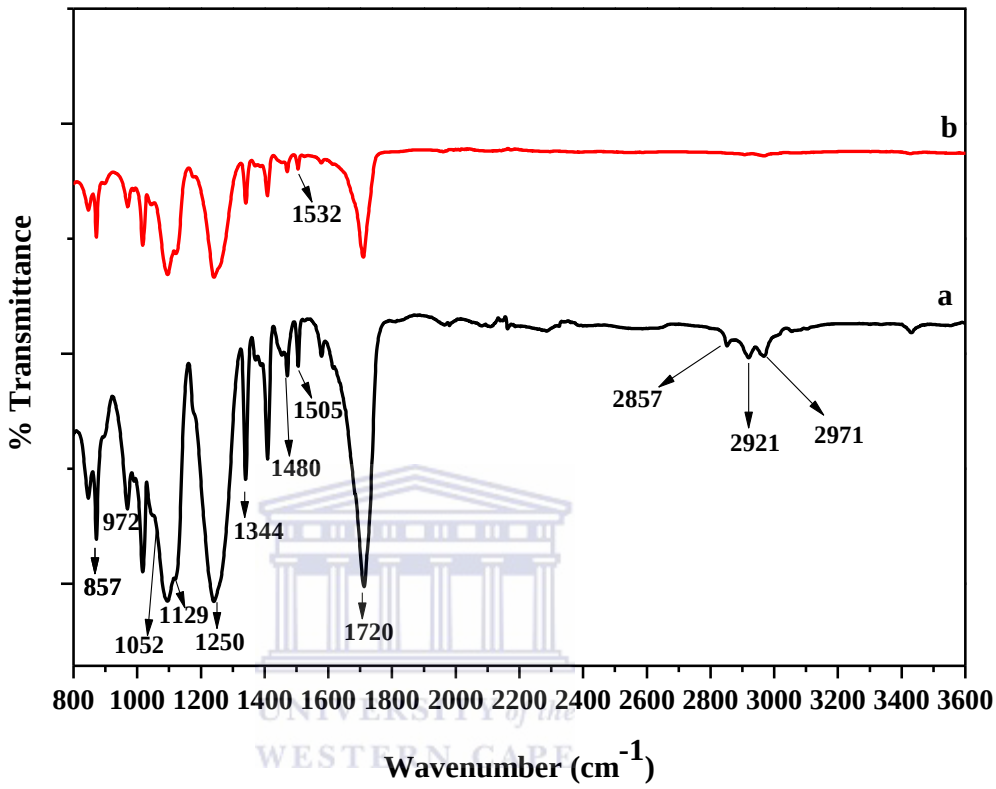

Figure 4-12: IR spectra of (a) ASPET (sample OA1a) and (b) PET (sample OA1b) polymer film etched in NaOH etched at 80 ˚C for 140 minutes

The summary of comparison of the IR bands in samples OA1a and OA1b is presented in Table 4-3.

Table 4-3: Comparison of selected functional groups in ASPET and etched PET polymer film

		Sample code	
Functional group assignment	**Wavenumber (cm^{-1})**	OA1a	OA1b
CH_2 rocking	857	Band is present with strong intensity	Band is present with medium intensity
CH_2 bending	1250	Band is present with strong intensity	Band unaltered but with reduced intensity
C=O	1720	Band is present and with strong intensity	Band did not shift but was with reduced intensity
Ethylene glycol residue	972 1052 1480	Bands are present but with medium intensities	Bands did shift and unaltered but with weak intensities
Aromatics	1532	Band is not present	Band is present with weak intensity
Aliphatic	1344	Band is present and with strong intensity	Band unaltered but appeared with weak intensity
Para-substituted aromatic	1129 1505	Band are present but with weak and medium	Bands unaltered and not shifted but appeared as

		intensities respectively	weak intensities for both bands
C-H $(CH)_2$	2857	Bands are present with medium intensities	Bands completely Band disappeared in sample
	2921		
	2971		

Figure 4-12a and 4-12b compares the IR spectrum of samples OA1a (a) and sample OA1b (b) PET polymer film respectively. It was observed that the characteristic functional groups band intensities were present in the IR results of both sample OA1a and OA1b (Figure 4-12a and 4-12b). These characteristic band intensities have been discussed after Figure 4-5. The IR result presented in Figure 4-12b (sample OA1b) showed some variations in the band intensities of the characteristic bands of sample OA1c compared with the IR result of sample OA1a. In sample OA1a (Figure 4-12a), the following IR bands peaks located at 2852 cm^{-1}, 2921 cm^{-1} and 2971 cm^{-1} completely disappeared for the IR result of sample OA1b (Figure 4-12b). These bands are indicative of the presence of C-H (CH_2) moieties. A similar trend of reduction in band intensities was reported by Steckenreiter et *al*., (1997). Although, Steckenreiter *et al*., (1997) used ion irradiation modification to treat PET polymer film, it was reported that the PET film experienced an overall reduction of band intensities as seen with the IR spectra collected for sample OA1c (Figure 4-12b). Also, it was observed from the IR result of sample OA1b (Figure 4-12b) that the overall band intensities for sample OA1b (Figure 4-12b) were reduced compared with the IR results of sample OA1a shown in Figure 4-12a. The response of PET polymer film (sample OA1b) to chemical etching from the IR analysis in Figure 4-12b showed the degree of PET polymer film susceptibility to chemical modification under mild conditions. This suggests that the use of chemical etchant such as NaOH solution to etched PET polymer is not limited to any specific functionality within the PET polymer structure as well as preferential chemical

attack on some functional groups with the disappearance of bands at located 2852 cm^{-1}, 2921 cm^{-1} and 2971 cm^{-1} as observed for sample OA1b (Figure 4-12b)

In the section 4.5, the results of chemically etched PMP (sample OA3b) polymer film will be presented and discussed. The chemical etching of PMP polymer film was performed in acidified chromium trioxide (7 M H_2SO_4 + 3 M CrO_3) at 80 ˚C for 150 minutes and characterized using SEM, etching kinetic and IR techniques. The SEM, etching kinetic and FTIR results for sample OA3b.

4.6 CHARACTERIZATION OF ETCHED PMP POLYMER FILM

Unlike polyethylene terephthalate (PET), polymethyl pentene (PMP) polymer film is poorly investigated under surface modification conditions such as swift heavy ion and chemical etching treatments. The crystalline nature of PMP polymer film requires that aggressive etchant such as acidified chromium trioxide (7 M H_2SO_4 + 3 M CrO_3) solution is preferred to mild etchant that was used for polyethylene terephthalate (PET) polymer film (Apel, 2001). In section 4.5.1, the SEM micrograph result of sample OA3b will be presented and discussed.

4.6.1 SCANNING ELECTRON MICROSCOPY ANALYSIS OF ETCHED PMP (SAMPLE OA3b) POLYMER FILM ETCHED IN ACIDIFIED CHROIMUM TRIOXIDE (H_2SO_4 + CrO_3)

The microscopy examination of chemically etched PMP (sample OA3b) polymer film by SEM can provide insight into the surface damage or defects experienced by PMP during etching. Also, deterioration of PMP during chemical etching can be considered to indicate the effects of the etchant solution on polymer film. The SEM micrograph surface morphology of chemically etched PMP (sample OA3b) polymer film is presented in Figure 4-13.

CHAPTER 4

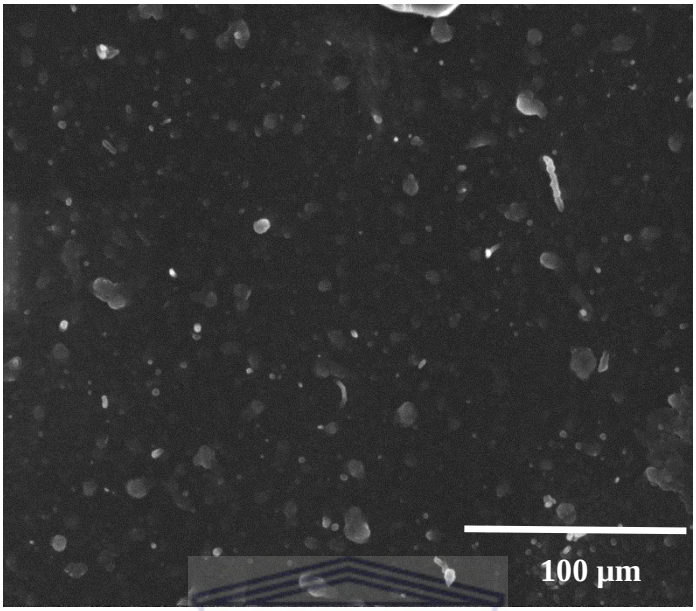

Figure 4-13: SEM micrograph of PMP (sample OA3b) polymer film etched in acidified chromium trioxide at 80 ˚C for 150 minutes

The SEM surface topography (Figure 4-13) of sample OA3b showed the presence of white spherical moieties fairly evenly distributed on the surface. Also, it was observed that there was no distinct pore formation on the polymer film except for the uniform surface defects induced by the etchant. Although the reason for the presence of the patches on etched PMP remains unclear, it could be dissolution or degradation of the polymer film considering the fact that a strong and aggressive oxidising agent in form of H_2SO_4 + CrO_3 solution was used. However, mild roughness of sample OA3b polymer film surface could possibly be due to the chemical resistance namely the surface inertness of PMP as well as its atomic composition which is mainly C-C and C-H bonds. In the study reported by Apel *et al*., (1997), polypropylene (PP) film was investigated and the relaxation transition of PP was considered to determine the etch rate. The relaxation transition of polymer was the term used by these authors to describe the return of excited species or radicals to ground state within the polymer after exposure of polymers to chemical etching or swift heavy ion irradiation. In this case, sample OA3b could

have experienced excited species due to the high etching temperature (80 ˚C). The significance of this study is that PP and PMP belong to the polyolefin group and are composed mainly of methyl and methylene groups.

In the next section, the etching kinetic result of sample OA3b due to weight loss as a function of etching time will be presented and discussed.

4.6.2 ETCHING KINETICS ANALYSIS OF ETCHED PMP (SAMPLE OA3b) ETCHED IN ACIDIFIED CHROIMUM TRIOXIDE (H_2SO_4 + CrO_3)

The measurement of polymer response via weight loss during chemical etching can be performed using the etching kinetic approach. This experiment explored two parameters that are used in chemical etching experiments i.e. nature of etchant and time. It is anticipated that polymers will experience deterioration in the form of weight loss due to etching time hence this analysis takes advantage of the simplicity of the measurement. This analysis was performed by periodic measurement of percentage weight change (loss) of etched PMP (sample OA3b) polymer film over etching time. The etching kinetic experiment of etched PMP (sample OA3b) polymer film was replicated three (3) times and the result of etched PMP polymer will be presented and discussed in Figure 4-14.

CHAPTER 4

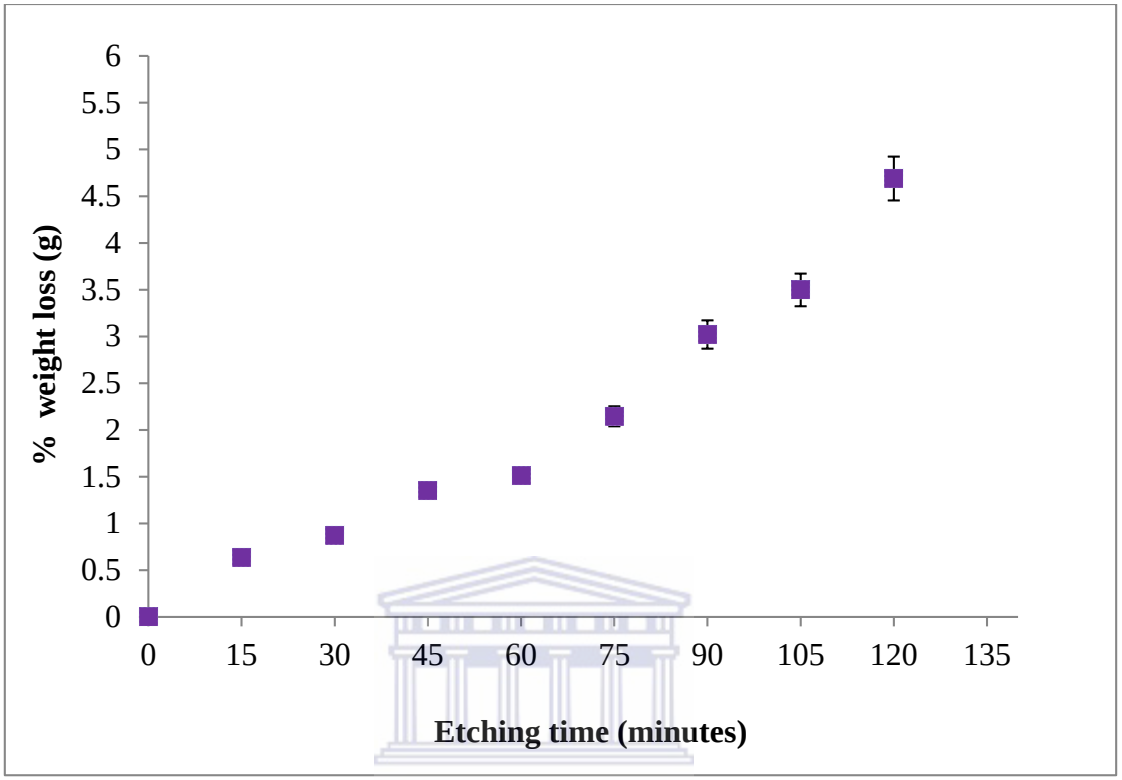

Figure 4-14: Chemical etching kinetic analysis of PMP (sample OA3b) polymer film

The etching kinetic study of PMP polymer film (sample OA3b) is shown in Figure 4.14. It was observed that the weight loss of sample OA3b PMP polymer film was about 1.5 % of the initial polymer weight after 60 minutes of chemical etching. In addition, sample OA3b weight loss 3.3 % after 2 hours (i.e. 120 minutes) of chemical etching as shown in Figure 4-14. The increase in weight loss within 60 minutes and 120 minutes showed that sample OA3b experienced twice its weight loss after 120 minutes. The effect of chemical etching on PMP polymer was lower than in the case of PET polymer film (Figure 4-11) even though a much aggressive etchant was used to etch PMP polymer film. This seems to suggest that the chemical resistance properties of sample OA3b is higher compared with sample OA1b. Also, the low weight loss experienced by sample OA3b could be attributed to the chain packing (Billigham and Walker, 1975) within the PMP polymer matrix thus a

gradual exposure of the polymer chains, especially the bulk side chains, which may not be readily available to chemical attack. The low susceptibility of PMP to chemical attack in an aggressive etching media such as acidified chromium trioxide can indicate the inertness of PMP and lack of loosely attached side chains with flexible and also its chemical resistance unlike the case of PET where higher percentage weight loss was observed. In section 4.6.3, the IR result of sample OA3b will be presented and discussed.

4.6.3 FTIR SPECTROSCOPY OF CHEMICALLY ETCHED PMP (SAMPLE OA3b) POLYMER FILM ETCHED IN ACIDIFIED CHROIMUM TRIOXIDE ($H_2SO_4 + CrO_3$)

The IR spectra in form of overlay for ASPMP (sample OA1a) and chemically etched PMP (sample OA3b) are presented in this section. The use of a strong oxidising agent such as sulphuric acid saturated with chromium trioxide as chemical etchant to treat a polymer such as polymethyl pentene (PMP) is anticipated to cause alterations in the polymer chain structures with selective or general attack on the functionalities present in PMP. Although, the susceptibility of PMP polymer to chemical etching and degree of chemical attack by etchant may vary, the associated functional groups at specific sites could be altered. The alteration of these functional groups can be identified via FTIR band intensities as is shown in Figure 4.15.

CHAPTER 4

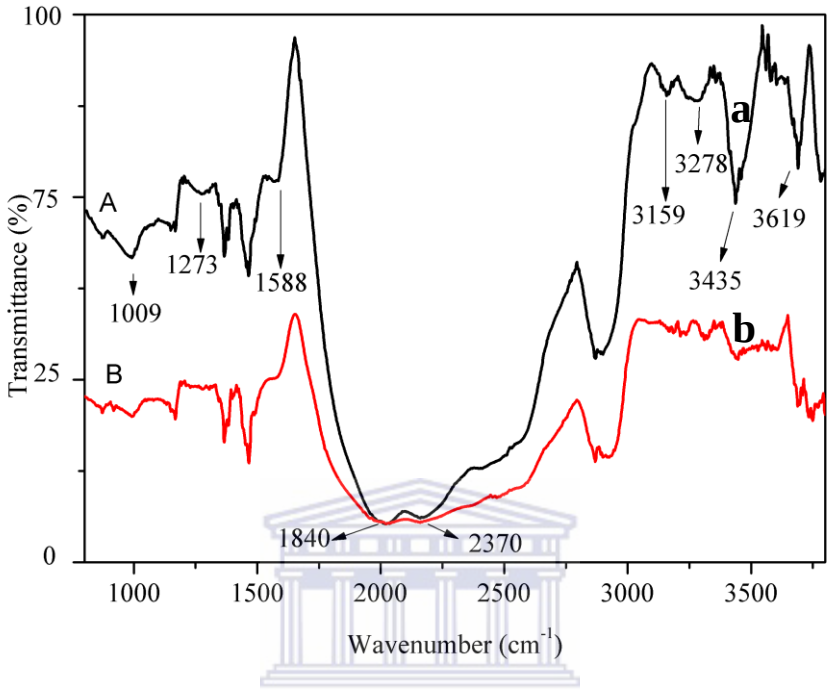

Figure 4-15: IR spectra of (a) ASPMP and (b) etched PMP (sample OA3b) polymer film

Table 4-4: Comparison of selected functional groups in ASPMP (sample OA3a) and etched PMP (sample OA3b) polymer film

		Sample code	
Functional group assignment	**Wavenumber (cm^{-1})**	OA3a	OA3b
Methyl (CH_3) rocking	1009	Band is present with weak intensity	Band remained unchanged in intensity
C-H	1273	Band is present with weak intensity	Band disappeared
Asymmetry and out-of-plane methyl (CH_3)	1588	Band is present as shoulder with weak intensity	Band was altered and emerged as bump with very weak intensity
Unsaturated alkyne	1840 and 2730	Bands are present as broad shoulders and with very weak intensities	Bands intensity were observed to disappeared and merged as a single broad band
CH_2 symmetry vibration	3159	Band is present with medium intensity	Band was observed to disappear
	3278	Band is present with medium intensity	Band disappeared in sample
	3435	Band is present with medium intensity	Band was observed with

			very weak intensity
	3619	Band is present with medium intensity	Band disappeared in sample

The IR spectra results of sample OA3a and sample OA3b (Table 3-3) polymer films are presented as shown in Figure 4-15. It was observed by comparison of the IR spectra for both samples OA3a (Figure 4-15a) and OA3b (Figure 4-15b) that OA3b (Figure 4-15b) experienced decrease in band intensities for some bands such as the bands located at 1840 cm^{-1} and 2370 cm^{-1}. Also, from the IR result of sample OA3b (Figure 4-15b) some bands were noted to disappear. For instance, there was complete disappearance of the transmittance band located at 1273 cm^{-1} which has been assigned to C-H. In addition, other bands that disappeared in sample OA3b include at 3159 cm^{-1}, 3278 cm^{-1}, 3435 cm^{-1} and 3619 cm^{-1}. These bands have been assigned to O-H end groups (Krim, 1960). There was no new band identified in the IR spectra of sample OA3b (Figure 4-15b). The effects of chemical etchant on sample OA3b which is acidified chromium trioxide (7 M H_2SO_4+ 3 M CrO_3) and the resulting disappearance of some IR bands in sample OA3b (Figure 4-15b) seems to indicate that as-received (commercial) PMP functional groups are selective to chemical attacks during etching. This can be attributed to the oxidising nature of chemical etchant and etching temperature on sample OA3b. However, even under these aggressive etching conditions, the bulk of the polymer structure appeared unaltered.

4.7 RESULT SUMMARY FOR ETCHED PET AND PMP POLYMER FILMS

Etching of PET and PMP polymer film showed significant variations on the surface morphology of each of the polymers and the IR analysis of these polymers film. In

the SEM analysis of sample OA1b (NaOH etched, unirradiated PET) polymer film, it was observed that there was an increase surface roughness of the film with the presence of coarse surface defects without distinct creation or presence of pores. The SEM result revealed that the surface of sample OA1b was extensively altered with the creation of surface defects. This suggests that chemical etching of PET was more effective at the surface region which could be due to the inability of the chemical etchant to penetrate into the PET polymer matrix. The etching kinetic study of sample OA1b (etched, unirradiated PET) also indicated a high weight loss as a function of etching time. It was observed that the average weight loss of PET polymer film was 8.5 % after etching for 2 hours. In the IR analysis of sample OA1b (etched, unirradiated PET) polymer film, there was continuous degradation of associated band intensities with the disappearance of peaks at 2587 cm^{-1}, 2921 cm^{-1} and 2971 cm^{-1} which have been assigned to the C-H (CH_2) functionality.

The etching of sample OA3b (etched, unirradiated PMP) polymer film observed from SEM showed the presence of surface defects with white spherical patches across polymer surface. Unlike sample OA1b (etched, unirradiated PET) in Figure 4-11b, sample OA3b (etched, unirradiated PMP) polymer film showed a low average weight loss of 2.4 % over a 2 hours etching period and this could be attributed to the chemical resistance of PMP. The IR result of sample OA3b (etched, unirradiated PMP) in Figure 4-15b polymer film showed the disappearance of several band intensities located at 1273 cm^{-1} , 3159 cm^{-1}, 3278 cm^{-1}, 3435 cm^{-1} and 3619 cm^{-1}.

4.8 CHARACTERIZATION OF SWIFT HEAVY ION IRRADIATED PET AND PMP POLYMER FILMS

The second control experiments involved the use of swift heavy ions to irradiate PET and PMP polymers. Swift heavy ions of xenon (Xe) and krypton (Kr) were used to irradiate PET and PMP polymer films respectively. In the case of PET

polymer film, the polymer film sample was *'shielded'* with Al film. The PMP polymer film was irradiated under two different irradiation procedures; *'shielded'* and *'direct'* irradiation. The details of the irradiation procedures for both *'shielded'* and *'direct'* irradiated polymer films have been explained in section 3.3.1 but will be briefly described. PMP polymer film was *'shielded'* with PET foil and thereafter irradiated with swift heavy of Kr. In the case of *'direct'* irradiation, PMP polymer film was not shielded with any material but directly irradiated wit swift heavy ion of Kr source. Although the use of swift heavy ion irradiation and chemical etching as treatment procedures on PET has been considerably investigated, however, as for PMP polymer film, there has not been any literature report on the use of swift heavy ion irradiation and chemical etching of PMP. It is therefore anticipated that the treatment of PMP under these conditions will provide unique information on specific properties of PMP in comparison with other known polyolefins such as polypropylene (PP) which has been reported in literature. During polymer irradiation, the physical, chemical, mechanical and thermal properties can be selectively or randomly altered. For instance, the various chemical bonds within the polymer structure and the effective destruction or emergence of new bonds in an orderly or randomly selective pattern can be achieved. This is because polymers are largely bonded covalently (Ulbricht *et al.*, 2006; Tjong *et al.*, 2006). The characteristics of covalent bonds include; high energies, short inter-atomic distances and relatively constant angles between the successive bond. In this section, the characterization results of swift heavy ion irradiated PET and PMP polymer films are presented. The *'shielded'* swift heavy ion irradiated PET and PMP polymer films were first simulated using the Stopping and Range of Ions in Matter (SRIM) software in order to obtain theoretical data and thereafter swift heavy ion irradiation of *'shielded'* PET and PMP polymer were experimentally determined. The results of SRIM simulated *'shielded'* swift heavy ion irradiated PET and PMP are presented and the experimentally determined swift heavy ion irradiation of *'shielded'* PET and PMP are characterized using TGA, XRD and FTIR and the results are presented. These analyses were performed on the swift

heavy ion irradiated PET and PMP polymer films after the removal of the *'shielded'* materials attached to the polymer films before being irradiated. The results of swift heavy ion *'shielded'* irradiated PET will be firstly presented followed by the results of swift heavy ion *layered'* and *'direct'* irradiated PMP. In Figure 4-16, the SRIM simulated result for *'shielded'* swift heavy ion irradiated PET (sample OA1c) is presented and discussed.

4.8.1 SRIM SIMULATED Xe ion IRRADIATION OF *'shielded'* PET (sample OA1c) POLYMER FILM

SRIM simulation was used as a theoretical model to understand the approximate conditions during swift heavy ion irradiation of *'shielded'* PET (sample OA1c) polymer film. In Figure 4-16, the results of the SRIM simulated conditions is presented and discussed.

CHAPTER 4

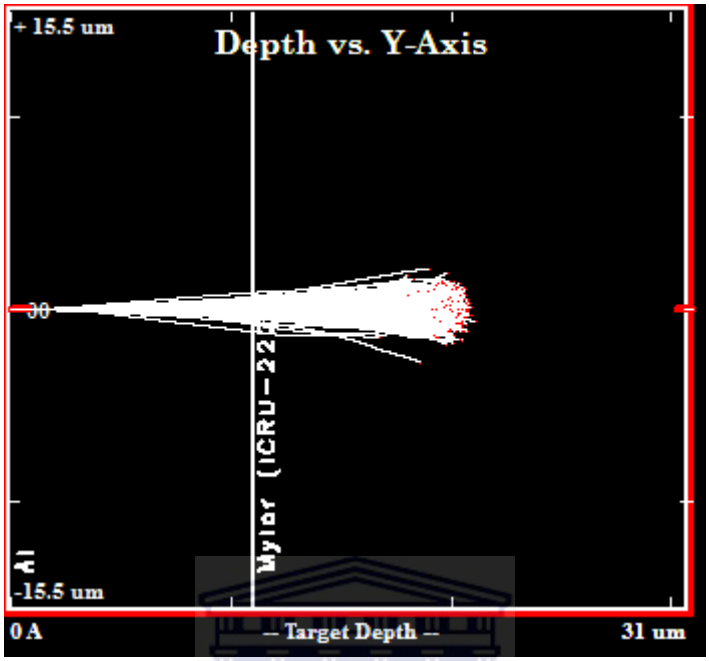

Figure 4-16: Theoretical SRIM simulated analysis for *'shielded'* swift heavy ion irradiated PET (sample OA1c) polymer film

The penetration of swift heavy ion of Xe source into *'shielded'* PET polymer film (Figure 4-16) showed that the Al foil (layer) restricted the depth of Xe ion into the PET polymer film (target depth). During SRIM analysis, the calculated Xe ion depth of into *'shielded'* PET polymer (sample OA1c) was approximately 18 µm which indicated that the Xe ion did not completely penetrate through the *'shielded'* PET polymer (sample OA1c) film. This simulated result for PET polymer film provided the basis for the choice of ion energy and shielded material. It also indicated the amount of energy loss and the maximum probable depth of Xe ion into the PET polymer film during swift heavy ion irradiation. In section 4.8.2, the TGA analysis of swift heavy ion irradiated *'shielded'* PET polymer film is presented and discussed.

CHAPTER 4

4.8.2 THERMOGRAVIMETRY (TGA) ANALYSIS OF SWIFT HEAVY ION OF XE IRRADIATED *'shielded'* PET (SAMPLE OA1c) POLYMER FILM

The impact of ion irradiation on polymers has been reported to initiate several degradations pathways within the polymer matrix and ultimately result in the deterioration of physical, chemical and thermal properties of the irradiated polymer (Jeon *et al*., 2004). The thermal properties of sample OA1c (after removal of the Al layer) with an overlay of TGA analysis of sample OA1a PET polymer film is investigated by TGA technique is presented in Figure 4-17. Figure 4-17a and 4-17b represents the TGA analysis of OA1a and OA1c samples which are as-received (commercial) PET and swift heavy ions irradiated PET polymer films respectively.

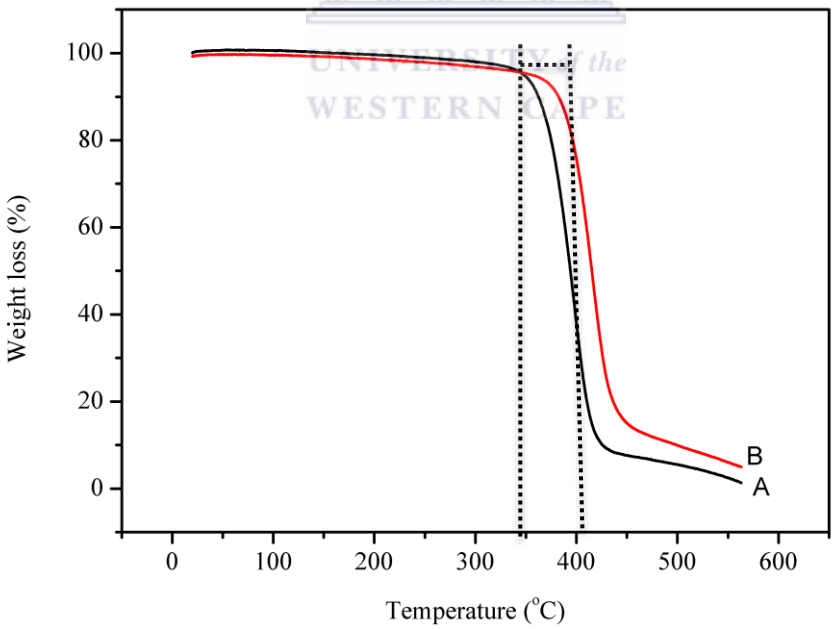

Figure 4-17: Thermal profile (TGA) analysis of (a) ASPET (sample OA1a) and (b) Xe ion irradiated PET (sample OA1c) polymer film

CHAPTER 4

The comparison of thermal stability between OA1a and OA1c polymer films showed that both sample OA1a (Figure 4-17a) and sample OA1c (Figure 4-17b) did not experience the evolution of volatile species or moisture at lower temperatures within the region of 100 ˚C. However, it was observed that sample OA1c (Figure 4-17b) started to undergo degradation at a higher temperature which resulted in an approximate increase of 50 ˚C compared with the thermal profile of sample OA1a (Figure 4-17a) polymer film. The increase in thermal stability of sample OA1c (Figure 4-17b) PET film could be attributed to a possible increase in chain rigidity due to the realignment of atoms after Xe ion interaction with PET polymer. Also, it could suggest that sample OA1c (Figure 4-17b) PET polymer thermal characteristic were affected during ion irradiation hence the observed increase in thermal stability. The Xe ion irradiation effects and more importantly the use of *'shielded'* Al foil to minimize Xe ion penetration into the polymer film could therefore be responsible for the improved thermal stability of sample OA1c (Figure 4-17b) PET polymer. In a study reported by Jeon *et al*., (2004), it was observed that PET polymer did not show any significant deterioration in its thermal profile after ion irradiation whereas the modification of PET via aminolysis by Carniero-da-Cunha *et al*., (2010) showed a decrease in thermal stability of the modified PET film. In section 4.8.3, the IR result of swift heavy ion *'shielded'* irradiated PET polymer film (sample OA1c) will be presented and compared with the IR result of sample OA1a.

4.8.3 FTIR SPECTROSCOPY OF SWIFT HEAVY ION OF XE IRRADIATED *'shielded'* PET (SAMPLE OA1c) POLYMER FILM

In this section, the IR (overlay) spectra result of sample OA1a and OA1c will be presented and discussed. The affected functional groups within polymer structure can be identified using IR technique hence this result will be compared with other studies that have been previously reported especially during polymer irradiation. The IR spectra result of samples OA1a and OA1c film is presented in Figure 4-18.

CHAPTER 4

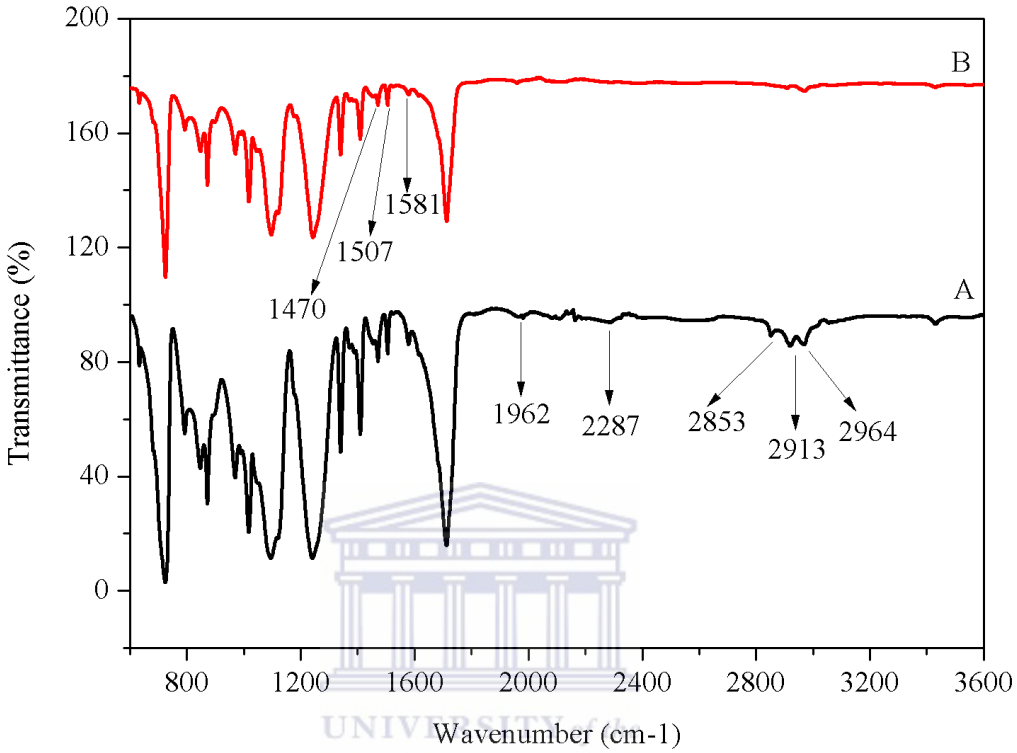

Figure 4-18: IR spectra (a) ASPET (sample OA1a) and (b) swift heavy ion irradiated *'shielded'* PET(sample OA1c) polymer film

In Figure 4-18, the IR spectra of OA1a and OA1c (Table 3-3) polymer film is presented. The characteristic peaks associated with some of the functional groups of PET were lost or less intense after swift heavy ion irradiation of the *'shielded'* irradiated PET polymer as seen for sample OA1c in Figure 4-18b. Also, in Figure 4-18b, the characteristic weak bands at 2853 cm^{-1}, 2913 cm^{-1} and 2964 cm^{-1} assigned to CH_2 (stretching), CH_2 (bending) and CH_3 (stretching) respectively (Krimm, 1960) were almost invisible for sample OA1c after swift heavy ion irradiation compared with sample OA1a in Figure 4-18a. The probable locations of chain scissions due to swift heavy irradiation of PET polymer film have been represented in Figure 4-19 while the respective fragments after the bond breakage have been highlighted in Figure 4-20. The predictions of the chain scission were

based on the band intensities from IR analysis. The IR analysis of sample OA1c (Figure 4.18b) suggests that swift heavy ion irradiation on PET polymer results in the selective depletion of some species within the polymer matrix which has also been reported by Liu *et al.*, (2000) and Abdesselam *et al.*, (2008). Also, the reduction in transmittance bands intensity associated with ethylene glycol residue at 1470 cm^{-1} of sample OA1c (Figure 4-18b) compared with sample OA1a (Figure 4-18a) has been reported to correspond with an increase in the amorphization of PET since this band is characteristic of the crystallinity of the polymer (Ciesla and Satrosta, 1995; Liu *et al*., 2000). In Figure 4-19, the probable chain scission location along the PET structure is presented and briefly discussed. Also, the associated fragment of different functional groups is presented in Figure 4-20.

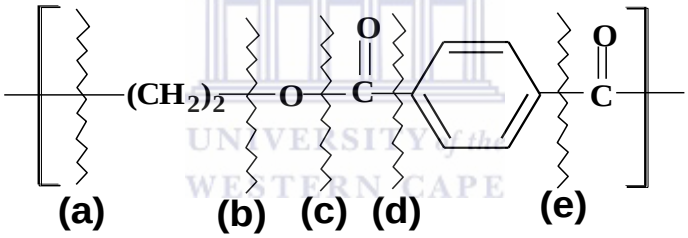

Figure 4-19: Probable chain scission locations (a), (b), (c), (d) and (e) in PET polymer during swift heavy ion irradiation

The effects of swift heavy ion on *'shielded'* swift heavy ion irradiated PET polymer film showed the possible locations of attack by the swift heavy ions within the PET structure. These selected locations have been identified by the IR analysis in Figure 4-18 and it was observed that the almost all the band intensities decreased after swift heavy ion irradiation of *'shielded'* PET polymer except for the bands located at 2853 cm^{-1}, 2913 cm^{-1} and 2964 cm^{-1} which completely disappeared. These bands have been assigned to CH_2 (stretching), CH_2 (bending) and CH_3 (stretching) respectively. The disappearance of these bands may be attributed to the rigidity behaviour of the PET back bone structure which is mainly the aromatic ring according to Burgess *et al.*, 2014. In Figure 4-20, the various functional groups

including radicals of *'shielded'* swift heavy ion irradiated PET polymer are presented.

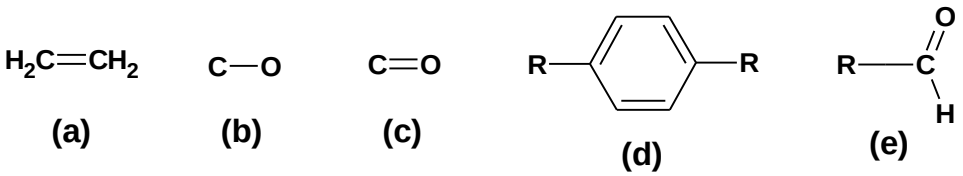

Figure 4-20: Fragments of functional groups from PET structure after swift heavy ion irradiation

The effects of swift heavy ion irradiation of *'shielded'* PET polymer film (Figure 4-20) identified *various* bond breakages resulting in the characteristic functional groups present within the PET backbone and side chain functional groups. The identified functional groups in the as-received PET (sample OA1a) have been compared with the *'shielded'* swift heavy ion irradiated PET (sample OA1c) presented and discussed in the IR analysis in Figure 4-18. In Table 4-5, the corresponding peak assignments for selected functional groups are described.

Table 4-5: Selected functional groups in PET polymer film and their corresponding wavenumbers

		Sample code	
Functional group assignment	**Wavenumber (cm^{-1})**	OA1a	OA1c
Ethylene glycol residue	1470	Band present with medium intensity	Band unaltered and did not shift but with very weak intensity
Para-substituted aromatics	1507	Band present with medium intensity	Band unaltered and did not shift but with very weak intensity
Asymmetry out-of-plane methyl (CH_3)	1581	Band is present but with very weak intensity	Band almost disappeared
Unsaturated alkyne	1962	Band present and very weak intensity	Band is altered resulting in complete disappearance
CH_2 (stretching) symmetry vibration	2287 2853	Band present and very weak intensity	Band is altered with complete disappearance
CH_2 (bending) symmetry vibration	2913	Band present and very weak intensity	Band is altered with complete disappearance

CH_3 (stretching) symmetry vibration	2964	Band present and very weak intensity	Band is altered with complete disappearance

The identities of the bands from the IR spectra obtained in Figure 4-18 showed the variation in the band intensities after swift heavy ion irradiation of *'shielded'* PET polymer (sample OA1c) in comparison with the as-received PET polymer (sample OA1a) in Table 4-5. The IR results which indicated changes in band intensities for sample OA1c have been previously presented and discussed in Figure 4-18.

In the next section, the SRIM (4.8.4) simulated result of *'shielded'* (sample OA3c) and *'direct'* (sample OA3d) swift heavy ion of Kr irradiated PMP polymer film is presented. Also, the TGA (4.8.5) and FTIR (4.8.6) analysis of *'shielded'* (sample OA3c) and *'direct'* (sample OA3d) swift heavy ion of Kr irradiated PMP polymer film will be presented and discussed. The irradiated PMP polymer film was performed under two different conditions; *'shielded'* irradiation and *'direct'* irradiation. The details of Kr ion irradiation conditions of both *'shielded'* and *'direct'* irradiated PMP have been described in section 3.3.1 and Table 3-3.

4.8.4 SRIM SIMULATED Kr ion IRRADIATION OF *'shielded'* AND *'direct'* PMP (sample OA3c and OA3d) POLYMER FILM

SRIM analysis of PMP of both *'shielded'* and *'direct'* swift heavy ion irradiated samples was investigated in order to generated theoretical data as well as understand the importance of layering material and determine the penetration capacity of the swift heavy ion prior to laboratory experiments. In Figure 4-21, the SRIM analysis of *'shielded'* swift heavy ion irradiated PMP polymer film is presented and briefly discussed while Figure 4-22 represents the SRIM result of *'direct'* swift heavy ion irradiated PMP polymer film.

CHAPTER 4

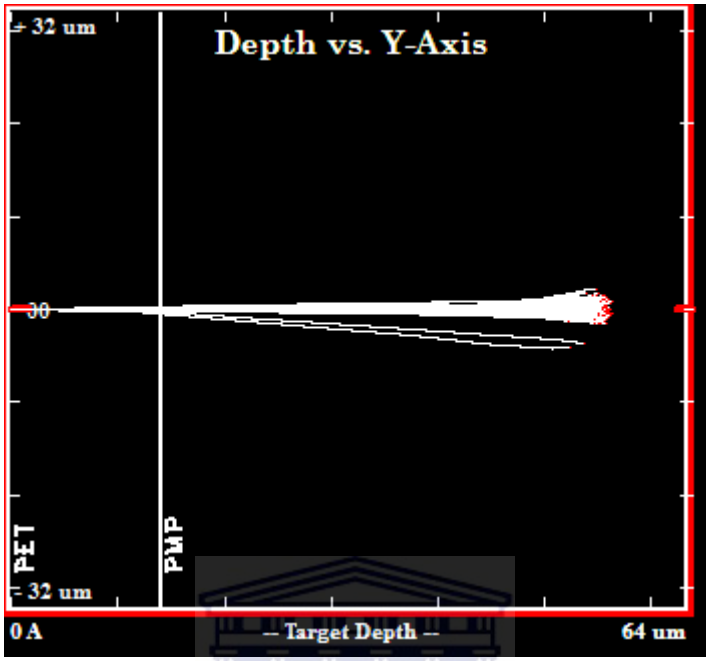

Figure 4-21: Theoretical SRIM simulated analysis of *'shielded'* swift heavy ion irradiated PMP

The use of PET foil as a shielded material on PMP (Figure 4-21) polymer prior to swift heavy ion irradiation by SRIM showed that the swift heavy ion of Kr source penetrated completely through the shielded material (PET foil) and also significantly into the target material i.e. PMP polymer film but not completely through the PMP polymer film as seen in Figure 4-21. In addition, the SRIM estimated average longitudinal ion depth was 54 µm which implies that the experimental swift heavy ion irradiation will result in the Kr ion not penetrating completely through the PMP polymer film. In Figure 4-22, the *'direct'* swift heavy ion irradiated PMP polymer film is presented.

CHAPTER 4

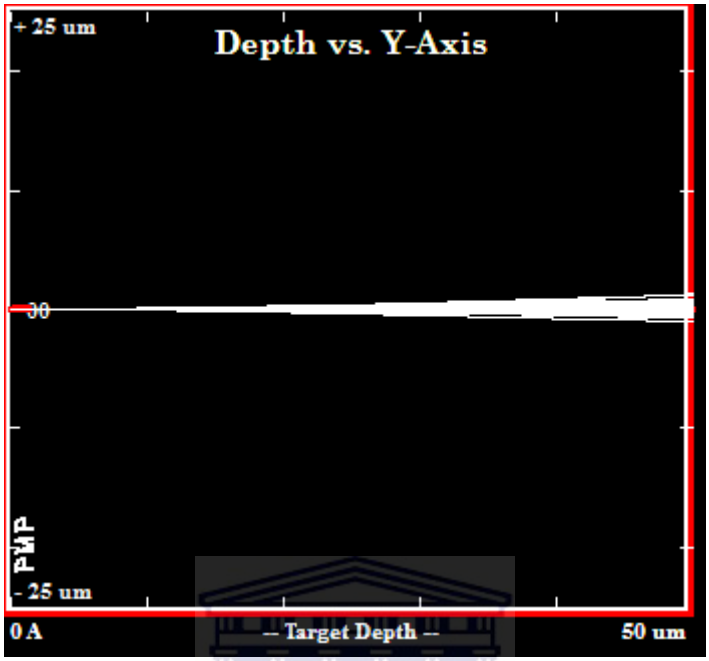

Figure 4-22: Theoretical SRIM analysis of swift heavy ion irradiated PMP

It was seen from Figure 4-22 that the SRIM simulated analysis of *'direct'* swift heavy ion irradiated PMP resulted in a complete penetration of swift heavy ion of Kr source through the PMP polymer film. Unlike the SRIM analysis in Figure 4-21, the Kr ion source in Figure 4-22 did not loss all of its energy within the PMP polymer film. In the case of *'direct'* swift heavy ion irradiated PMP (Figure 4-22), the stopping power against the irradiation ion is only from PMP polymer since it does not have any shielded surface as *'shielded'* swift heavy ion irradiated PMP in Figure 4-21. This implies that the depth of Kr ion could not be restricted with the PMP polymer. Also, the energy of Kr ion could have been high enough to ensure that swift heavy Kr completely penetrate the PMP polymer film.

CHAPTER 4

4.8.5 THERMOGRAVIMETRY (TGA) ANALYSIS OF SWIFT HEAVY KR ION IRRADIATED PMP (SAMPLES OA3c and OA3d) POLYMER FILM

In this section, the thermal analysis (TGA) results of ASPMP, *'shielded'* and *'direct'* swift heavy ion irradiated PMP polymer films which are sample OA3a, OA3c and OA3d respectively will be presented. The thermal stability of polymers is crucial to their applications considering the variation in environmental conditions that they may be exposed to. It is therefore important that polymers do not undergo significant change in thermal stability or even have thermal properties improved after modifications such as ion irradiation. The prevailing reaction mechanism during modification can trigger several reaction mechanisms and have an overall effect on polymer thermal properties. PMP polymer film was irradiated under two different conditions; *layered* and *'direct'* irradiation. In the *'shielded'* PMP polymer film, PET foil was used as *'shielded'* material and the *'direct'* irradiated PMP was performed without any shielded material. The TGA profile analysis of ASPMP (Figure 4-23a) with swift heavy ion irradiated PMP polymer films for samples OA3c (Figure 4-23b) and sample OA3d (Figure 4-23c) are presented in Figure 4-23. Sample OA3c represents *'shielded'* irradiated PMP polymer and sample OA3d was *'direct'* irradiated PMP polymer film.

CHAPTER 4

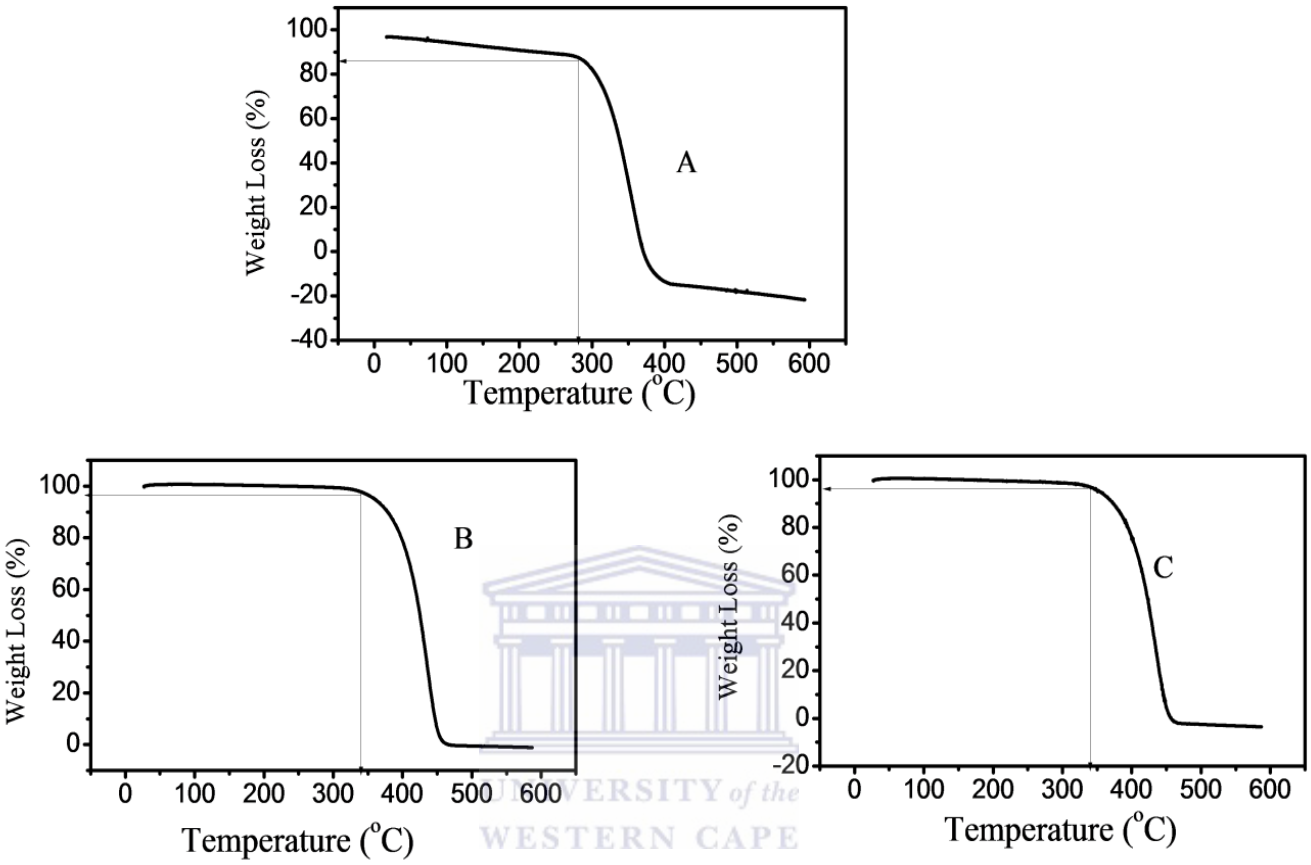

Figure 4-23: TGA analysis of (a) ASPMP polymer, (b) *'layered'* irradiated PMP (sample OA3c) and (c) *'directly'* irradiated PMP polymer film (sample OA3d)

The thermal analysis (weight loss and degradation pattern) of ASPMP (sample OA3a) as presented in Figure 4-23a showed the slow and gradual evolution of volatile species between 20 ˚C and 300 ˚C with a weight loss of about 20 %. The thermal stability of sample OA3a indicated a single thermal degradation which started at about 300 ˚C up to 375 ˚C. In Figure 4-23b and 4-23c which represented *'shielded'* and *'direct'* swift heavy ion irradiated PMP polymer film, it was observed that there was an improvement in the thermal stability by approximately 50 ˚C in stability before degradation for the swift heavy ion irradiated PMP polymer

i.e. samples OA3c (Figure 4-23b) and OA3d (Figure 4-23c) compared with the ASPMP (Figure 4-23a) i.e. sample OA3a. Also, the TGA analysis of swift heavy ion irradiated PMP film samples OA3c (Figure 4-23b) and OA3d (Figure 4-23c) did not show any difference in their thermal stability as well as very little mass loss for both swift heavy ion irradiated PMP polymer film samples. The single thermal degradation of both swift heavy ion irradiated PMP films i.e. sample OA3c and OA3d in Figure 4-23b and Figure 4-23c respectively showed that the thermal profile of PMP was not affected by the two methods of swift heavy ion irradiation applied i.e. *'shielded'* and *'direct'* irradiated PMP polymer films. This is unique because the process of interaction between swift heavy ions and polymer film has been reported to depend on irradiation conditions such ion dose, fluence as well as the irradiated polymer structural configuration including the composition of polymer side chains (Jeon *et al*., 2004). Also, the swift heavy ion irradiation of polyolefins has been reported to initiate scission of C-C and C-H bonds resulting in the formation of alkyl and allyl radicals which are stable in vacuum and can as well recombine (Hama *et al*., 1996; Murray *et al*., 2013). It therefore seems that the alkyl and ally radicals which are presented in Figure 4-26a and 4-26b generated in the swift heavy ion irradiated PMP polymer matrix could have diffused into the polymer matrix hence improve the thermal stability for both samples OA3c and OA3d (swift heavy ion irradiated PMP) polymer film. In section 4.8.6, the IR results of swift heavy ion irradiated PMP will be presented and discussed.

4.8.6 FTIR SPECTROSCOPY OF KR IONS IRRADIATED *'shielded'* PMP (SAMPLES OA3c and OA3d) POLYMER FILM

The use of Kr ion irradiation to modify PMP polymer film has not been reported in literature. In this section, the FTIR results of the swift heavy ion irradiated PMP polymer films are presented. The use of IR analysis to investigate polymers especially PMP can provide insight into the inter-molecular and intra-molecular interactions. Another important point to note about the interactions (intra and inter)

and ion-polymer interaction especially for PMP is that it has two (2) main potential sites of attack due to the presence of the tertiary carbon located on the polymer backbone and in the pendant isobutyl group (EL-Naggar *et al*., 1990). In addition, Samuel and Mohan (2004) have provided an elaborate IR analysis of PMP which be employed to assign the different IR bands in this section. The study by Samuel and Mohan (2004) discussed 3 (three) modes of vibrational spectroscopy unique to this class of polyolefin polymer. These 3 (three) modes are; side chain, main chain and mixture of both the side and main chains. The IR spectra results of ASPMP and swift heavy ion irradiated PMP polymer films are presented in Figure 4-24. In Figure 4-24a, 4-24b and 4-24c, the IR spectra overlay correspond to ASPMP (sample OA3a), *'shielded'* OA3c (Figure 4-24b) and *'direct'* sample OA3d (Figure 4-24b) Kr ions irradiated PMP polymer film respectively.

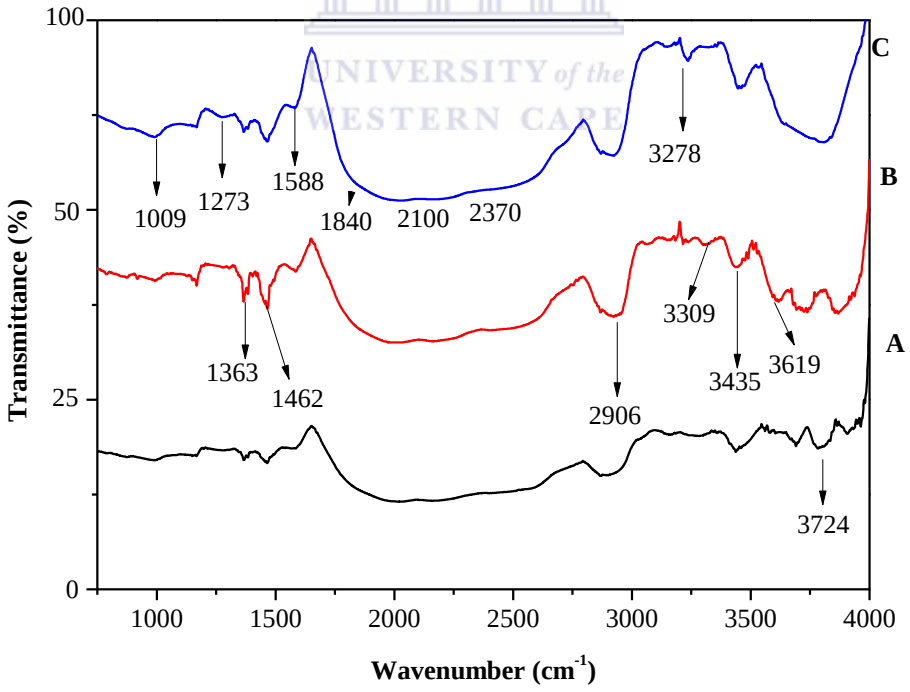

Figure 4-24: IR spectra analysis of (a) ASPMP, (b) *'layered'* PMP polymer film irradiated with Kr ion irradiated (sample OA3c) and (c) PMP polymer film *'directly'* irradiated with Kr ion without layering (sample OA3d)

CHAPTER 4

The IR analysis of ASPMP (sample OA3a) in Figure 4-24a revealed the presence of the following functional groups; 1009 cm^{-1} (CH_3 rocking), 1170 cm^{-1} (CH_3 wagging), 1368 cm^{-1} and 1468 cm^{-1} (asymmetry and out-of-plane CH_3 bend alkene), 1840 cm^{-1} and 2370 cm^{-1} (unsaturated alkyne), 2873 cm^{-1} (CH_2 symmetry vibration), 2948 cm^{-1} and 3165 cm^{-1} (methylene (CH_2) asymmetrical stretch). The *'shielded'* swift heavy ion irradiated PMP polymer film (sample OA3c) in Figure 4-24b showed the emergence of new band with weak intensity at 1273 cm^{-1} (unsaturated C-H). Also, a shift in band intensities was observed at 1363 cm^{-1} and 1462 cm^{-1} which have been assigned to asymmetry and out-of-plane methyl compared with sample OA3a (ASPMP) polymer film. The *'shielded'* swift heavy ion irradiated PMP polymer film (sample OA3c) in Figure 4-24b showed bands at 2906 cm^{-1} (CH_2 asymmetry stretching of alkanes) with strong intensity as well as a new weaker band at 3309 cm^{-1} (hydroxyl group). The IR analysis of *'direct'* swift heavy ion irradiated PMP (sample OA3d) polymer film in Figure 4-24c indicated broad band at 1840 cm^{-1} and 2370 cm^{-1} (unsaturated alkyne). Also, the bands at 3435 cm^{-1}, 3619 cm^{-1} and 3724 cm^{-1} have been assigned to CH_2 symmetry vibration. Figure 4-25 represents the probable chain scission location of PMP polymer after swift heavy ion irradiation.

CHAPTER 4

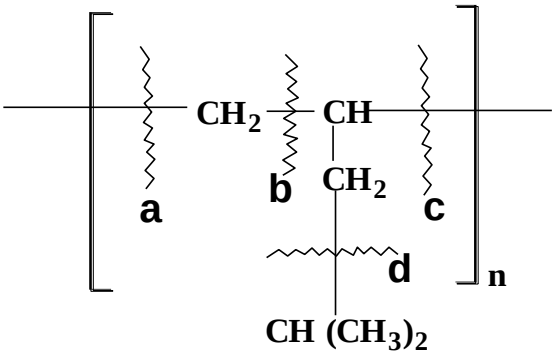

Figure 4-25: Probable chain scission locations on PMP polymer structure locations after swift heavy ion irradiation

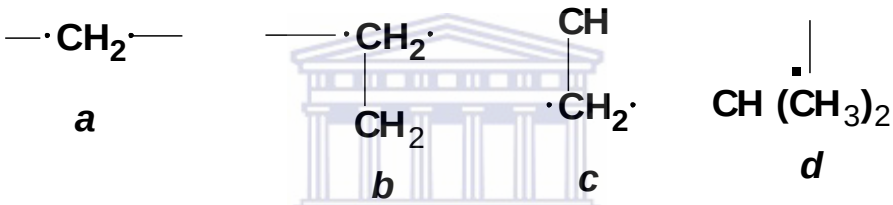

Figure 4-26: Fragments of moieties from PMP structure after swift heavy ion irradiation

The probable chain scission locations in PMP polymer after swift heavy ion irradiation (Figure 4-25) showed that the available fragment of moieties from PMP polymer due to swift heavy ion irradiation resulted in mainly unsaturated chains such as alkyl, allyl, methylene etc (Figure 4-26). The locations and available fragment of the functional groups have been confirmed from the IR analysis of sample OA3a, OA3c and OA3d in Figure 4-21. In Table 4-6, the comparison of band intensities for samples OA3a (ASPMP), OA3c (*'shielded'* swift heavy ion irradiated) and OA3d (*'direct'* swift heavy ion irradiated) PMP polymer film is presented. The table describes the changes in the band intensities as well as the emergence of new and disappearance of existing bands.

CHAPTER 4

Table 4-6: Comparison of selected functional groups for samples OA3a, OA3c and OA3d PMP polymer film

		Sample code		
Functional group assignment	**Wavenumber (cm^{-1})**	OA3a	OA3c	OA3d
Methyl (CH_3) rocking	1009	Band is not present	Present with weak intensity	Present with weak intensity
C-H	1273	Band is not present	Band not present	Present as a bump with weak intensity
Asymmetry and out-of-plane CH_3 bending	1363	Band is present with weak intensity	Present with medium intensity	Present with weak intensity
	1462	Band is present with weak intensity	Present with medium intensity	Present with weak intensity
Asymmetry and out-of-plane methyl (CH_3)	1588	Band is present with weak intensity	Band is present with weak intensity	Band is present with bump of weak intensity
Unsaturated alkyne	1840 2730	Band is present as broad and with weak intensity	Band intensity is Unaltered	Band intensity is Unaltered
	2906	Band is present with weak intensity	Present and unaltered but	Present and unaltered but

			with medium intensity	with medium intensity
CH_2 symmetry vibration	3278	Band is not present	Band is not present	Band is present but with weak intensity
	3435	Band is present with weak intensity	Band is present and unaltered in intensity	Band is present and unaltered in intensity
	3619	Band is not present	Band is present and with weak intensity	Band is not present

It was observed that the irradiation of PMP polymer film with swift heavy ion of Kr ions (OA3c and OA3d) and unirradiated PMP polymer film (OA3a) polymer film showed specific variations with the emergence of band bands at 1273 cm^{-1} and 3278 cm^{-1} for samples OA3c and OA3d respectively compared with sample OA3a of the PMP polymer film. Otherwise, the other bands such as 1363 cm^{-1} and 1468 cm^{-1} experienced a shift for samples OA3c and OA3d PMP polymer films. The IR analysis of samples OA3a, OA3c and OA3d showed that the main functional groups are unsaturated C-H confined within the alkenes and alkynes functional groups (Samuel and Mohan, 2004). As expected, the effects of heavy ions on sample OA3d seems to have significant effect and this could be due to the stopping power (ion energy loss) of the PMP polymer film and its overall intensity effect within the polymer side and main chains. The resultant effect of "*layer*" and "*direct*" irradiation approaches seem to have varying effects on the PMP configurations with the generation of more unsaturated species associated with PMP from the IR analysis of sample OA3c in Figure 4-24b. This could be due to the ease of bond breakage in the surface or near surface regions of functional groups present in PMP structure.

CHAPTER 4

4.8.7 RESULT SUMMARY FOR SWIFT HEAVY ION IRRADIATED PET AND PMP POLYMER FILM

The effects of swift heavy ion irradiated PET and PMP polymer films have been investigated and considered within thermal profile and IR analysis of the polymer films. The thermal studies of swift heavy ion irradiated PET (sample OA1c) showed an improved thermal stability compared with the ASPET (sample OA1a) polymer film. The thermal stability of swift heavy ion irradiated PET (sample OA1c) was approximately 50 ˚C higher than the sample OA1a PET polymer film. The IR analysis of sample OA1a and OA1c showed overall reduction in band intensities along with the presence of weak bands at 2853 cm^{-1}, 2913 cm^{-1} and 2964 cm^{-1} assigned to CH_2 (stretching), CH_2 (bending) and CH_3 (stretching) respectively. The TGA and IR results of the swift heavy ion irradiated PMP (samples OA3c and OA3d) polymer showed that the thermal profile analysis of PMP polymer was unaltered by the two methods of swift heavy ion irradiation i.e. *'shielded'* and *'direct'* irradiation. However, the thermal profiles of ion irradiated PMP (samples OA3c and OA3d) film increased by approximately 14 % in thermal stability above 400 ˚C compared with ASPMP (sample OA3a). The IR results of ion irradiated PMP (sample OA3c and sample OA3d) polymer films were observed to result in the presence new band intensities at 1273 cm^{-1} and 3278 cm^{-1} for samples OA3c and OA3d respectively. Also, there were shift in band for samples OA3c and OA3d.

4.9 CHAPTER SUMMARY

The results obtained from the analysis of as-received (commercial) PET and PMP polymer films has provided an insight into the individual effects of chemical etching and ion irradiation on the polymers. The degradation of as-received (commercial) PET due to chemical etching and ion irradiation experiments was observed. This suggests that the as-received (commercial) PET film is highly susceptibility to modifications by either route. The functional groups' identities

obtained by IR technique indicated overall depletion of all functional groups that exist within the PET polymer matrix during swift heavy ion irradiation. This suggests that the polymer backbone structure and side chain could have been distorted. Also, the thermal studies showed an improvement in thermal stability of the swift heavy ion irradiated PET polymer by extra 50 ˚C between the chemically etched and ion irradiated PET polymer.

The as-received (commercial) PMP polymer film was not easily degraded as observed in the chemical etching kinetics measurement, IR and TGA results presented in this chapter. This can be attributed to the inertness of polyolefin. Also, the surface morphology studies and roughness of etched as-received (commercial) PMP polymer film did not indicate distinct surface irregularity or presence of pores but solubility of surface species were observed. This was attributed to the slow etching rate due to the chemical inertness of the polymer. The IR spectra results of ASPMP (OA3a) and swift heavy ion irradiated PMP (OA3c and OA3d) polymer showed the emergence of new functional groups and a shift in band intensities for samples OA3c and OA3d PMP polymer films. Lastly, the etching kinetic studies for as-received (commercial) PET and PMP polymer films showed that the degree of polymer deterioration in chemical etchant differs significantly and much higher with PET than PMP. This is because of the distinct variation in the etchant concentration and composition as well as the types of polymers. In the next chapter, the results of track-etched analysis of as-received (commercial) PET and PMP polymers film will be presented and discussed.

CHAPTER 5

CHAPTER FIVE

5 CHARACTERIZATION OF *'shielded'* SWIFT HEAVY ION IRRADIATED ETCHED POLYETHYLENE TEREPHTHALATE (PET) AND POLYMETHYL PENTENE (PMP) POLYMER FILMS

5.1 INTRODUCTION

This chapter will present the characterization results of track-etched PET and PMP polymer films. Traditionally, track-etching is a procedure which involves swift heavy ion irradiation of polymer film and the polymer film is thereafter treated with appropriate chemical solutions in order to reveal the ion irradiated regions with the formation of pores along the path of the ion track within the polymer. The PET and PMP polymer films that were etched and investigated in this section were the swift heavy ion irradiated *'shielded'* PET and PMP polymer films. The ion irradiated polymers were then etched in chemical solutions. Xe ion irradiated *'shielded'* PET polymer film was etched in 1 M NaOH at 80 ˚C up to a maximum etching time of 12 minutes at 3 minutes intervals. Also, the swift heavy ion irradiated *'shielded'* PMP polymer film was etched in acidified chromium oxide (7 M H_2SO_4 + 3 M CrO_3) solutions for up to 2 hours 30 minutes at 30 minutes intervals and the etching temperature was varied between 60 ˚C and 80 ˚C . The ion irradiation and chemical etching experimental procedures used in this study to treat PET and PMP polymer films have been described in sections 3.3.1 and 3.3.2. This chapter describes the various analytical techniques used to investigate morphological, chemical and thermal properties of track-etched PET and PMP polymer films by SEM, FTIR, TGA and XRD analytical techniques. In addition, etching kinetic (i.e. weight loss as a function of etching time) study was performed on the track-etched PET and PMP polymer film. However, the etching kinetic study was limited to track-etched PMP polymer film. This was because of ease of weight loss experienced by the irradiated PET polymer film during chemical etching after

CHAPTER 5

12 minutes. The results of each characterization for the track-etched PET and PMP polymer films will be presented and discussed.

5.2 CHARACTERIZATION OF *'shielded'* SWIFT HEAVY ION IRRADIATED ETCHED PET POLYMER FILM

Track-etched PET polymer film has been extensively studied and the overall effects of swift heavy ion and chemical etching on polymer physical, chemical, thermal and morphological properties have been discussed. In this section, the characterization results of track-etched *'shielded'* PET i.e. samples OA2a, OA2b, OA2c and OA2d (Table 3-3) will be presented and discussed. These samples were swift heavy ion irradiated *'shielded'* PET polymer films etched in 1 M NaOH solution at 80 ˚C for maximum duration of 12 minutes at different etching time intervals. The code for each sample indicates the duration of etching time i.e. 3, 6, 9 and 12 minutes etching for samples OA2a, OA2b, OA2c and OA2d respectively. The characterization of track-etched PET polymer films will be investigated using SEM, XRD and FTIR techniques.

5.3 SCANNING ELECTRON MICROSCOPY MORPHOLOGY ANALYSIS OF *'shielded'* SWIFT HEAVY ION IRRADIATED ETCHED PET POLYMER FILM

Scanning electron microscopy (SEM) is traditionally used to probe the surface morphology of solid samples. This analytical technique has been regarded to be a powerful tool as it facilitates visual inspection of sample surface topography. As for track-etched polymers, SEM can be used to correlate the emergence of surface deformities and microscopic changes (Aggarwal *et al*., 2012) resulting from the exposure of polymers to surface modifications such as swift heavy ion irradiations and chemical etching. Also, the SEM analytical technique is used to investigate the general profile of pores i.e. shape, size and distribution including depth and the

presence of surface defects due to pores. The surface morphology of track-etched polymer film helps to understand the effects of swift heavy ion irradiation as well as the chemical etching process. In Figure 5-1, the SEM analysis of ASPET (sample OA1a) and compared with the SEM micrograph results of track-etched PET (samples OA2a, OA2b, OA2c and OA2d) polymer films is presented.

CHAPTER 5

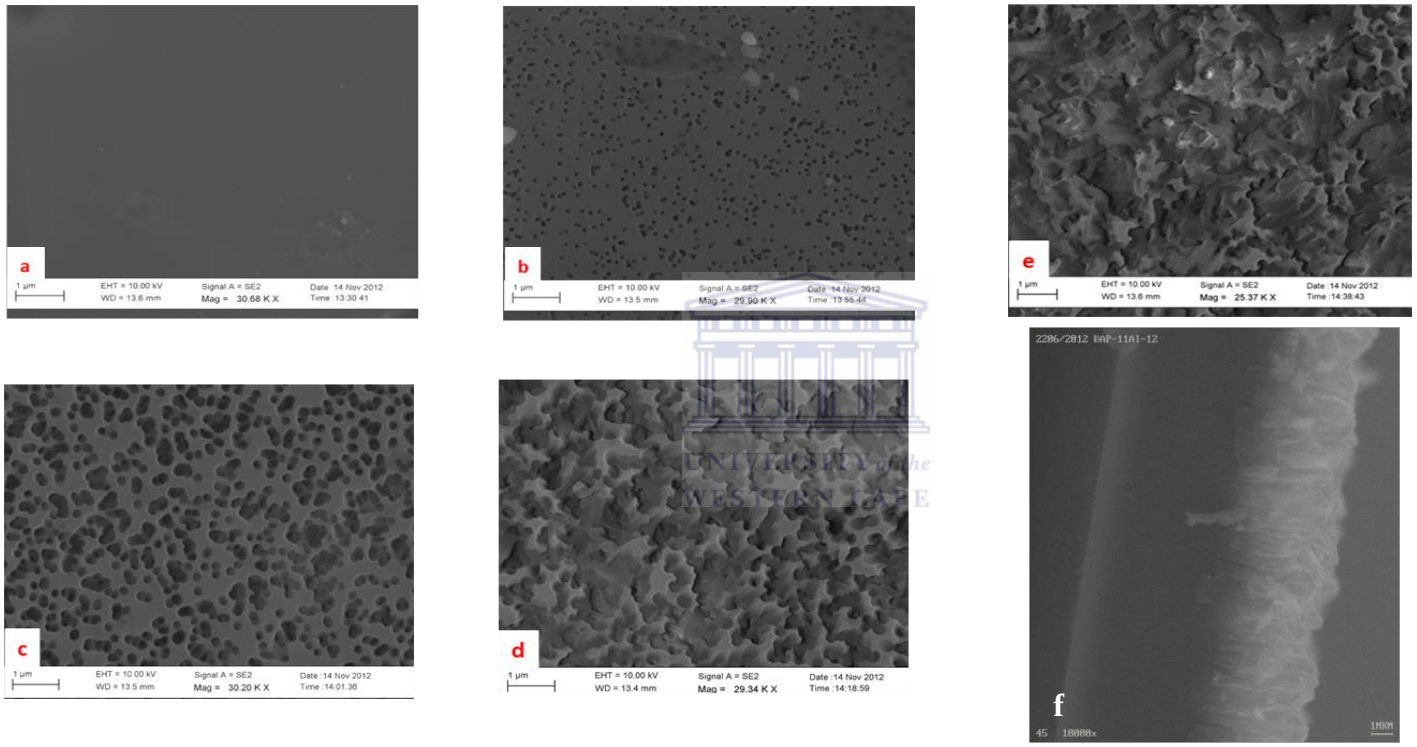

Figure 5-1: SEM micrograph surface morphology of (a) ASPET (OA1a), *'shielded'* swift heavy ion irradiated etched PET polymer film (b) OA2a, (c) OA2b, (d) OA2c and (e) OA2d due to various etching time and (f) SEM cross-section of sample OA2d PET polymer film

CHAPTER 5

It was observed that sample OA1c i.e. unetched irradiated PET polymer film (Fig. 5-1a) showed a smooth surface without any visible defects such as formation of pores or emergence of blisters. The absence of blisters as well as distinct surface roughness can indicate that the swift heavy ion irradiated PET (sample OA1c) polymer film did not experience the escape of volatile species as was confirmed with the IR and TGA results in Figures 4-16 and 4-17. The effect of chemical etching on irradiated polymer is often related to the emergence of pores on polymer surfaces. As a result, after 3 minutes etching swift heavy ion irradiated PET polymer (sample OA2a) in Figure 5.1b, surface pores of sample OA2a was observed to increase although with uniform size and evenly distributed on ion irradiated PET polymer film. Also, the pores appeared as isolated and are mono dispersed and mostly with circular shapes. In Figure 5-1c, the SEM micrograph image of sample OA2b showed a gradual increase in pore size after 6 minutes of etching which in turn resulted in the presence of bi-circular pores on the track-etched PET polymer film surface. Also, the pores were moderately irregular in shape with increased surface roughness but the single pore shapes were still maintained in circular forms. Although sample OA2a (Figure 5-1b) showed a fairly smooth surface due to the uniformity of pores compared with sample OA2b, the early formation of pore observed for sample OA2b surface after 3 minutes of etching at 80 ˚C suggests that the chemical resistance properties of PET polymer is low and this could be due to the ion energy loss within the polymer film and the aggressive NaOH etchant used. In Figure 5-1d, the SEM micrograph of sample OA2c showed an increase in pore geometry after the 9 minutes of chemical etching. The pores were observed to experience extensive overlapping with multi-connected pores and the continuous chemical attack on ion irradiated PET film resulted in distorted and irregularly shaped pores with eroded pore surface. The *'widening'* of pores could also indicate that the track-core regions extended into the swift heavy ion irradiated PET polymer matrix hence the increase in etch rate (Apel, 2001).

CHAPTER 5

Figure 5-1e represents sample OA2d for 12 minutes etching of track-etched PET polymer film. The progressive enlargement of the pores by the etchant increased the surface roughness of the PET film due to the amalgamation of voids as pores enlarged was observed in sample OA2d (Figure 5-1e). The SEM images of sample OA2d showed that after 12 minutes of etching, the pore profiles (shape and geometry) were compromised and resulted in highly disfigured '*undefined*' pores shape with extremely irregular orientation. Although the pores were undefined and highly irregular, sample OA2d was observed to still retain its asymmetrical membrane structure. It was observed that an increase in etching time has a direct influence on the overall pore geometry as seen with the transformation of pores on the surface of the ion irradiated PET polymer film i.e. defined orientation to defaced undefined pore geometry. The etching conditions (etchant concentration, etching time and temperature) on ion irradiated PET and the subsequent surface defects such as pore geometry and dramatic weight loss indicated the low resistance of PET to chemical etching as were shown in the analysis of unirradiated PET samples (OA1a and OA1b). Also, the degree of transformation of the pore shape on the swift heavy ion irradiated PET could be as a result of the uneven distribution or rate of energy loss of ions during irradiation. This is because during swift heavy ion irradiation of polymers, the ion induced changes are known as track *'core'* and track *'halo'* areas of the polymer hence during chemical etching the rate of etching on track *'core'* regions is faster than in the track *'halo'*. However, due to swift heavy ion irradiation, the fragility of damaged bonds within the main and side chains of irradiated PET could be responsible for the overall functional group susceptibility to etching even under mild conditions. This behaviour of polymer was explained by Aggarwal *et al*., 2012 in which both etchant concentration and time of etching must be carefully controlled within restricted parameters of time and temperature in order not to completely destroy the surface structure. The importance of controlled pore profile is significant in polymer applicability for gas separation i.e. improved polymer permeability and selectivity properties. It is interesting to

CHAPTER 5

observe that even in the case of the most intensely altered PET surface after 12 minutes of etching, the SEM cross-sectional measurement by Image J software of sample OA2d (Figure 5-1f) showed anisotropic *'dissimilar'* layers with about 65 % dense layer of PET remaining whereas surface morphology (Figure 5-1e) study showed completely irregular pore geometry. This was attributed to the use of *'shield'* material on PET polymer film surface prior to swift heavy ion irradiation. The stopping power of both *'shield'* material and PET polymer film restricted the ion depth penetration into the polymer film during swift heavy ion irradiation.

5.4 X-RAY DIFFRACTION ANALYSIS OF *'shielded'* SWIFT HEAVY ION IRRADIATED ETCHED PET POLYMER FILM

It is well known that polymer crystalline properties influence the final applicability of the polymer whereas the distortion of atomic orientation within the polymer structure due to multiple modifications can be investigated using the XRD technique. In Figure 5-2, the XRD results of ASPET (sample OA1a) and *'shielded'* swift heavy ion irradiated and etched PET (samples OA2a, OA2b, OA2c and OA2d) polymer films is presented and discussed. Samples OA2a, OA2b, OA2c and OA2d represent the swift heavy ion irradiated PET polymer films etched in 1 M NaOH at 80 ˚C for 3, 6, 9 and 12 minutes respectively.

CHAPTER 5

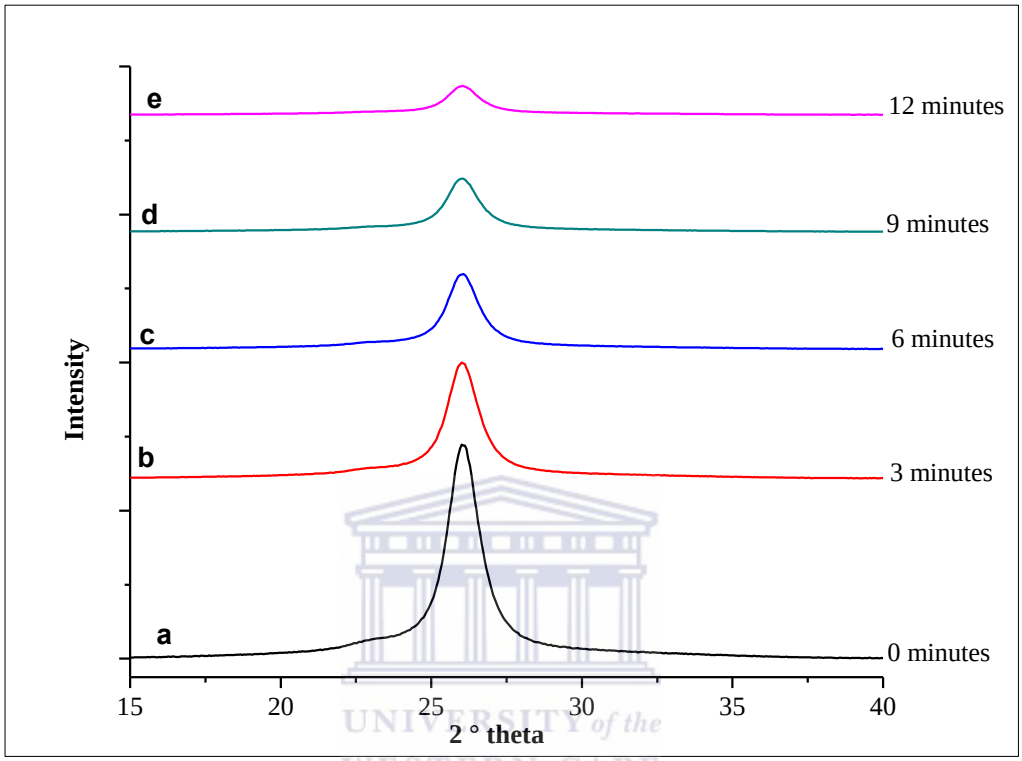

Figure 5-2: X-ray diffraction analysis of (a) ASPET, (sample OA1a) and *'shielded'* swift heavy ion irradiated etched PET polymer film (b) OA2a, (c) OA2b, (d) OA2c and (e) OA2d as a function of various etching time

A single diffraction peak was observed for all samples shown in Figure 5-2. The XRD peak seen for sample OA1a at 25.95˚ theta was shown in Figure 4-2. However, in the case of the swift heavy ion irradiated and etched PET polymer film i.e. OA2a, OA2b, OA2c and OA2d, the XRD peak was marginally shifted to lower angles of 25.89° theta, 25.89° theta, 25.84° theta and 25.78° theta respectively. The other observed trend in the XRD analysis of samples OA2a, OA2b, OA2c and OA2d in Figure 5-2 was the continuous broadening of diffraction peaks for longer etching times which suggests that the ordered region of the polymer matrix became more disordered and thus decrease in crystallinity (Liu *et al*., 2000). This could indicate that the effect of the energetic swift heavy ion irradiation and chemical

etching may initiate the delocalization of some regularly aligned atoms within the side chain and back bone structure of the PET as is indicated the broadening of peaks. The single diffractogram peaks observed in Figure 5-2 correspond to the (1 0 0) planes of PET (Liu *et al*., 2000). The broadening of peaks of *'shielded'* swift heavy ion irradiated and etched PET polymer samples OA2a, OA2b, OA2c and OA2d could imply an increase the distortion of the structure. Also, the distortion of atoms within the swift heavy ion irradiated and etched PET polymer structure could result in the increase in fractional volume due to atomic mobility either in the side chain or main chain of the PET polymer structure. Although the diffraction peaks' intensity decreased with increase in etching time, this may not directly translate to loss crystalline structure (Aggarwal *et al*., 2012) within *'shielded'* swift heavy ion irradiated and etched PET polymer. The degree of chain order as well as the presence of aromaticity in the PET may have facilitated the crystalline distortion (Balta *et al.*, 2000). This is because the presence of aromaticity (i.e. phenyl ring) which can be easily flip in the PET polymer has been reported to limit the polymer stability thereby making the atom species in the crystalline regions highly susceptible to energetic ions and chemical treatment (Burgess *et al*., 2014).

In a study by Awasthi *et al*., (2010), it was reported that the semicrystalline polymers can be converted into the amorphous phase after irradiation by suitable ions to initiate an amorphization process in the polymer via the impact of swift heavy ion irradiation on polymer matrix. However, this process of polymer amorphization does not necessarily translate to complete migration of atoms from their lattices site to neighbouring domain. Awasthi *et al*., (2010) suggested that long molecular chains are merely damaged not completely destroyed as their neighbouring chains are partially preserved.

The concept of crystallinity in polymer is relatively different compared with that of other solids. The decrease in the diffractogram peak intensity and the shift in the

CHAPTER 5

angular position towards higher angles can be considered as a decrease in lattice spacing. Similarly, the broadening of diffractogram peaks often suggests the transformation of the polymer toward a more disordered state and consequently changes in crystalline size. These phenomena are often cited when polymer undergo ion irradiation (Biswas *et al*., 1999; Virik and Srivastava, 2001; Youmei *et al*., 2003 *cited in* Awasthi *et al*., 2010). The combined effects of ion irradiation and chemical etching of polymer can be determined with respect to the polymer crystallinity properties.

5.5 FOURIER TRANSFORMED INFRA-RED (FTIR) SPECTROSCOPY ANALYSIS OF *'shielded'* SWIFT HEAVY ION IRRADIATED ETCHED PET POLYMER FILM

Infra-red spectra analysis of *'shielded'* swift heavy ion irradiated and etched PET polymer film (i.e. samples OA2a, OA2b, OA2c and OA2d) can assist to profile the functional groups configuration of the polymer. Also, the IR analysis of samples OA2a, OA2b, OA2c and OA2d in comparison with ASPET (samples OA1a) can provides an insight into the chemical and structural orientation via the vibrational spectra of these functional groups that are associated with the polymer. The *'shielded'* swift heavy ion irradiated etched PET polymer film are samples OA2a, OA2b, OA2c and OA2d and have characteristic functional groups that are identified at specific absorbance or transmittance bands. The samples; OA2a, OA2b, OA2c and OA2d are swift heavy ion irradiated PET polymer films etched in 1 M NaOH at 80 ˚C for 3, 6, 9 and 12 minutes respectively. In Figure 5-3, the overlay of IR spectra in transmittance mode for ASPET (OA1a) and *'shielded'* swift heavy ion irradiated etched PET (OA2a, OA2b, OA2c and OA2d) polymer is presented. The IR spectra in transmittance mode were collected from 2000 cm^{-1} to 600 cm^{-1}.

CHAPTER 5

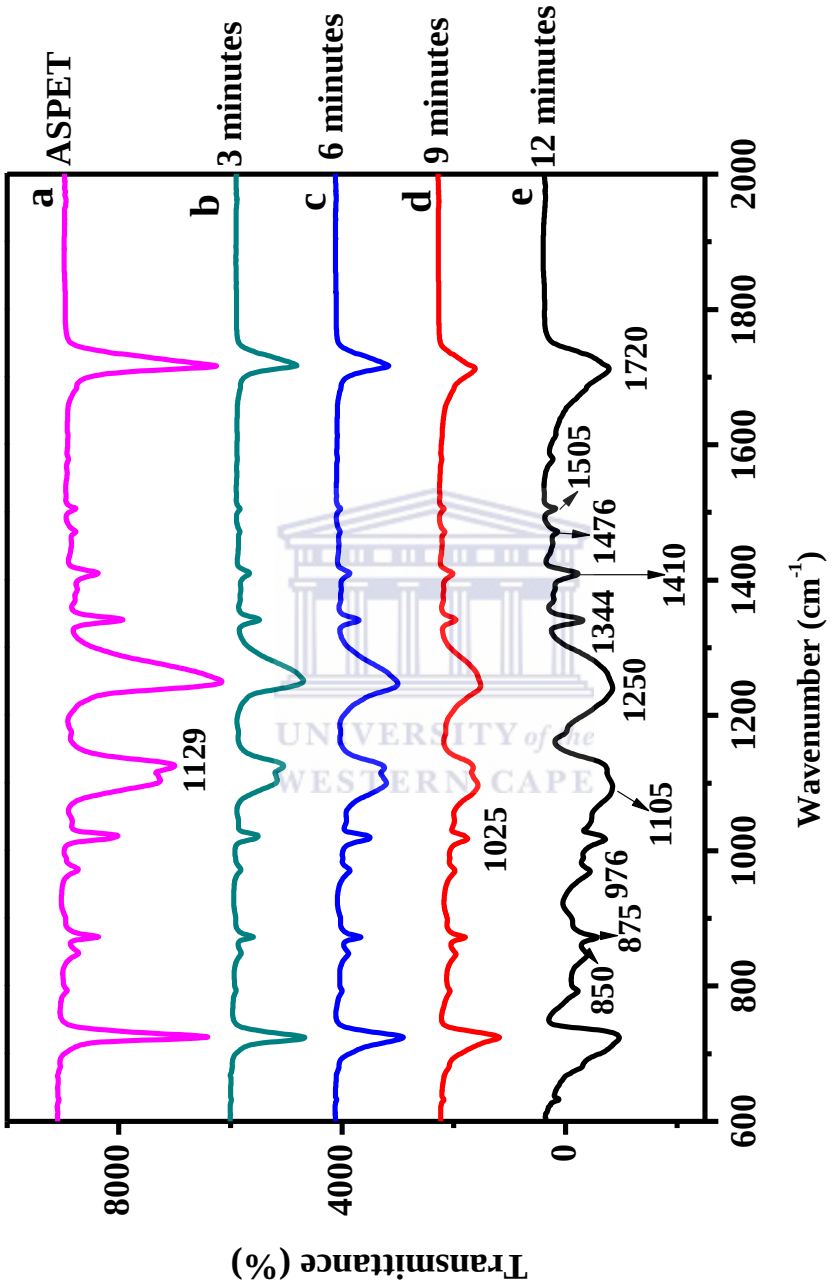

Figure 5-3: IR analysis of (a) ASPET (sample OA1a) and *'shielded'* swift heavy ion irradiated etched PET polymer film (b) OA2a, (c) OA2b, (d) OA2c and (e) OA2d as a function of various etching time.

CHAPTER 5

The IR result in Figure 5-3 showed the presence of the following bands in the ASPET (sample OA1a); 850 cm^{-1} (C-H rocking), 875 cm^{-1}, C-O stretching vibration at 976 cm^{-1}, , aliphatic at 1344 cm^{-1}, the aromatic (1105 cm^{-1}, 1250 cm^{-1},1410 cm^{-1}, 1505 cm^{-1}), CH_2 bending moiety was observed at 1476 cm^{-1} and 1720 cm^{-1}. It was observed that these IR peaks occurred at different intensities ranging from weak, medium to strong bands. The IR spectra for ASPET (OA1a) and *'shielded'* swift heavy ion irradiated etched PET (OA2a, OA2b, OA2c and OA2d) polymer showed that there was continuous decrease in spectra peak intensity as the etching time increases for samples OA2a, OA2b,OA2c and OA2dcompared with sample OA1a. Also, the IR spectra analysis of samples OA2c and OA2d showed the presence of new band at 1129 cm^{-1} which has been assigned to disubstituted in the para positions of the benzene ring in the PET structure as shown in Figure 4-17 and 4-19. The new band 1129 cm^{-1} was a transformation of the band at 1105 cm^{-1} which is also assigned to disubstituted benzene in the para positions. Table 5-1, below give a summary of the alterations in band intensity as function of etching time for the ASPET and track-etched PET i.e. samples OA2a, OA2b, OA2c and OA2d polymer film.

CHAPTER 5

Table 5-1: Comparison of selected functional group and wavenumber present in PET for ASPET and *'shielded'* swift heavy ion irradiated etched PET polymer film and their corresponding wavenumbers

		Sample code				
Functional group assignment	**Wavenumber (cm^{-1})**	OA1a	OA2a	OA2b	OA2c	OA2d
CH_2 rocking	850	Band is present with very weak intensity	Band is present, unaltered but became extremely weak intensity	Band is present, unaltered but became extremely weak intensity	Band is present, unaltered but became extremely weak intensity	Band is present, unaltered but became extremely weak intensity
C-O stretch	976	Band is present with very weak intensity	Band is present, unaltered but became extremely weak in intensity	Band is present, unaltered but became extremely weak in intensity	Band is present, unaltered but became extremely weak in intensity	Band is present, unaltered but became extremely weak in intensity

C-C-C bending	1025	Band is present with medium intensity	Band is unaltered but became very weak in intensity	Band is unaltered but became very weak in intensity	Band is unaltered but became very weak in intensity	Band is unaltered but became very weak in intensity
CH_2 bending	1476	Band appeared with very weak intensity	Band remained unaltered in intensity	Band remained unaltered in intensity	Band remained unaltered in intensity	Band remained unaltered in intensity
C-O stretch	1250	Band present with strong intensity	Band is present and unaltered but became weak in intensity	Band is present and unaltered but became weak in intensity	Band is present and unaltered but became weak in intensity	Band is present and unaltered but became weak in intensity
Aliphatic	1344	Band is present with medium intensity	Band is present and became weak in intensity	Band is present and became weak in intensity	Band is present and became weak in intensity	Band is present and became weak in intensity
Aromatics (Di substitution in para position in benzene)	875 1105 1129 1410 1505	All bands were present with weak and very weak intensity	Band at 875 cm^{-1} was unaltered but became weak in intensity. Band at 1105 cm^{-1} was altered and appeared as bump.	Band at 875 cm^{-1} was unaltered but became weak in intensity. Band at 1105 cm^{-1} was altered and appeared as bump.	Band at 875 cm^{-1} was unaltered but became weak in intensity. Band at 1105 cm^{-1} was altered and appeared as bump.	Band at 875 cm^{-1} was unaltered but became weak in intensity. Band at 1105 cm^{-1} was altered and appeared as bump. Band at 1129

			Band at 1129 cm^{-1} was reduced into medium intensity, bands at 1410 and 1505 cm^{-1} were both unaltered in intensity.	Band at 1129 cm^{-1} was reduced into medium intensity, bands at 1410 and 1505 cm^{-1} were both unaltered in intensity.	Band at 1129 cm^{-1} was reduced into medium intensity, bands at 1410 and 1505 cm^{-1} were both unaltered in intensity.	cm^{-1} completely disappeared, bands at 1410 and 1505 cm^{-1} were both unaltered with reduced intensity
C=O carbonyl	1720	Band is present with very strong intensity	Band is present and unaltered but with medium intensity	Band is present, unaltered and with reduced intensity	Band is present, unaltered and with reduced intensity	Band is present, unaltered and with reduced intensity and became broad

CHAPTER 6

The backbone structure of PET is mainly constituted by the benzene ring i.e. para and normal modes as previously shown in Figure 4-19 and summarized in Table 5-1 (Burgess *et al*., 2014). However, the emergence of new band at 1129 cm^{-1} (para-disubstituted benzene) could be as a result of continuous and simultaneous degradation of both side and main chain structures of PET. Since the aromatic structure in PET is responsible for its stability (Burgess *et al*., 2014), the effects of irradiation and chemical etching altered the existing bonds within the PET polymer. The aliphatic band group at 1344 cm^{-1} are attributed to the crystallinity region of the PET polymer due to the presence of specific bands associated with trans configuration of ethylene glycol residue which is responsible for dense packing of PET polymer chains (Liu *et al*., 2000). The effects of swift heavy ion irradiation and chemical etching on PET polymer showed that the response of characteristics band intensities in the PET polymer structure was not selective in bond deformation of both the side chains and backbone structures of PET. Although samples OA2a, OA2b and OA2c experienced continuous decrease in characteristic PET bands, no new molecular rearrangement due to the reported chain scission or crosslinking could be seen (Steckenreiter *et al*., 1997 and Awasthi *et al*., 2010). This is because the chain scission or molecular rearrangement should have resulted in the emergence of several new spectra in the swift heavy ion irradiated etched PET polymer film which was only observed at 1129 cm^{-1} for sample OA2d. The evidence of the presence of the olefinic group at 1652 cm^{-1} could not be confirmed in the IR analysis of all samples as previously reported in other studies (Steckenreiter *et al*., 1997 and Awasthi *et al*., 2010). However, these studies focused only on the structural degradation of PET polymers as a function of ion fluence and irradiation environments such as vacuum and air. The IR analysis of swift heavy ion irradiated etched PET has provided insight into the possibility that the unirradiated regions of the PET polymer mainly has retained its original properties as anticipated. It is possible that the diffusion of gases or migration of radicals from porous to non-porous regions of the PET could have resulted in the change in the overall properties of the non-porous layer of PET as seen in sample OA2d. This is possible due to the

multiple reaction processes (Figure 2.5) that PET undergoes after swift heavy ion irradiation. These processes have been described by Steckenreiter *et al*., (1997) to include; formation of alkyne end groups, overall degradation of PET by oxidation process, amorphization of the crystalline fraction and finally scission of the main chain at the para position of the substituted benzene ring. Energy dissipation along the latent damaged tracks of polymer and the availability of some of the free radicals (Apel *et al*., 1997) to react with the chemical etchant is crucial to understanding polymer susceptibility to ion irradiation and chemical etching. Consequently, the degree of band intensity, disappearance of bands or emergence of new bands can be related to the effects of the modification and whether the attack on the polymer chains is random, coordinated or selective (Awasthi *et al*., 2010). In this study, only amorphization could be detected by both XRD and FTIR and no clear case could be made for the formation of new bonds from the FTIR results.

In the next section, relative absorbance (A_o) of ASPET (sample OA1a) and *'shielded'* swift heavy ion irradiated etched PET polymer (samples OA2a, OA2b, OA2c and OA2d) which is represented as (A) is presented. The ratio of A/A_o can be used to determine the susceptibility of the isolated functional groups as well as their degradations within the polymer matrix (Mathakari *et al.*, 2009), calculated by extrapolating the wavenumber of a specific functional and using the ratio A/A_o which in this case represents sample OA1a with the swift heavy ion irradiated etched PET polymer film (OA2a, OA2b, OA2c and OA2d). The extrapolated plot is used to define the susceptibility of some specific functional groups to irradiation and chemical etching. In Figure 5-4, the relative absorbance (A/A_o) *'shielded'* swift heavy ion irradiated etched PET polymer OA2a, OA2b, OA2c and OA2d for some selected functional groups will be presented and discussed.

CHAPTER 6

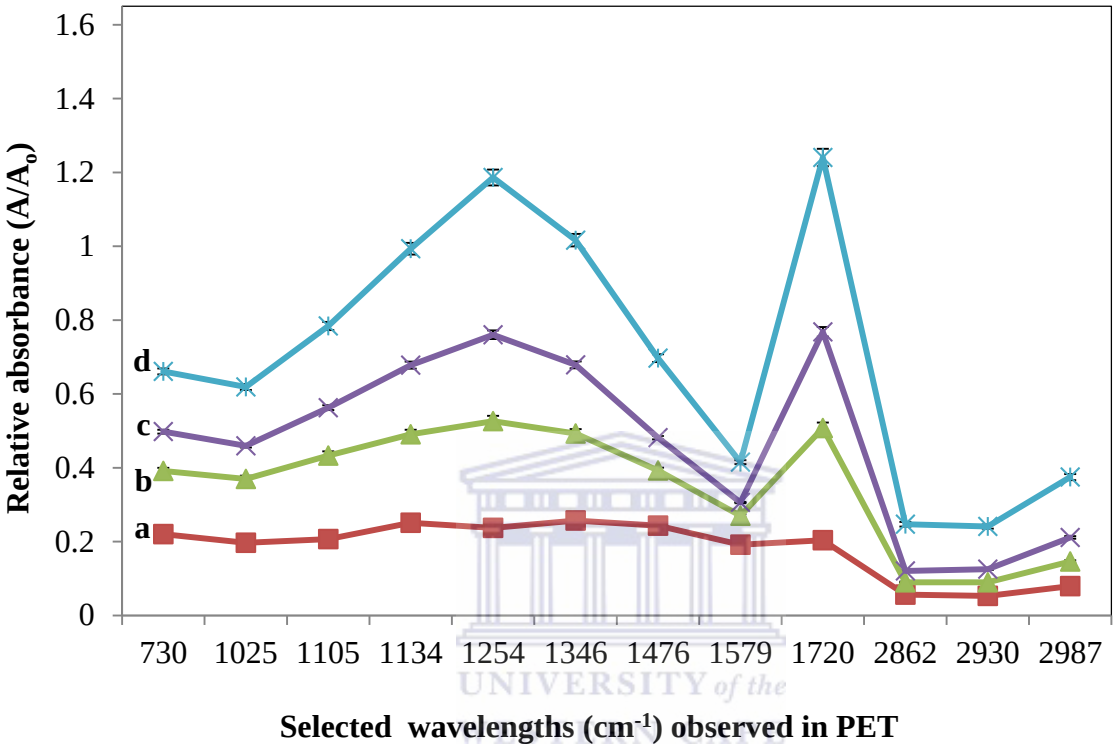

Figure 5-4: The relative absorbance *'shielded'* swift heavy irradiated etched PET polymer (a) OA2a, (b) OA2b, (c) OA2c and (d) OA2d as a function of etching time

Samples OA2a (Figure 5-4a) and OA2b (Figure 5-4b) did not show significant differences across all bond configurations which could indicate that the bonds (scission or crosslinked) for sample OA2a (Fig. 5-4b), the PET film was not severely affect the polymer matrix hence no significant degradation was observed. However, sample OA2c (Figure 5-4c) PET polymer showed a slight variation in intensity for para substituted benzene groups i.e. 1105 cm^{-1}, 1134 cm^{-1}, 1254 cm^{-1}, 1346 cm^{-1} and 1476 cm^{-1} (CH_2 bending). In the case of sample OA2d (Figure 5-4d) which represents 12 minutes etched *'shielded'* swift heavy ion irradiated PET film the intensities showed an abrupt and significant variation in the para-substituted benzene region which is

indicative of the loss of groups in the benzene ring present in the PET polymer. The relative absorbance analysis showed that the etching process caused a degree of amorphization due to chemical attack on the benzene ring in the PET structure (Figure 4-17 and Figure 4-19). In the next section (5.5), the characterization results of *'shielded'* swift heavy ion irradiated etched PMP will be extensively presented and discussed. Also, some results of the *'direct'* swift heavy ion irradiated etched PMP will be presented and discussed.

5.6 CHARACTERIZATION OF *'shielded'* and *'direct'* SWIFT HEAVY ION IRRADIATED ETCHED PMP POLYMER FILM

The study of polymethyl pentene (PMP) under swift heavy ion irradiation and chemical etching treatment has not been widely investigated. In this study, PMP polymer was irradiated with swift heavy ion of Kr with ion energy of 3.57 MeV or 4.5 MeV. The procedure for the swift heavy ion irradiation involved the use of *'shielded'* material (PET film) on the PMP polymer for the 3.57 MeV Kr ion irradiation experiment. The *'direct'* irradiated PMP polymer was not *'shielded'* when irradiated with Kr ion. This section presents some selected experimental results that show the response of swift heavy ion irradiated PMP to chemical etching conditions.

5.7 ETCHING KINETICS OF *'shielded'* SWIFT HEAVY ION IRRADIATED ETCHED PMP POLYMER FILM

The continuous depletion of polymer film due to weight loss experienced during chemical etching can be determined especially after such polymers have been exposed to conditions such as swift heavy ion irradiation and chemical etching. The use of swift heavy ion irradiation and chemical etching are known to significantly alter polymer physical properties (Aggarwal *et al*., 2012). Consequently, etching kinetic studies can

be used as an appropriate analytical approach to determine the degree of polymer weight loss as a function of time. This analytical approach can also be used to investigate and predict other properties such as track profile, pore configuration and breakthrough i.e. complete pore opening of a symmetry membrane structure (Apel *et al*., 1998). Figure 5-5 shows the comparative weight loss study as a function of etching time for samples OA3b and OA4d PMP polymer film. Sample OA3b represents ASPMP etched in acidified chromium trioxide solution while sample OA4d is *'shielded'* swift heavy ion irradiated etched PMP polymer. Sample OA4d was *'shielded'* with PET film and irradiated with 3.57 MeV, etching Kr ion irradiated PMP was performed in acidified chromium trioxide (H_2SO_4+CrO_3) at 80 ˚C for 150 minutes. The etchability (weight loss) of samples OA3b and OA4d as a function of time is presented and discussed in Figure 5-5.

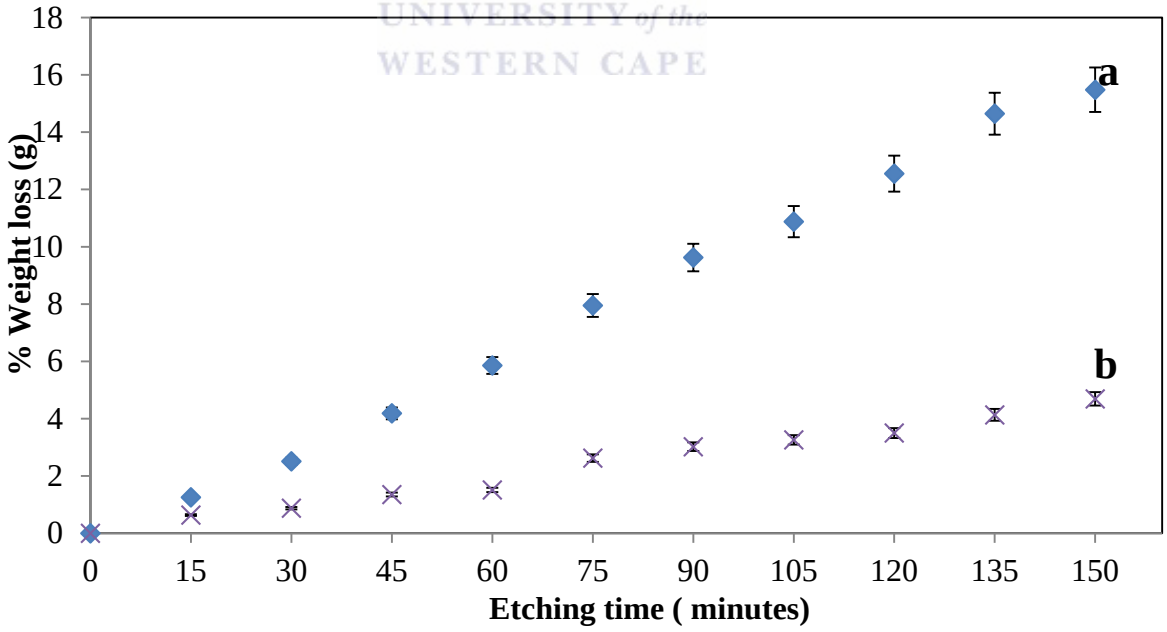

Figure 5-5: Etching kinetics (weight loss) analysis of (a) *'shielded'* swift heavy ion irradiated etched PMP (sample OA4d) and (b) ASPMP (sample OA3b) polymer film

It was observed that sample OA3b PMP polymer film (Figure 5-5b) and OA4d (Figure 5-5a) showed a significant difference in weight loss as a function of etching time. The weight loss of sample OA4d was intense and continued to increase with increase in etching time. However, sample OA3b (Figure 5-5b) experienced slight increase in weight loss which almost became relatively stable after 105 minutes. In the case of sample OA4d (Figure 5-5a), the weight loss was approximately 6 % within 60 minutes of etching time compared with the corresponding weight loss of 1.5 % for sample OA3b (Figure 5-5b) PMP polymer. The increase in weight loss of sample OA4d (Figure 5-5a) during chemical etching could be as a result of the damaged latent tracks by swift heavy ion irradiation of sample OA4d hence the significant variation in weight loss between sample OA3b and samples OA4d as observed in Figure 5-5a and 5-5b respectively (Apel *et al*., 1998). Swift heavy ion irradiated polymer experience latent damage along the trajectory of the ion irradiation in polymer film. As a result, it is possible that atoms and bonds with the structure of the swift heavy ion irradiated polymer will undergo excitation and therefore cause ease of etching as in the case of sample OA4d (Liu *et al*., 2000).

In the next section, the etching kinetic (weight loss) study as a function of etching time for samples OA3b and OA9d is presented in Figure 5-6. Sample OA3b represents ASPMP etched in acidified chromium trioxide solution (H_2SO_4+CrO_3) at 80 ˚C for 135 minutes while sample OA9d is *'direct'* swift heavy ion irradiated etched PMP polymer using 4.5 MeV of Kr ion. The direct swift heavy ion implies that the PMP polymer film was not *'shielded'* prior to Kr ion irradiation. The chemical etching conditions were the same as sample OA3b. In Figure 5-6, the etchability (weight loss) analysis of samples OA3b and OA9d as a function of time is presented and discussed.

CHAPTER 6

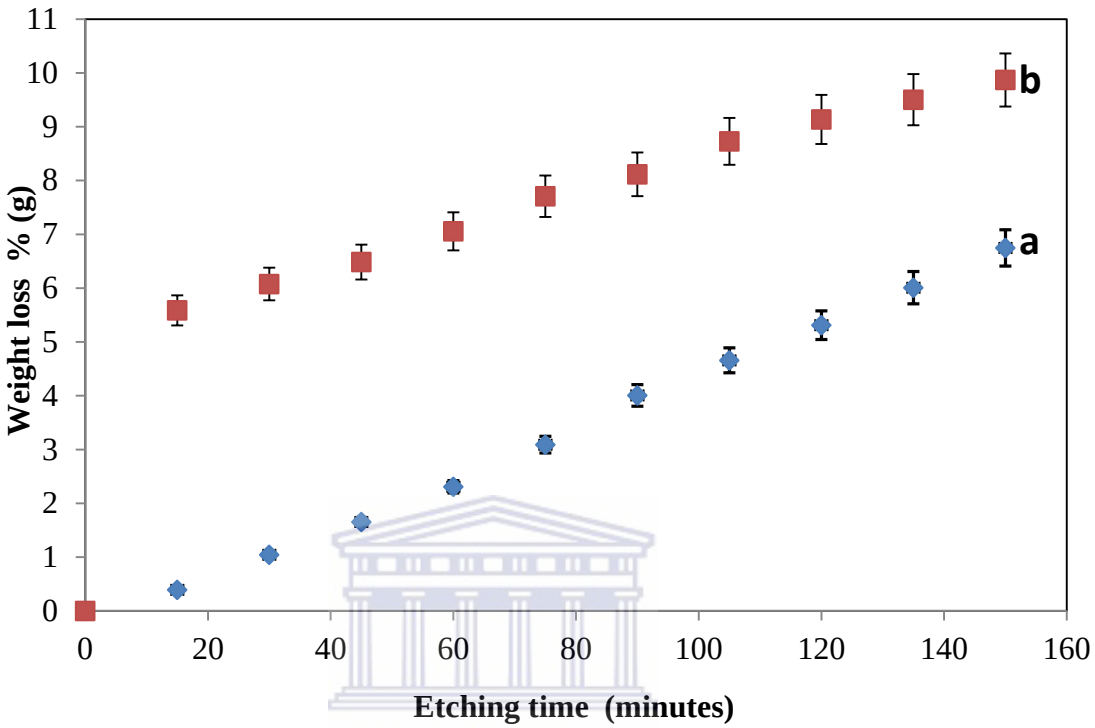

Figure 5-6: Etching kinetics analysis of (a) etched ASPMP and (b) track-etched PMP film

It was observed that the weight loss of samples OA3b (Figure 5-6a) and OA9d (Figure 5-6b) continues to increase as a function of increase in etching time. Sample OA9d experienced over 5 % in weight loss within the first 20 minutes of chemical etching time. In comparison, sample OA3b did not experience intense degradation with less than 1 % in weight loss of PMP polymer film. Also, it was observed that weight loss of sample OA9d continues to increase with increase in etching time. The spontaneity of degradation due to weight loss of sample OA9d could be as a result of *'direct'* swift heavy ion irradiation of PMP high latent tracks which are susceptible to chemical etching (Aggarwal *et al*., 2012). According to Apel *et al*., 1997c the molecular mobility and relaxation transition activities of polypropylene (PP) and polyethylene terephthalate (PET) were identified as the predominant factors that influences the etch rate of PET and PP.

In comparison, the etching kinetic study result presented in sample OA4d (Figure.5-5a) and sample OA9d (Figure 5-6b) were both irradiated with swift heavy ion of krypton. However, sample OA4d was *'shielded'* while sample OA9d was *'direct'* irradiated with Kr ion. The weight loss for samples OA4d (1.5 %) and OA9d (5.5 %) were different and higher for sample OA9d compared with sample OA4d. This showed that the effects of *'shielded'* material on PMP polymer as in the case of sample OA4d prior to swift heavy ion irradiation could have altered the stopping power of PMP polymer film. It is possible that that stability of atoms in the near surface regions for sample OA4d in Figure 5-5a is much stronger compared with atoms in similar surface regions of sample OA9d in Figure 5-6a.

5.8 SCANNING ELECTRON MICROSCOPY MORPHOLOGY ANALYSIS OF ETCHED UNIRRADIATED, *'shielded'* AND *'direct'* SWIFT HEAVY ION IRRADIATED ETCHED PMP POLYMER FILM

SEM technique is one of the most versatile techniques used to investigate surface morphology of samples. This analytical technique is useful as it help to profile the polymer with respect to the observed physical characteristics such as presence of pores including their shape, size and distribution as well as other defects. Polyolefins are mostly considered to be inert (Mike Chung, 2002) hence the need to create active sites with high reactivity properties is crucial. Consequently, these reactive sites can be susceptible to reveal the extent of latent damaged regions via a representative pore profile. In Figure 5.7, the SEM morphological analysis results of ASPMP, *'shielded'* and *'direct'* swift heavy ion irradiated etched PMP polymer film are presented. Samples OA3b, OA4d and OA9d represent the unirradiated PMP, *'layered'* and *'direct'* swift heavy Kr ion irradiated etched PMP polymer films respectively. The ASPMP (sample OA3b) was etched without exposure to swift heavy ion irradiation while sample OA4d was *'shielded'* with PET foil prior to swift heavy ion irradiation by Kr ion and etched. Sample OA9d was not shielded with any material but *'direct'*

irradiated with swift heavy Kr ion and etched. All the three (3) samples i.e. OA3b, OA4d and OA9d were etched in acidified chromium trioxide at 80 ˚C for 150 minutes.

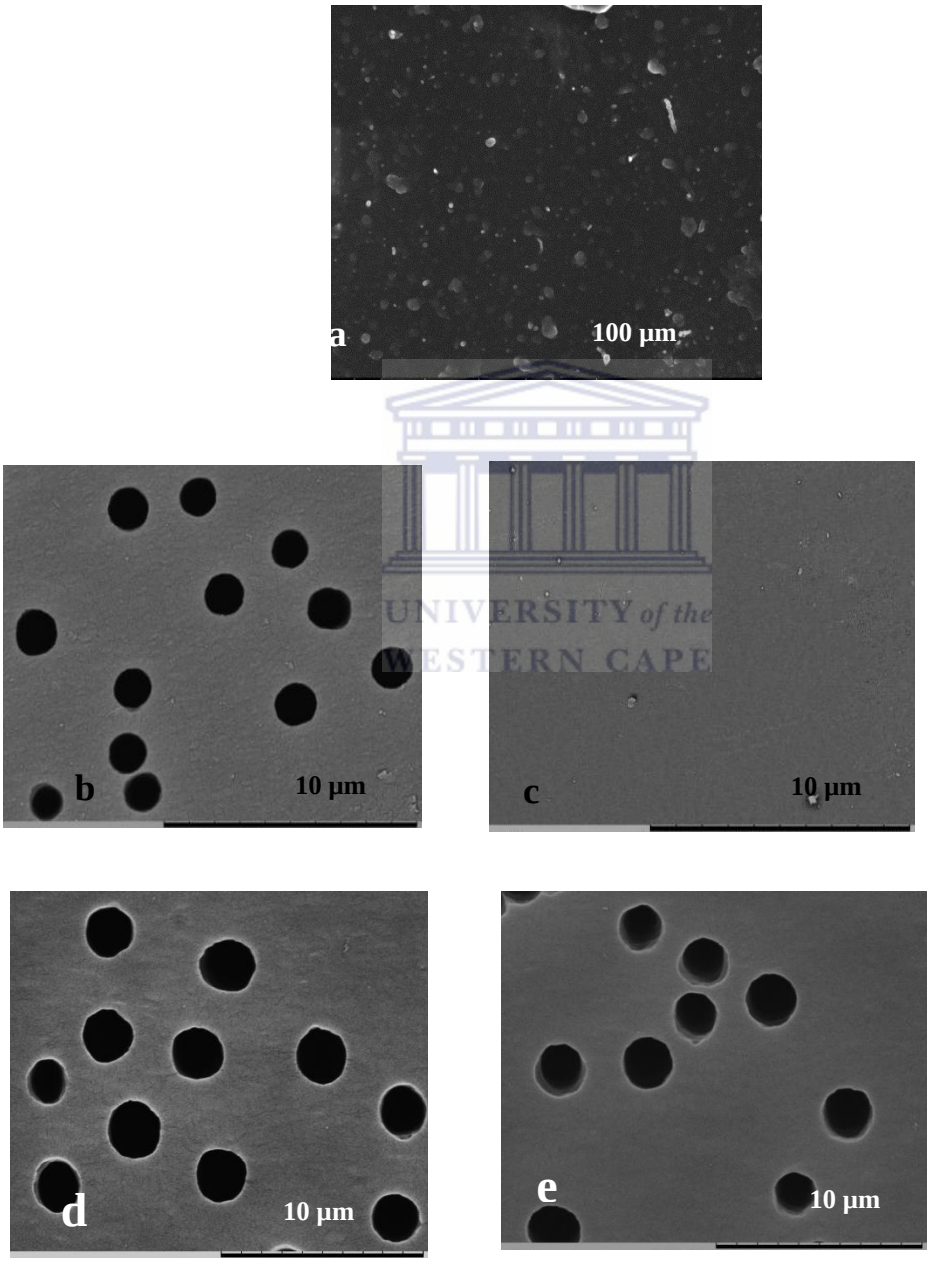

Figure 5-7: **SEM surface micrograph (a) sample OA3b, *'shielded'* (sample OA4d) with (b) irradiated side and (c) back side, (d) and (e) *'direct'* swift heavy ion irradiated PMP (sample OA9d)**

CHAPTER 6

It was observed from SEM micrograph that the etching of sample OA3b (Figure 5-7a) did not result in the formation of surface or through pore. As for sample OA4d (Figure 5-7b and 5-7c), the *'shielded'* swift heavy ion irradiated PMP polymer film showed the presence of pores on the irradiated side of sample OA4d (Figure 5-7b). The pores formed on sample OA4d (Figure 5-7b) polymer film surface were observed to be spherical and did not overlap hence there was no bi-circular pores. The average pore of sample OA4d (Figure 5-7b) was approximately 1 µm and these pores were fairly distributed on the surface of sample OA4d. On the contrary, the unirradiated side of sample OA4d (Figure 5-7c) did not indicate the presence of pores and the surface of the unirradiated side of sample OA4d (Figure 5-7c) was smooth without any distinct surface defects. The *'direct'* swift heavy ion irradiated etched PMP (sample OA9d) revealed the presence of pores after chemical etching and these pores were observed for both sides of sample OA9d (Figure 5-7d and 5-7e)PMP polymer film. Also, the pores were spherical, isolated with an average diameter of 1.5 µm. The pores density observed for sample OA9d (Figure 5-7d) was slightly more than the other side of sample OA9d (Figure 5-7e).

The use of *'shielded'* material by PET film as in the case of sample OA4d (Figure 5-7b and 5-7c) seems to have resulted in combined ion stopping power of both the *'shielded'* material and the PMP film. This could be responsible for the formation of single-sided pores which are restricted to the swift heavy ion irradiated side PMP polymer film even though a strong chemical etchant was used. Sample OA9d (Figure 5-7d and 5-7e) was *'direct'* irradiated etched PMP polymer film and the emergence of pores on both sides of the OA9d suggests that the swift heavy ion irradiation exited the PMP polymer film during irradiation even though the pore density between Figure 5-7d and 5-7e varied. Sample OA9d side with high pore density (Figure 5-7d) was the side that was exposed to swift heavy ion irradiation and serves as the entry point of the heavy ions.

CHAPTER 6

In Figure 5-8, the SEM cross-section micrograph of samples OA4d (Figure 5-8a and 5-8b) and OA9d (Figure 5-8c and 5-8d) are presented. Sample OA4d and OA9d represent the *'shielded'* and *'direct'* swift heavy ion irradiated etched PMP polymer film. The *'shielded'* material for sample OA4d was PET film which was attached to one of the surface side of PMP polymer film before being irradiated with 3.57 MeV of swift heavy Kr ion. Sample OA9d was *'directly'* irradiated with 4.5 MeV of swift heavy Kr ion without the use of any shielded material on the PMP polymer film. The samples (OA4d and OA9d) were both etched in acidified chromium trioxide (H_2SO_4 + CrO_3) solution at 80 ˚C for 150 minutes.

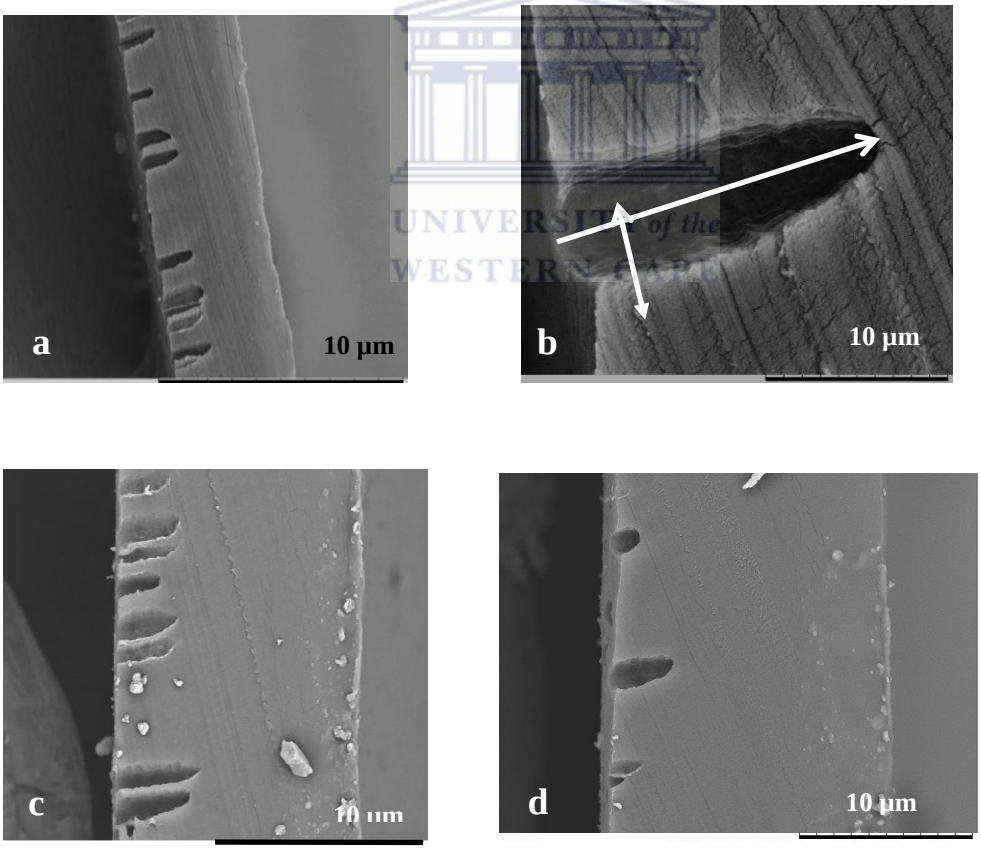

Figure 5-8: Cross section of SEM micrograph of *'shielded'* (sample OA4d) (Fig. 5-8a and 5.8b) and *'direct'* (sample OA9d) (Fig. 5-8c and 5.8d) swift heavy ion irradiated etched PMP polymer film

CHAPTER 6

The SEM cross-section micrograph of sample OA4d (Figure 5-8a) revealed the presence of pores on a single side of the sample which resulted in the formation of asymmetry membrane structure for sample OA4d (Figure 5-8a). Also, it was observed that the orientation of pores in sample OA4d (Figure 5-8a) were approximately 10 µm deep into the polymer film with extensive dense layer which were not affected during chemical etching as there was no pores formed. The shape of the pore for sample OA4d in Figure 5-8b showed that the pore was conical in shape with wide opening and narrow base. The formation of asymmetrical membrane structure of sample OA4d showed that the use of *'shielded'* material affected the penetration of swift heavy ion into the PMP polymer film. The stopping power of both the *'shielded'* material and PMP polymer is one of the possible reasons for the pores depth that was observed for sample OA4d (Figure 5-8a). Also, the conical shape of the pore in Figure 5-8b) implied that during chemical etching of sample OA4d, radial etching was more predominant that lateral chemical etching. This is because lateral chemical etching would have resulted in the formation of cylindrical shaped pores. The radial chemical etching that was observed resulted in the increase in pore diameter rather than pore length. Also, the pore density agreed with the theoretical SRIM calculated value i.e. 10^6. Apel *et al*., 1997d explained that the rate of energy loss within a polymer matrix and the spatial distribution of ion-induced damaged directly relates to pattern of etching.

It is likely that the reactive species that are available within sample OA4d after swift heavy ion could have been decreased as chemical etching continued. Also, during chemical etching, the etchable zones could have been consumed after which the original structural configuration of the sample OA4d PMP polymer may have been encountered within the polymer matrix hence the slow rate of etching. The relaxation of generated radicals as well as their shelf life could have been recovered during etching process. Ultimately, since the PMP polymer investigated in this study was

commercially purchased hence the inclusion of filler or additives could have influenced the etchable zones.

5.9 XRD ANALYSIS OF ETCHED UNIRRADIATED, *'shielded'* AND *'direct'* SWIFT HEAVY ION IRRADIATED PMP POLYMER FILM

In this section, the result of XRD analysis for samples OA3b, OA4d and OA9d are presented. XRD analysis was performed in order to gain insight into the structural orientations between the unirradiated etched PMP (sample OA3b) and *'shielded'* (sample OA4d) and *'direct'* (sample OA9d) swift heavy ion irradiated PMP polymer film. The swift heavy ion irradiated PMP polymer films i.e. samples OA4d and OA9d were irradiated with Kr ion and etched in acidified chromium trioxide (H_2SO_4+CrO_3). The etching conditions include 80 ˚C temperatures and etching time was 150 minutes. In Figure 5-9, the XRD analysis of samples OA3b, OA4d and OA9d PMP polymer films are presented and discussed.

CHAPTER 6

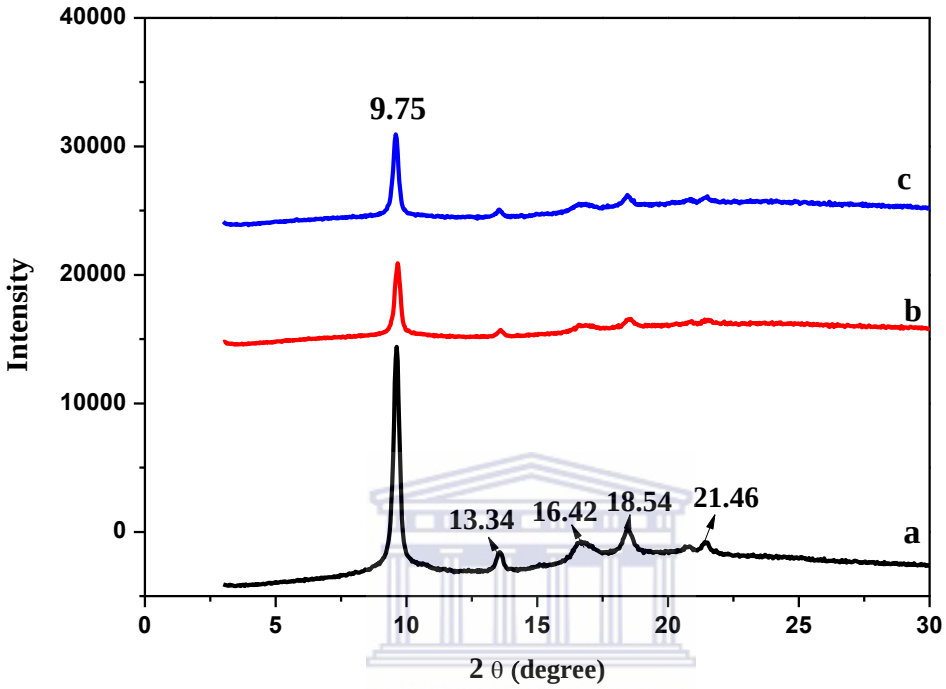

Figure 5-9: XRD analysis (a) sample OA3b, (b) *'shielded'* (sample OA4d) (c) *'direct'* (sample OA9d) swift heavy ion irradiated PMP polymer film

In Figure 5-9, the XRD diffractogram peaks in sample OA3b (Figure 5-9a) were observed at 9.75 °, 13.34 °, 16.42 ° and 18.54 ° 2θ. In addition, the diffraction peak at 9.75 ° 2θ was present for samples OA4d and OA9d but became less intense in OA4d (Figure 5-9b) and OA9d (Figure 5-9c). Also, the diffraction peak at 9.75 ˚ (2θ) that was observed for sample OA3b (Figure 5-9a) did not shift for samples OA4d and OA9d PMP polymer film. The diffraction peaks at 13.34, 16.42, 18.54 and 21.46 disappeared for samples OA4d and OA9d. The decrease in 9.75 ˚ (2θ) peak intensity for samples OA4d and OA9d could be as a result of the etching temperature of samples OA4d and OA9d which is above the glass transition temperature of PMP polymer film. Ghosa and Freeman (1993) suggested that at temperature higher than polymer glass transition temperature, polymer structure may be altered.

CHAPTER 6

5.10 FOURIER TRANSFORMED INFRA-RED SPECTROSCOPY ANALYSIS FOR ETCHED UNIRRADIATED, *'shielded'* and *'direct'* SWIFT HEAVY ION IRRADIATED PMP POLYMER FILM

In this section, the IR results of samples OA3b, OA4d and OA9d PMP films will be presented. Sample OA3b represents unirradiated etched PMP polymer film while samples OA4d and OA9d are *'shielded'* and *'direct'* swift heavy ion irradiated etched PMP polymer film. The etching temperature, solution and time are 80 ˚C, acidified chromium trioxide (H_2SO_4+CrO_3) and 150 minutes. The IR was performed to investigate the changes in functional groups due to chemical etching on samples OA3b, OA4d and OA9d PMP polymer film. In Figure 5-10, the IR spectra analysis results of samples OA3b, OA4d and OA9d is discussed.

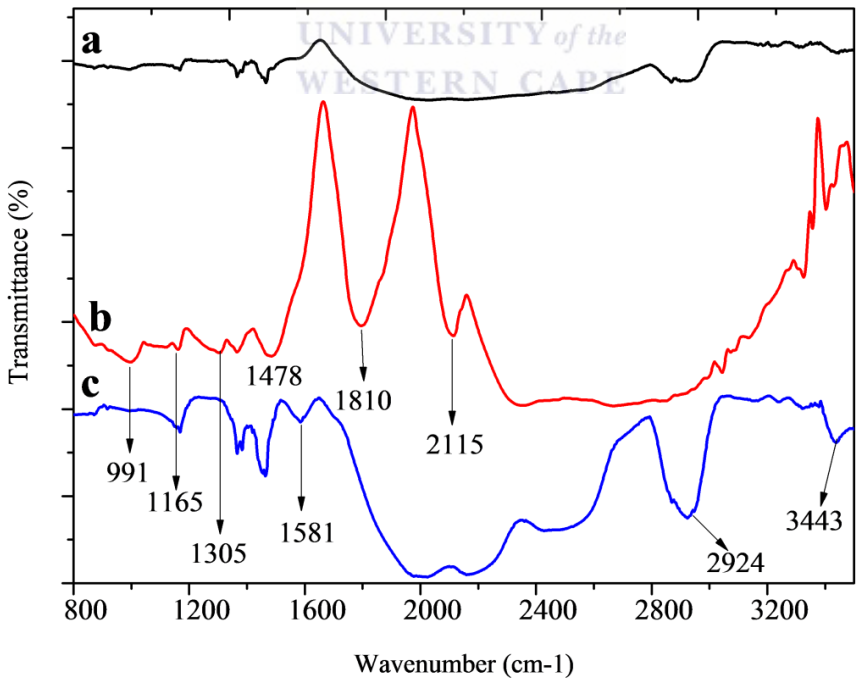

Figure 5-10: FTIR spectra analysis (a) sample OA3b, (b) *'shielded'* (sample OA4d) and (c) *'direct'* (sample OA9d). Figure 5.10b and 5-10c were swift heavy ion irradiated etched PMP polymer film

In sample OA4d (Figure 5-10b), the IR analysis showed the presence of a medium band intensities at 991 cm^{-1} which represents CH_3 rocking. This band was not present in in sample OA9d (Figure 5-10c). In addition, the following bands were present in sample OA4d; 1165 cm^{-1} (twisting modes of (CH_3) methyl groups), 1305 cm^{-1} (CH_2 wagging), 1478 cm^{-1} (degenerate deformation modes of the (CH_2) methylene groups, 1810 cm^{-1} (CH_3 asymmetry deformation and C-C in plane bending) and 2115 cm^{-1} which have both the methylene (CH_2) rocking and methyl (CH_3) asymmetry deformation. The IR analysis of sample OA9d (Figure 5-11c) showed the presence of bands at 1581 cm^{-1}, 2924 cm^{-1} (CH asymmetric stretching in CH_2) and 3443 cm^{-1} (in-plane bending of C-C). The response of samples OA3b, OA4d and OA9d to etching temperature was observed to show the presence of some characteristic bands. At 80 ˚C of etching, it is possible that reactive species and inter and intra chain relaxation within the PMP undergo various changes (Samuel and Mohan, 2004). Table 5-2, describes some selected functional group assignments present in PMP.

Table 5-2: Selected functional groups in *'shielded'* and *'directly' irradiated* PMP polymer film and their corresponding wavenumbers

Functional group	Wavenumber (cm^{-1})
Methyl (CH_3) rocking	991
CH_2, CH_3 wagging	1165
Methylene groups	1305,1478
CH_3 (asymmetry deformation)	1810
CH_3 and CH_2	2115
Asymmetry and out-of-plane methyl (CH_2)	1588
C-H asymmetry stretching	2924
CH_2 asymmetry	3443

CHAPTER 6

5.11 RELATIVE TRANSMITTANCE ANALYSIS OF *'shielded'* AND *'direct'* SWIFT HEAVY ION IRRADIATED PMP POLYMER FILM

In order to understand the degree of degradation within the PMP polymer structure, some selected functional groups of *'shielded'* and *'direct'* swift heavy ion irradiated etched PMP (samples OA4d and OA9d) polymer films were considered and their relative transmittance from IR analysis (Figure 5-10) was determined. The selected functional groups from IR bands of samples OA4d and OA9d represents the side chains and main chain regions of samples OA4d and OA9d. The relative transmittance (IR) of samples OA4d and OA9d is presented in Figure 5-11 below.

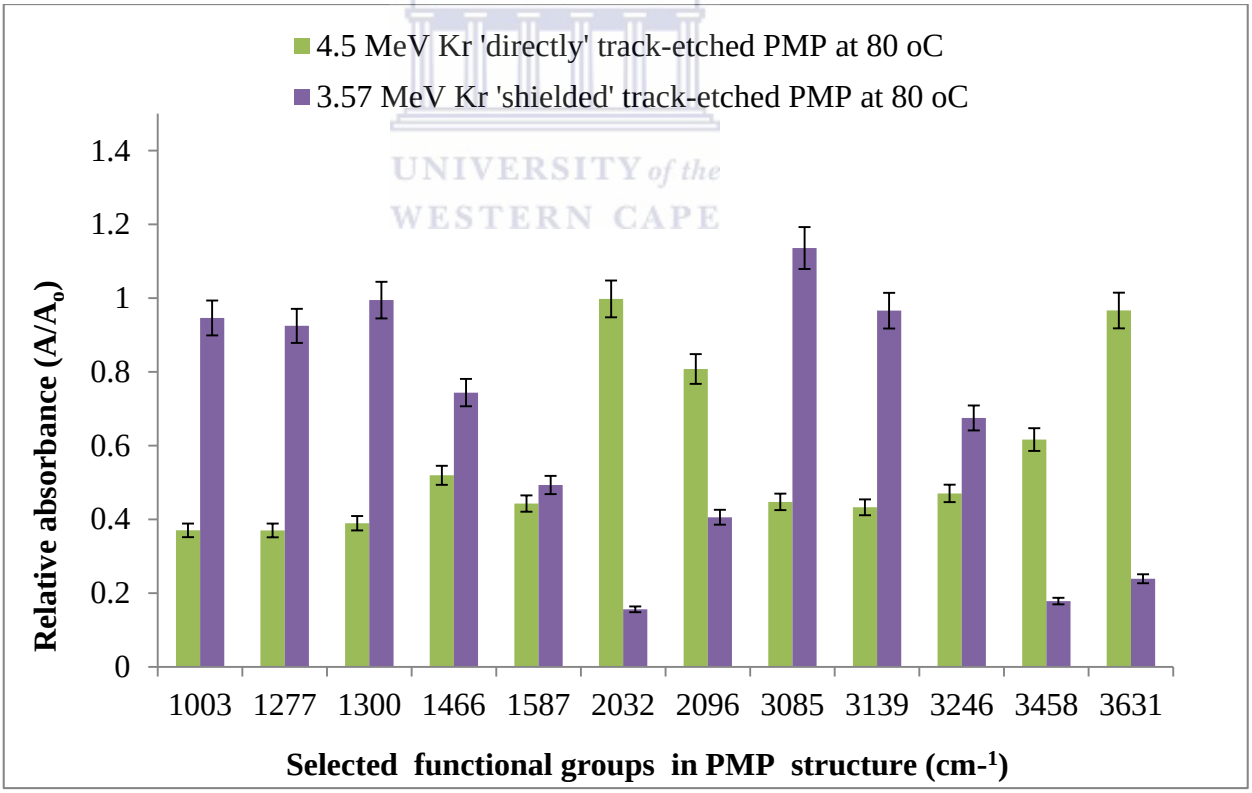

Figure 5-11: Relative absorbance (A/A_o) analysis of selected characteristic functional groups for *'shielded'* and *'direct'* swift heavy ion irradiated etched PMP polymer films

CHAPTER 6

Figure 5-11 represents the IR relative absorbance results of some selected functional groups for sample OA4d and OA9d. These selected functional groups constitute the main chains and side groups of PMP polymer film (Samuel and Mohan, 2004). The relative transmittance analysis of the selected functional groups showed that the chemical attack functional groups in sample OA4d during etching was more intense for most of the functional groups than for sample OA9d. For instance, sample OA4d showed significant variation in the susceptibility of functional groups of band intensities at 2032 cm^{-1}, 3458 cm^{-1} and 3631 cm^{-1} compared with sample OA9d. In the case of sample OA9d, the effect of chemical etching on the selected functional groups showed similar intensity except for 2032 $^{-1}$, 2096 $^{-1}$ and 3631 cm^{-1}. These functional groups have been assigned to methyl (CH_3) bending, C-C stretching and CH symmetric stretching in CH_3 respectively (Samuel and Mohan 2004). The band intensities at 3085 cm^{-1} is assigned to CH asymmetric deformation in CH_3, 3139 cm^{-1} for CH asymmetric deformation in CH_3 and C-H out of plane bending, 3246 cm^{-1} and 3458 cm^{-1} (CH symmetric stretching in CH_2). These functional groups experienced gradual decrease in the band intensities especially for sample OA9d PMP polymer.

5.12 CHAPTER SUMMARY

Track-etched PET polymer film analysis showed regular and consistent degradation as a function of etching time. The SEM morphological study showed the presence of pore with different orientation and geometry while a complete collapse of pore walls and decrease in dense layer thickness was observed after 12 minutes of etching. XRD analysis result for track-etched PET polymer showed continuous decrease in diffractogram peaks with peak broadening. IR results showed that track-etched PET polymer did not experience the introduction of new functional group but continuous deterioration with overall decrease in characteristic band intensities present in the polymer structure. The SEM analysis of track-etched PMP polymer film showed the

presence of single-sided pores that were sparsely distributed after etching for 2 hours and 30 minutes. The thickness of the dense layer was observed to decrease as a result of increase in etching time but did not lead to collapse of pore walls as observed in the case of track-etched PET polymer film. The pores diameter increased as a function of etching time which is indicative of radial etching being predominant. The XRD results for the track-etched PMP showed the decrease in diffraction peaks. However, this may not have translated into loss of crystallinity in polymer but realignment of atoms within the polymer structure. This is because PMP is known as a polymorph which implies that it has the ability to crystalize in several crystal lattices (Farmer, 1996). The investigation of track-etched PET and PMP polymer film especially using IR analysis has shown that the available species susceptible to attack after exposing PMP to are mainly located in the side chain reactions. This agreed with the report of EL-Naggar *et al*., (1990) that tertiary carbon atoms in a polymer structure are highly susceptible to irradiation than their secondary counterparts. In addition, the IR study and assignment of side chain and main degradation experienced by PMP polymer showed that several reactive species are generated in the side and thus easily attacked during chemical etching (Samuel and Mohan, 2004). As a result of the preferential availability of reactive species within PMP structure after ion irradiation and chemical etching, it is evident that the stability (i.e. longevity) of these reactive species can play an important role in the continuous degradation of the polymer.

CHAPTER 6

CHAPTER SIX

6 GAS PERMEABILITY AND SELECTIVITY

6.1 INTRODUCTION

In this chapter, the gas permeability and selectivity results of *'shielded'* swift heavy ion irradiated etched PET and PMP polymer film are presented and discussed. The PET polymer film samples that were analysed for their gas permeability and selectivity include; ASPET (sample OA1a), unirradiated etched PET (sample OA1c) and *'shielded'* swift heavy ion irradiated etched PET (OA2a, OA2b, OA2c and OA2d) polymer film. Also, this chapter presents the gas permeability and selectivity results of PMP polymer film samples. These samples are ASPMP (sample OA3a), unirradiated etched PMP (sample OA3b) and *'shielded'* swift heavy ion irradiated etched PMP (sample OA4a, OA5a, OA6a, OA6b, OA6c, and OA6d).

This chapter will first discuss the gas permeability and selectivity results of PET (i.e. samples OA1a and OA1c, OA2a, OA2b, OA2c and OA2d) polymer films in section 6.2. In section 6-3, the gas permeability and selectivity results of PMP (i.e. samples OA3a, OA3b, OA3c, OA4a, OA5a, OA6a, OA6b, OA6c, and OA6d) polymer films will be presented and discussed. The details of gas permeability and selectivity measurement set-up and conditions have been described in section 3.4.5. The gas permeability and selectivity analysis of swift heavy ion irradiated PET and PMP polymer films was restricted to the *'shielded'* etched PET and PMP polymer samples. The choice of presenting gas permeability and selectivity results for the *'shielded'* irradiated polymer film samples was based on the objective of this study as described in section 1.7, time constraints and to also ensure a representation of PET and PMP polymer films due to the similarity. As a result, the gas permeability and selectivity

studies for all the *'direct'* ion irradiated polymer samples as in the case of PMP polymer film are not reported.

6.2 GAS PERMEABILITY AND SELECTIVITY ANALYSIS OF POLYETHYLENE TEREPHTHALATE (PET)

This section presents the gas permeability and selectivity analysis of ASPET (sample OA1a), *'shielded'* swift heavy ion irradiated without chemical etching (sample OA1c) and the etched *'shielded'* swift heavy ion irradiated PET samples (i.e. OA2a, OA2b, OA2c, and OA2d) polymer films. Aluminium foil was used as the layering material of the swift heavy ion irradiated PET polymer. The *'shielded'* swift heavy ion irradiated PET polymer films were etched in 1 M NaOH at 80 ˚C for different etching time (i.e. 3, 6, 9 and 12 minutes). The single gas permeability for the PET polymer samples was calculated using equation 3.5 and the gas permeability and ideal selectivity measurement were performed at room temperature. The permeability of He, CO_2 and CH_4 gases were investigated across the ASPET and *'shielded'* swift heavy ion irradiated unetched PET polymer which are samples OA1a and OA1c respectively. In Table 6-1, the gas permeability analysis of ASPET (OA1a) and *'shielded'* swift heavy ion irradiated unetched PET (OA1c) polymer film are presented and discussed.

Table 6-1: Gas permeability analysis of ASPET (sample OA1a) and *'shielded'* irradiated PET (sample OA1c) polymer films

Sample	P (cm cm^3/cm^2 s cm Hg)		
	He	**CO_2**	**CH_4**
OA1a	1,0E-10	1,2E-11	1,3E-12
OA1c	1,1E-10	1,6E-11	1,5E-12

CHAPTER 6

It was observed that the permeability of He, CO_2 and CH_4 gases for ASPET (samples OA1a) and *'shielded'* swift heavy ion irradiated unetched PET (sample OA1c) decreased from He to CH_4. Helium gas was the most permeable gas for both samples OA1a and OA1c while CH_4 gas was the least permeable. Samples OA1a and OA1c showed similar He gas permeability whereas CO and CH_4 gases were slightly higher in permeability for sample OA1c compared with samples OA1a. The similarity in gas permeability properties for all the three (3) gases in both sample OA1a and OA1c indicated that the use of Al foil as *'shield'* and swift heavy ion irradiation for sample OA1c did not significantly affect the permeability of He, CO_2 and CH_4. This could be because the unaffected 'region' of the *'shielded'* swift heavy ion irradiated unetched PET polymer film may have been unaffected as in the case of sample OA1c. In addition, the similarity in gas permeability properties of samples OA1a and OA1c can be related to the chain mobility within the PET which may have compensated for the micro voids created due to latent tracks damage after the swift heavy ion irradiation process. Also, the fact that the gas permeability measurement for both samples OA1a and OA1c was conducted at room temperature (25 ˚C) may have restricted significant physical changes in the *'shielded'* swift heavy ion irradiated unetched PET (sample OA1c) polymer film as it is lower than the glass transition temperature of PET polymer film.

In the next section, the ideal gas selectivity analysis of ASPET (sample OA1a) and *'shielded'* swift heavy ion irradiated without chemical etching (sample OA1c) is presented. The ideal selectivity measurements were performed at room temperature. The ideal gas selectivity that was performed for He/CO_2, CO_2/CH_4 and He/CH_4 gases were investigated across the ASPET and *'shielded'* swift heavy ion irradiated unetched PET polymer which are samples OA1a and OA1c respectively. The ideal gas selectivity analysis of samples OA1a and OA1c was calculated using equation 3.7 and presented in Table 6-2.

Table 6-2: Ideal gas selectivity of ASPET (sample OA1a) and *'shielded'* irradiated PET (sample OA1c) polymer films

Sample	A		
	He/CO_2	He/CH_4	CO_2/CH_4
OA1a	8,7	80	9,2
OA1c	6,7	73	10

The ideal selectivity results of the pairs of He/CO_2, He/CH_4 CH_4/CO_2 and He/ gases were observed to marginally decrease for He/CO_2 and He/CH_4 gas pairs for sample OA1c compared with sample OA1a. On the contrary, the ideal selectivity results for CO_2/CH_4 gas pair was observed to increase for sample OA1c compared with sample OA1a. The difference in ideal gas selectivity properties of samples OA1a and OA1c could be due to the rigidity of PET chains that was imposed on the overall structure of PET especially by the unaffected regions of PET structure during swift heavy ion irradiation for sample OA1c. The decrease in ideal gas selectivity for samples OA1 and OA1c in Table 6-2 could be as a result of the gas permeability property of helium gas presented in Table 6-1 which seems to compensate for the ideal gas selectivity properties of samples OA1a and OA1c.

This section presents the gas permeability results of *'shielded'* swift heavy ion irradiated etched PET samples (i.e. OA2a, OA2b, OA2c, and OA2d) polymer film. Aluminium foil was used as the layering material of the swift heavy ion irradiated PET polymer. The *'shielded'* swift heavy ion irradiated PET polymer films were etched in 1 M NaOH at 80 ˚C for different etching times (i.e. 3, 6, 9 and 12 minutes). The single gas permeability for the PET polymer samples was calculated using equation 3.5 and the gas permeability was performed at room temperature. The dependence of chemical

etching time on gas permeability of *'shielded'* swift heavy ion irradiated etched PET (OA2a, OA2b, OA2c and OA2d) polymer film is presented in Figure 6-1, in which the gas permeability analysis stated above are presented and the results are discussed.

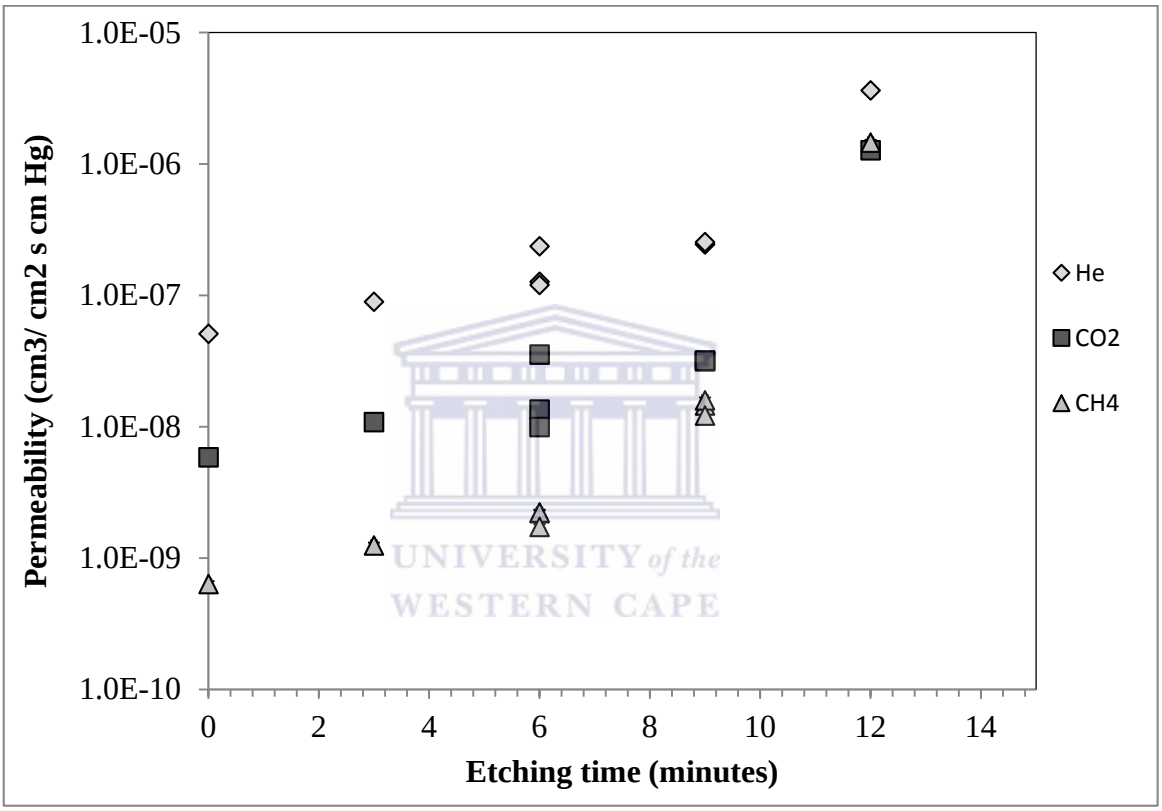

Figure 6-1: The dependence of gas permeability on etching time *'shielded'* ion irradiated PET films

It was observed that the permeability measurement of all gases through samples OA2a, OA2b, OA2c and OA2d increased with etching time (Figure 6-1). Also, the CO_2 and CH_4 gases showed identical permeability value in Figure 6-1 for samples OA2b and OA2c etched for 6 and 9 minutes respectively. The permeability of helium gas was observed to be fastest while CH_4 was the least permeable gas for all the samples (OA2a, OA2b, OA2c and OA2d). In addition, the values of CO_2 gas permeability through

samples for OA2b and OA2c which were etched for 6 and 9 minutes respectively was almost identical but increased for sample OA2d etched for 12 minutes. The preference of He gas permeability for all samples may be directly attributed to the pore geometry (i.e. size and depth) of the pores in the surfaces of the *'shielded'* swift heavy ion irradiated etched PET polymer and the presence of micro-defects in the dense layer region that were large enough to allow the passage of helium gas. The SEM surface morphology result of the *'shielded'* swift heavy ion irradiated etched PET polymer presented in Figure 5-1a -5-1f, showed that the pores after 3 minutes of etching (sample OA2a) and 6 minutes etching (sample OA2b) increased in size as a function of etching time with defined pore sizes (Figure 5-1b and Figure5-1c) whereas the pore sizes became agglomerated without defined pore size after 9 and 12 minutes of time i.e. samples OA2c and OA2d respectively. Although agglomerated pores were observed in samples OA2c and OA2d due to continuous chemical etching i.e. 9 and 12 minutes respectively, the pores formed in these samples (i.e. OA2c and OA2d) did not exist as through pore across polymer film samples OA2c and OA2d. In Figure 6-2, the gas selectivity properties of ASPET (sample OA1a) and the *'shielded'* swift heavy ion irradiated etched PET (OA2a, OA2b, OA2c and OA2d) polymer are presented.

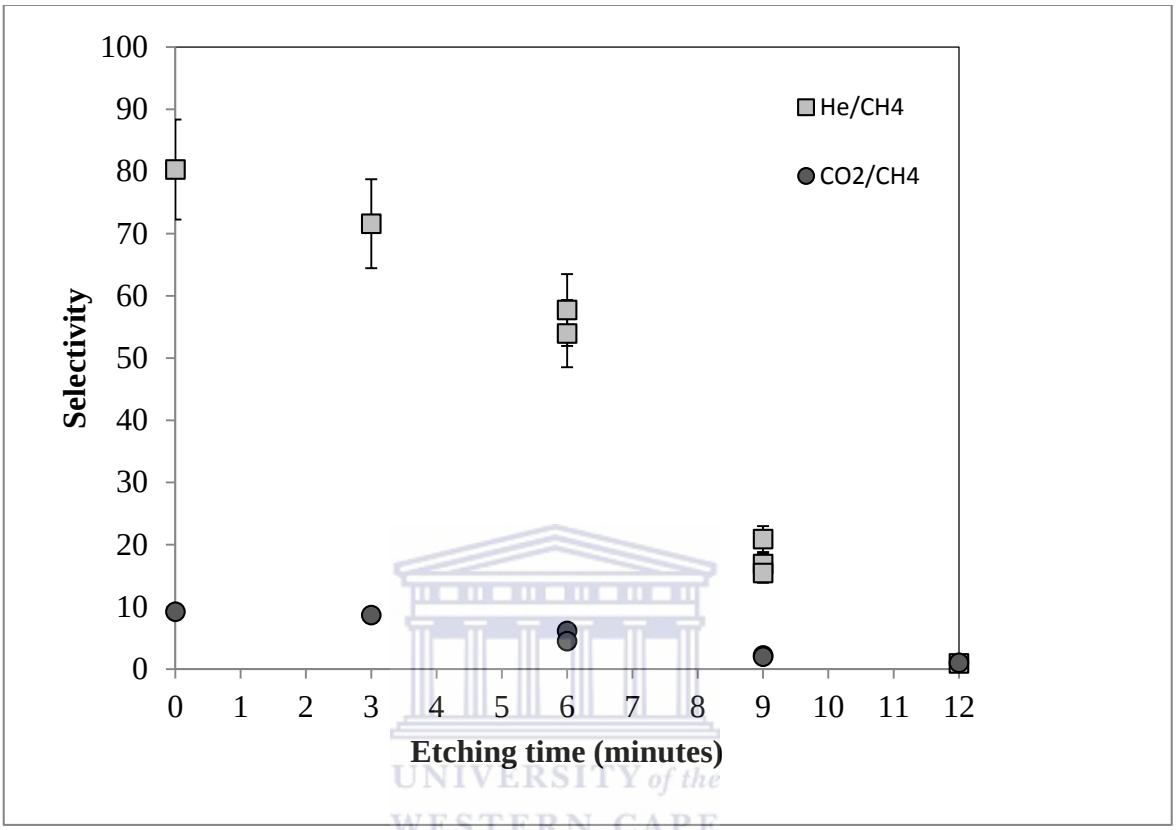

Figure 6-2: The dependence of ideal gas selectivity on etching time *'shielded'* Xe ion irradiated PET polymer films

It was found that the gas selectivity properties decreased as a function of etching time but varied significantly with each gas pair of He/CH_4 and CO_2/CH_4 in Figure 6-2. The *'shielded'* swift heavy ion irradiated etched PET (i.e. OA2a, OA2b, OA2c and OA2d) revealed a spontaneous decrease in selectivity for He/CH_4 gas pair over etching time. It was observed that a decrease in selectivity of approximately 80 % occurred within 12 minutes of chemical etching time for sample OA2d. However, the selectivity of the *'shielded'* swift heavy ion irradiated etched PET (i.e. OA2a, OA2b, OA2c and OA2d) for CO_2/CH_4 pair (Figure 6-2) showed low selectivity (less than 10) which slowly decreased over etching time (3, 6 and 9 minutes for samples OA2a, OA2b and OA2c

respectively) to no selectivity after 12 minutes for sampleOA2d). Also, the selectivity for CO_2/CH_4 of sample OA1a was identical with the selectivity of sample OA2a. The comparison of gas permeability (Fig. 6-1) and selectivity in Fig. 6-2 for sample OA1a and swift heavy ion irradiated etched PET polymer (i.e. samples OA2a, OA2b, OA2c and OA2d) showed that the dependence of gas selectivity on etching time decreases with time of etching whereas the permeability increases as a function of etching time.

In the next section, the gas permeability and selectivity analysis of PMP polymer will be presented and a brief description of the selected samples will be provided.

6.3 GAS PERMEABILITY AND SELECTIVITY STUDY OF POLYMETHYL PENTENE (PMP)

In this section, the gas permeability and ideal selectivity results are presented. ASPMP (OA3a) and some selected samples of *'shielded'* swift heavy ion irradiated etched polymethyl pentene is presented. These samples include OA3b, OA3c, OA4a, OA5a, OA6a, OA6b, OA6c and OA6d). The basis for selecting these samples especially samples OA6a, OA6b, OA6c and OA6d was to ensure a similarity with the gas permeability and selectivity of *'shielded'* swift heavy ion irradiated PET polymer samples OA2a, OA2b, OA2c and OA2d. In brief, sample OA3b represents unirradiated etched PMP polymer film which was etched for 150 minutes in acidified chromium (H_2SO_4+CrO_3) solution with etching temperature of 80 ˚C. Sample OA3c was *'shielded'* swift heavy ion irradiated unetched PMP polymer film. The shielded material was PET foil while the irradiation ion was Kr with ion energy of 3.57 MeV. Samples OA4a and OA5a are *'shielded'* swift heavy ion irradiated PMP etched in acidified chromium solution at etching temperature 60 ˚C or 70 ˚C respectively and both PMP polymer samples were etched for similar etching time of 40 minutes. The following samples (i.e. OA6a, OA6b, OA6c and OA6d) were etched in acidified chromium (H_2SO_4+CrO_3) solution at 80 ˚C under different etching times of 40, 60, 120

and 150 minutes respectively. In the gas permeability set-up, the working area of the PMP polymer film was 32 cm^2. The single gas permeability for He, CH_4 (gas purity 99.9 % vol) and CO_2 (gas purity 98.9 % vol) was measured by a differential method with gas chromatography analysis as described in Figure 3.4. Helium and argon were used as gas-carriers and the partial pressure drop was equal to 1 atm. The gas permeability of selected results of PMP (OA3a, OA3b, OA3c, OA4a, OA5a, OA6a, OA6b, OA6c and OA6d) polymer film is presented in Table 6-3 and the ideal gas selectivity is presented in Table 6-4.

Table 6-3: Gas permeability analysis of swift heavy Kr ion irradiated PMP films '*layered*' with PET polymer foil

Sample codes and description	Selectivity (P) (cm cm^3/cm^2 s cm Hg)		
	He	**CO_2**	**CH_4**
As-received PMP polymer film (sample OA3a)	2.43E-06	2.58E-06	4.35E-07
Etched unirradiated PMP polymer film (sample OA3b)	6.13E-06	6.15E-06	9.76E-07
layered swift heavy ion irradiated etched PMP polymer film sample (OA3c)	2.43E-06	3.00E-06	4.46E-07
layered swift heavy ion irradiated etched PMP polymer film, etched at 60 ˚C for 40 minutes (sample OA4a)	2.39E-06	2.09E-06	3.36E-07
layered swift heavy ion irradiated etched PMP polymer film, etched at 70 ˚C for 40 minutes (sample OA5a)	4.09E-06	3.31E-06	2.97E-06
layered' swift heavy ion irradiated etched PMP polymer film, etched at 80 ˚C for 40 minutes (sample OA6a)	2.84E-06	3.60E-06	5.12E-07

layered' swift heavy ion irradiated etched PMP polymer film, etched at 80 ˚C for 60 minutes (sample OA6b)	3.63E-06	4.27E-06	6.77E-07
layered' swift heavy ion irradiated etched PMP polymer film, etched at 80 ˚C for 120 minutes (sample OA6c)	3.94E-06	4.58E-06	6.72E-07
layered swift heavy ion irradiated etched PMP polymer film, etched at 80 ˚C for 150 minutes (sample OA6d)	1.54E-05	1.16E-05	5.07E-06

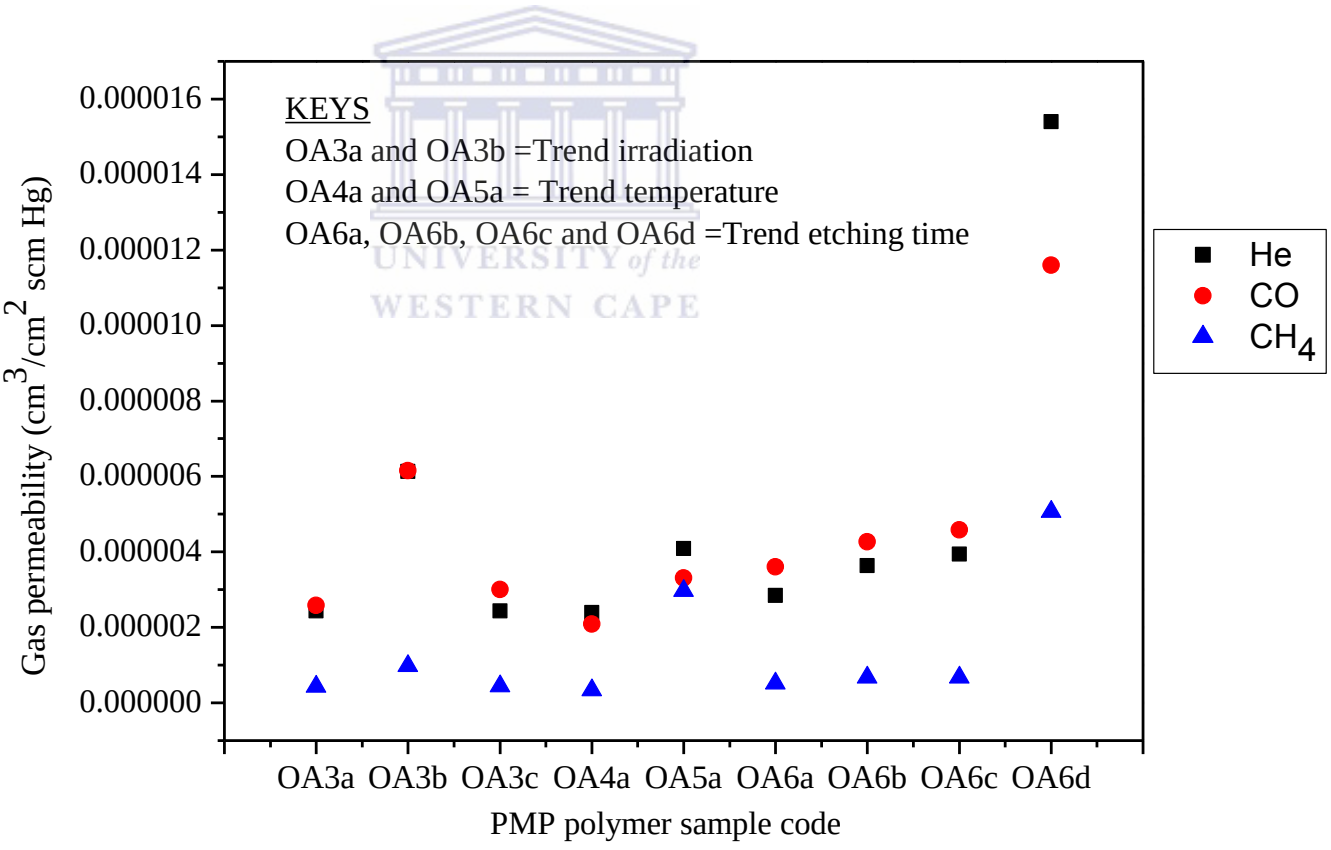

Figure 6-3: The dependence of gas permeability on ASPMP and *'shielded'* swift heavy Kr ion irradiated etched PMP films

CHAPTER 6

It was observed that the permeability of CO_2, CH_4 and He gases increased for all the swift heavy ion irradiated and etched selected PMP polymer samples although CH_4 was the least permeable gas while He gas was the most permeable especially for the *'shielded'* swift heavy ion irradiated etched PMP as seen for samples OA4a, OA5a, OA6a, OA6b, OA6c and OA6d. The permeability of CH_4 gas across the selected PMP samples remained unchanged for most of the samples except for samples OA5a (etched at 70 ˚C for 40 minutes) and OA6d etched for 150 minutes at 80 ˚C. Also, it was observed that the permeability of CO_2 gas was highest for samples OA3b and OA6d, the difference being due to high etching time in the case of sample OA3b whereas in the case of sample OA6d, it was a combination of high etching time and use of swift heavy ion irradiation to treat the PMP polymer film. The preference for He gas permeability as observed for samples OA6a, OA6b, OA6c and OA6d could be attributed to the multiple effects of swift heavy ion irradiation and increasing chemical etching time as in the case of samples OA6a, OA6b, OA6c and OA6d treatment i.e. ion irradiation and chemical etching of PMP polymer film. This was because the emergence of pores due to swift heavy ion irradiation and decrease in PMP thickness was accomplished after extended time of etching i.e. 2 hours 30 minutes (Figure 5-7b and 5-7c). Also, this could be due to the increase in the fractional volume within the polymer structure. The fractional volume seems to therefore result in the increase in mobility of He and CO_2 gases across the membrane. The presence of micro voids, intra-segmental and inter-segmental chain mobility and realignment of atoms or functional groups due to swift heavy ion irradiation and chemical etching are ascribed to the increase in gas permeability observed for samples OA6a, OA6b, OA6c and OA6d (Babari et al., 1988; Ghosa and Freeman, 1993; George and Thomas, 2001; Thorton et al., 2009). According to Ghosa and Freeman (1993), it was reported that changes in polymer matrix due to chemical and thermal effects could facilitate high gas permeability in polymers.

CHAPTER 6

In the next section (Table 6-5), the ideal gas selectivity results of selected PMP samples (OA3a, OA3b, OA3c, OA4a, OA5a, OA6a, OA6b, OA6c and OA6d) will be presented and discussed. The ideal gas selectivity for CO_2/CH_4 and He/CH_4 of some selected PMP (OA3a, OA3b, OA3c, OA4a, OA5a, OA6a, OA6b, OA6c and OA6d) polymer is presented in Figure 6-4.

Table 6-4: Ideal gas selectivity of ASPMP and track-etched PMP polymer film

Sample	Ideal selectivity (α)	
	He/CH_4	**CO_2/CH_4**
As-received PMP polymer film (sample OA3a)	5.6	5.9
Etched unirradiated PMP polymer film (sample OA3b)	6.3	6.3
layered swift heavy ion irradiated etched PMP polymer film sample (OA3c)	5.4	6.7
layered swift heavy ion irradiated etched PMP polymer film, etched at 60 ˚C for 40 minutes (sample OA4a)	7.1	6.2
layered swift heavy ion irradiated etched PMP polymer film, etched at 70 ˚C for 40 minutes (sample OA5a)	1.4	1.1
layered' swift heavy ion irradiated etched PMP polymer film, etched at 80 ˚C for 40 minutes (sample OA6a)	5.5	7.0
layered' swift heavy ion irradiated etched PMP polymer film, etched at 80 ˚C for 60 minutes (sample OA6b)	2.8 1.5 0.8	2.3 1.0 0.7

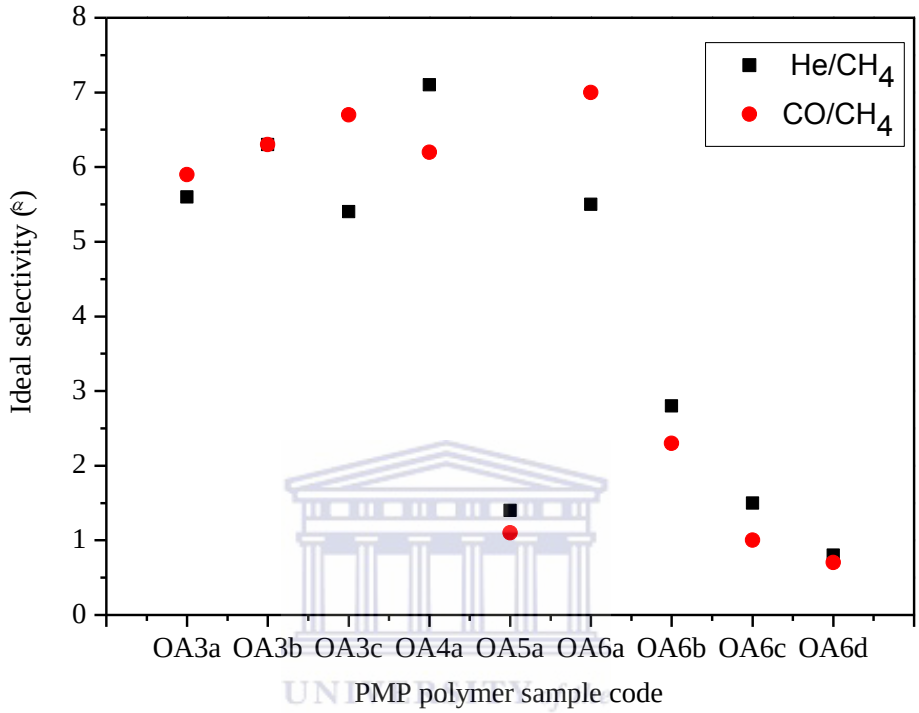

Figure 6-4: The dependence of ideal gas selectivity on ASPMP and *'shielded'* swift heavy Kr ion irradiated etched PMP films

The gas selectivity results in Figure 6-4 indicated that the gas selectivity for CO/CH_4 gas pairs was highest for all samples compared with the gas selectivity for CH_4/He gas pair. Samples OA4a and OA5a were both *'shielded'* swift heavy ion irradiated PMP polymer etched for 40 minutes but at different temperatures. Sample OA4a was etched at 60 ˚C while OA5a was etched at 70 ˚C. It was observed that the gas selectivity for samples OA4a was higher than sample OA5a (Figure 6-4). This may suggest that the availability of fractional free volume (FFV) in sample OA4a was less than in sample OA5a and this may be as a result of the etching temperature of sample OA5a. Also, it was observed that the gas selectivity properties decreased for both CH_4/CO_2 and He/CH_4 for samples OA6a, OA6b, OA6c and OA6d in comparison with sample OA3a

which represents the ASPMP. The decrease in gas selectivity that was observed for samples OA6a, OA6b, OA6c and OA6d could be as a result of etching temperature and etching time used for these samples. The etching temperature was 80 ˚C while the etching time was varied from 40 minutes (OA6a), 60 minutes (OA6b), 120 minutes (OA6c) and 150 minutes for samples OA6d. It is therefore possible that the increase in etching time resulted in chain mobility within PMP polymer structure hence decrease in gas selectivity. The gas selectivity properties of polymers have been associated with the nature of polymer, structure as well as polymer class (George and Thomas 2001).

6.4 CHAPTER SUMMARY

The overall effects of swift heavy ion-irradiation and chemical etching on PET and PMP polymer films under different heavy ion irradiation conditions showed that the gas permeability of swift heavy ion irradiated etched PET and PMP improved considerably as a function of etching time. Also, it was observed that the permeability of He gas was highest while CH_4 gas showed lowest gas permeability for both swift heavy ion irradiated etched PET and PMP polymers. The permeability of He compared with other gases could indicate that the pores sizes formed during chemical etching of the swift heavy ion irradiated PET and PMP polymer films favoured the passage of small gas like He. The increase in gas permeability of the swift heavy ion irradiated etched PET and PMP polymer samples could be attributed to atomic reorientation within the polymer matrix, available micro void for gas penetrants and decrease in dense layer thickness as in the case of swift heavy ion irradiated etched PET polymer film while the extended chemical etching time could have facilitated the physical and chemical changes in swift heavy ion irradiated etched PMP polymer samples.

CHAPTER 7

CHAPTER SEVEN

7 CONCLUSION AND RECOMMENDATION

This chapter presents and consolidates the key findings in this study. Also, this chapter presents a summary of results. The suggestions in the form of recommendations for future studies are discussed in this chapter.

7.1 OVERVIEW OF FINDINGS

The PET and PMP polymer films investigated in this study showed that the physico-chemical properties of these polymers were altered during ion track bombardment followed by selective etching. In the case of swift heavy ion *'shielded'* irradiated etched PMP, saturated and unsaturated moieties of C-H and C-C were predominant while the swift heavy ion *'shielded'* irradiated etched PET polymer film showed the presence of C-H, C=O, C-H and C-C species which undergo various chemical processes via reaction mechanisms such as deprotonation, alkylation, carboxylation and carbonylation. For instance, the IR analysis of swift heavy ion *'shielded'* irradiated etched PET and PMP polymer film indicated various asymmetry or symmetry wagging, twisting and, bending vibrations with the emergence of weak, medium or strong intensities. The structural composition and IR analysis of swift heavy ion *'shielded'* irradiated etched PMP has provided understanding with respect to the positions in the PMP structure that are being attacked during swift heavy ion irradiation as well as the variation of possible bond fragmentation, free radical generation and molecular or chain reorientation that can be initiated using ion irradiation and chemical etching as modification approach. Also, the "*location*" and "*carrier*" of free radicals in the polymer chain due to swift heavy ion irradiation and chemical treatment of PMP and PET polymers showed the possible pattern of degradation and asymmetry that will occur as well as the emergence of new bonds.

CHAPTER 7

The ultimate purpose of this study was to prepare asymmetrical membrane structure using *'shielded'* material on two (2) polymer films (PET and PMP) prior to swift heavy ion irradiation and chemical etching in order to improved gas permeability properties of the swift heavy ion *'shielded'* irradiated etched PET and PMP. In addition, this main objective is considered within the scope of determining the effects of *'shielded'* materials on the PET and PMP physico-chemical properties after irradiation and their gas permeability and selectivity profile after chemical etching of the *'shielded'* irradiated PET and PMP polymer films.

7.2 SUMMARY OF KEY FINDINGS

a. A systematic experimental approach was used to prepared asymmetrical membranes first by mechanical attachment of a *'shielded'* material on the surface of the polymer film prior to swift heavy ion irradiation and after irradiation, the *'shielded'* material was removed and the swift heavy ion irradiated PET and PMP polymer films were etched in chemical solution. This method is simple and novel as it has never been reported in literature.

b. The *'shielded'* material attached to the polymer film prior to swift heavy ion irradiation was able to control the penetration depth of the swift heavy ion into the polymer film during irradiation thus asymmetrical membrane was achieved from SEM results.

c. Swift heavy ion irradiated *'shielded'* etched PET polymer film was successfully used as a template to create the asymmetrical polymer membrane structure and the same approach was successfully adopted to produce asymmetrical PMP polymer film after layering the PMP polymer film with PET foil.

d. The gas permeability properties of the *'shielded'* PET and PMP polymer films were significantly improved as a function of etching time while their gas selectivity properties were retained relatively unchanged or completely lost as observed in the case of swift heavy ion irradiated *'shielded'* PMP polymer film upon extensive etching therefor allowing the control of gas permeability and selectivity properties of PMP.

e. This study has presented a new avenue to explore towards creating asymmetrical membranes from polymer film and also to further investigate the intrinsic properties of PMP polymer film

The use of *'shielded'* material approach during swift heavy ion irradiation of polymer film proved to be a novel and simple route to tailor polymer film into a gas selective asymmetrical membrane. This method *'shielded'* swift heavy ion irradiation of polymer film showed a significant reduction in etching time especially in the case of PET polymer film in which the dense layer thickness was considerably reduced within 12 minutes of etching in alkaline solution. In the case of PMP polymer, the use of *'shielded'* swift heavy ion irradiation of PMP polymer film and chemical etching showed that PMP polymer undergo selective chemical changes with the emergence of new spectra at 1478 cm^{-1}, 1810 cm^{-1} and 2115 cm^{-1} as observed in the IR analysis. In addition, the effect of chemical etchant on *'shielded'* swift heavy ion irradiated PET showed that PET polymer films experienced overall reduction in band intensities from the IR results. This characteristic further highlights the chemical resistant properties of PET and PMP polymer films. The use of *'shielded'* materials before swift heavy ion irradiation of PET and PMP polymer films resulted in the formation of asymmetrical membrane structure with porous surface on dense layer. The pores size was observed to increase as a function etching time for swift heavy ion irradiated etched PET and PMP polymer film whereas the orientation of the pores formed in PET polymer films

were cylindrical in shape but the etched PMP polymer film showed the formation of conical shaped pores.

7.3 RECOMMENDATIONS

The core objective of this study was to prepare gas selective asymmetrical membrane with porous surface on a dense layer using a simple and novel approach. Although swift heavy ion irradiated *'shielded'* PET polymer film was used as a template, swift heavy ion irradiation experiments of PMP polymer showed that asymmetrical membrane was prepared. However, swift heavy ion irradiated PMP polymer film was developed using two different conditions i.e. the use *'shielded'* material on PMP prior to swift heavy ion irradiation and *'direct'* irradiation which does not involve the use of *'shielded'* material on the PMP polymer film. The scope of this study did not cover an extensive investigation of PMP polymer under *'direct'* swift heavy ion irradiation. As a result, it will be valuable to understand the effects of swift heavy ion on PMP polymer using *'direct'* irradiation approach.

Although the objectives of this study were successfully accomplished, the following areas of polymer ion irradiation could be considered for future studies.

a. An extensive investigation of the effects of swift heavy ion irradiation conditions such as ion energy, stopping power of PMP and their effects on PMP polymer side chains and backbone structures.

b. The use *'direct'* swift heavy ion irradiation on PMP polymer film should be investigated in order to understand the alterations in the physico-chemical, thermal properties of swift heavy ion *'direct'* etched PMP polymer film.

c. Gas permeability and selectivity of swift heavy ion irradiated PMP polymer film should be investigated especially in the case of *'direct'* swift heavy ion irradiation without the use of shielded material.

8. REFERENCES

1. ABDESSELAM, M., STOQUERT, J. P., DJEBARA, M.., CERRUTI, C., CHAMI, A. C. AND MONTGOMERY, P. (2011). Stoichiometry evolution of polyethylene terephthalate under 3.7 MeV He^{+} irradiation. *Nuclear Instruments and Methods in Physics Research B*, 269. pp. 140–144.

2. ABEDINI, R. AND NEZHADMOGHADAM, A. (2010). Application of membrane in gas separation processes: its suitability and mechanisms. *Petroleum & Coal*, 52(2) pp. 69-80.

3. ACHARYA, N. K., KULSHRESTHA, V., AWASTHI, K., KUMAR, R., JAIN, A. K., SINGH, M., AVASTHI, D. K. AND VIJAY, Y. K. (2006). Gas permeation study of Ti-coated, track-etched polymeric membranes. *Vacuum*, 81**,** pp. 389-393.

4. ADHIKARI, S. AND FERNANDO, S. (2006). Hydrogen Membrane Separation Techniques**.** *Ind. Eng. Chem. Res.* 45, pp. 875-881.

5. AGGARWAL, P., SINGH, V., SINGH, A., SCHERER, U. W. SINGH, T., SINGLA, M. L. AND SRIVASTAVA, A. (2012). Physico-chemical transformations in swift heavy ion modified poly (ethylene terephthalate). *Radiation Physics and Chemistry*, 81, pp. 284–289.

6. AHARONI, S. M., CHARLET, G. AND DELMAS, G. (1981). Investigation of Solutions and Gels of Poly (4-methyl-l-pentene) in Cyclohexane and Decalin by Viscosimetry, Calorimetry, and X-ray

Diffraction. A New Crystalline Form of Poly (4-methyl-l-pentene) from Gels. *Macromolecules,* 14. pp. 1390-1394.

7. AKAMATSU, K., IKEDA, S. AND NAWAFUNE, H. (2003). Site-Selective Direct Silver Metallization on Surface-Modified Polyimide Layers. *Langmuir,* 19**,** pp. 10366-10371.

8. APEL, P. Yu. (1995). Heavy particle tracks in polymers and polymeric track membranes. *Radiation Measurements,* 25. pp. 667—674.

9. APEL., P. YU., DIDYK, A. YU., FURSOV, B. I., KRAVETS, L. I., NESTEROV, V . G., SAMOILOVA, L. I. AND ZHDANOV, G. S. (1997). Registration temperature effect in polymers: physico-chemical aspects. Radiation Measurements, 28. pp. 19-24.

10. APEL, P., SCHULZ, A., SPOHR, R., TRAUTMANN, C. AND VUTSADAKIS, V. (1997b). Tracks of very heavy ions in polymers. *Nuclear Instruments and Methods in Physics Research B*, 131. pp. 55-63.
11. APEL, P., SCHULZ, A., SPOHR, R., TRAUTMANN, C., AND VUTSADAKIS, V. (1998). Track size and track structure in polymer irradiated by heavy ions. *Nuclear Instruments and Methods in Physics Research B* 146. pp. 468-474.

12. APEL, P. (2001). Track-etching technique in membrane technology. *Radiation Measurements,* 34**,** pp. 559-566.

13. APEL, P. Y., BLONSKAYA, I. V. DIDYK, A. Y., DIMITRIEV, S. N. ORELOVITCH, O. L., ROOT, D., SAMILOVA, L. I. AND

VUTSADAKIS, V. A. (2001a). Surfactant-enhanced control of track-etch pore morphology. *Nuclear Instruments and Methods in Physics Research B,* 179**,** pp. 55-62.

14. APEL, P. (2003). Swift ion effects in polymers: industrial applications. *Nuclear Instruments and Methods in Physics Research B,* 208**,** pp. 11-20.

15. APEL, P. Y., AKIMENKO, A. P., BLONSKAYA, I. V., CORNELIUS, T., NEUMANN, R., SCHWARTZ, K., SPOHR, R. AND TRAUTMANN, C. (2006). Etching of nanopores in polycarbonate irradiated with swift heavy ions at 15K. *Nuclear Instruments and Methods in Physics Research B,* 245**,** pp. 284-287.

16. AVASTHI, D. K. (2009). Modification and Characterisation of Materials by Swift Heavy Ions. *Defence Science Journal*, 59. pp. 401-412.

17. AWASTHI, K., KULSHRESTHA, V., AVASTHI, D. K. AND VIJAY, Y. K. 2010. Optical, chemical and structural modification of oxygen irradiated PET. *Radiation Measurements,* 45**,** pp. 850-855.
18. BABARI, T. A., KOROS, W. J., AND PAUL, D. R. (1988). Gas Sorption in Polymers Based on Bisphenol-A. *Journal of Polymer Science Part B Polymer Physics,* 26**,** pp. 729-744.

19. BAGLIN, E. E. E. (1992). Ion beam enhancement of metal-insulator adhesion. *Nuclear Instruments and Methods in Physics Research B,* 65**,** pp. 119-128.

20. BAKER, R. W. (2002). Future directions of membrane gas separation technology. *Industrial Engineering Chemical Research,* 41**,** pp. 1393-1411.

21. BAKER, R. W. A. L., K. (2008). Natural Gas Processing with Membranes: An Overview. *Industrial Engineering Chemical Research,* 47**,** pp. 2109-2121.

22. BALANZAT, E., BETZ, N. AND BOUFFARD, S. (1995). Swift heavy ion modification of polymers *Nuclear Instruments and Methods in Physics Research B,* 105**,** pp. 46-54.

23. BALTA CALLEJA, F. J., GARCI´A GUTIERREZ, M. C., RUEDA, D. R. AND PICCAROLO, S. (2000). Structure development in poly (ethylene terephthalate) quenched from the melt at high cooling rates: X-ray scattering and microhardness study. *Polymer,* 41. pp. 4143–4148.

24. BANDYOPADHYAY, J., SINHA RAY, S. AND BOUSMINA, MOSTO. (2007). Thermal and Thermo-mechanical Properties of Poly (ethylene terephthalate) Nanocomposites. *J. Ind. Eng. Chem.,* 13. pp. 614-623.

25. BASTANI, D., ESMAELI, N. AND ASADOLLAHI, M. (2013). Polymeric mixed matrix membranes containing zeolites as a filler for gas separation applications: A review. *Journal of Industrial and Engineering Chemistry,* 19**,** 375-393.

26. BERNARDO, P., DRIOLI, E. and GOLEMME, G. (2009). Memb*rane Gas Sepa*ration: A r**ev**iew/State of the art. *Industrial Engineering Chemical Research*, 48, pp. 4638-4663.

27. BILLINGHAM, N. C., AND WALKER, T. J. (1975). Autoxidation of Poly-4-methylpentene-1. The role of Diffusion in Autoxidation kinetics. *Journal of Polymer Science Polymer Chemistry Edition,* 13**,** pp. 1209-1222.

28. BISWAS, A., LOTHA, S., FINK, D., SINGH, J. P., AVASTHI, D. K., YADAV, B. K., BOSE, S. K., KHATING, D. T., AND AVASTHI, A. M. (1999). The effects of swift heavy ion irradiation on the radiochemistry and melting characteristics of PET. *Nuclear Instruments and Methods in Physics Research B,* 159. pp. 40-51.

29. BRIGGS, D. AND HEARN, M. J. (1986). Interaction of ion beams with polymers with particular reference to SIMS. *Vacuum,* 36**,** pp. 1005-1010.

30. BUDD, P. M. AND McKWEON, N. B. (2010). Highly permeable polymers for gas separation membranes. *Polymer Chemistry,* 1, pp. 63-68.

31. BURGESS, S. K., LEISEN, J. E., KRAFTSCHIK, B. E. MUBARAK, C. R., KRIEGEL, R. M. AND KOROS, W. J. (2014). Chain Mobility, Thermal, and Mechanical Properties of Poly(ethylene furanoate) Compared to Poly(ethylene terephthalate). *Macromolecules,* 47, pp. 1383-1391.

32. CALCAGNO, L., COMPAGNINI, G. AND FOTI, G. (1992). Structural modification of polymer films by ion irradiation. *Nuclear Instruments and Methods in Physics Research B,* 65**,** pp. 413-422.

33. CHAPPA, V. C., del GROSSO, M. F., Garcıa-Bermudez, G., Mazzei, R.O. (2006). Infrared spectroscopy analysis of physico-chemical modifications induced by heavy ions in ultra-high molecular weight polyethylene. *Nuclear Instruments and Methods in Physics Research B,* 243, pp. 58–62.

34. CHAPIRO, A. (1988). Chemical modifications in irradiated polymers. *Nuclear Instruments and Methods in Physics Research B32*, pp. 111-114.

35. CHECCHETTO R., BAZZANELLA, N. PATTON, B. MIOTELLO, A. (2004). Palladium membranes prepared by r.f. magnetron sputtering for hydrogen. *Surface and Coatings Technology*, 177 –178. pp. 73–79.

36. CHEN, T.-X., YAO, S-D., WANG, K., WANG, H., DING, Z-B. AND CHEN, D. (2009). Structure Characterization of Modified Polyimide Films Irradiated by 2MeV Si Ions. *Chinese Physical Letter,* 26**,** pp. 1-3.

37. CHMIELEWSKI, A. G., HAJI-SAEID, M. AND AHMED, S. (2005). Progress in radiation processing of polymers. *Nuclear Instruments and Methods in Physics Research B,* 236**,** pp. 44-54.

38. CHMIELEWSKI, A. G. A. H.-S., M. (2004). Radiation technologies: past, present and future. *Radiation Physics and Chemistry,* 71**,** pp. 16-20.

39. CIESLA, K AND STAROSTA, W. (2000). Heavy ions track structure in a PETP. *Nuclear Instruments and Methods in Physics Research B,* 105. pp. 115-119.

40. CLOUGH, R. L. (2001). High-energy radiation and polymers: A review of commercial processes and emerging applications. *Nuclear Instruments and Methods in Physics Research B,* 185**,** pp. 8-33.

41. DELGADO, A. O., M.A. RIZZUTTO, M. A., TABACNIKS, M. H., ADDED, N., AND FINK, D. (2009). Infrared analysis of ion beam irradiated polymer. *Nuclear Instruments and Methods in Physics Research B 267,* pp. 1546–1548.

42. DUNSON, D. L. (2000). Synthesis and characterization of thermosetting polyimide oligomers for microelectronics packaging. PhD thesis, Virginia Polytechnic Institute and State University.

43. EL-NAGGAR, A. M., LOPEZ, L. C. AND WILKES, G. L. (1990). Effect of Electron Beam Radiation on the Mechanical and Thermal Properties of Poly (4-Methylpentene-1). *Journal of Applied Polymer Science,* 39**,** pp. 427-446.

44. ENSINGER, W. (2007). Formation of nanopore membranes and nanowires by high energy ion irradiation of polymer foils. *Surface and Coatings Technology* 201, pp. 8442–8447.

45. FINK, D. (2004). Fundamentals of Ion irradiated polymers: Springer Series, Materials Sciences 63.

46. FLEISCHER, R. L., PRICE, P. B. AND WALKER, R. M., (1975). Nuclear Tracks in Solids. *Principles and Applications*. University of California. Press, Berkeley.

47. FREEMAN, B. D. (1999). Basis of permeability/selectivity trade-off relations in polymeric gas separation membranes. *Macromolecules,* 32**,** pp. 375-380.

48. GRAY, J. E., NORTON, P. R. AND GRIFFITHS, K. (2005). Mechanism of adhesion of electroless-deposited silver on poly (ether urethane). *Thin Solid Films,* 484. pp. 196-207.

49. GHOSH, S., KLETT, R., FINK, D., DWIVEDI, K. K., VACIK, J., HNATOWICZ, V. AND CÏERVENA, J. (1999). On the penetration of aqueous solutions into pristine and radiation damaged polyimide. *Radiation Physics and Chemistry*, 55**,** pp. 271-284.

50. GHOSAL, K. AND FREEMAN, B. D. (1993). Gas Separation Using Polymer Membranes: An Overview. *Polymers for Advanced Technologies Volume*, 5, pp. 673-697.

51. GODDARD, J. M. AND HOTCHKISS, J. H. (2007). Polymer surface modification for the attachment of bioactive compounds. *Progress in polymer Science*, 32. pp. 698-725.

52. GEORGE, S. C., AND THOMAS, SABU. (2001). Transport phenomenon through polymeric systems. *Progress in polymer sciences,* 26. pp. 985-1017.

53. GUENTHER, M., GERLACH, G., SUCHANECK, G., SAHRE, K., EICHHORN, K. -J., WOLF, B., DEINEKA, A. and JASTRABIK, L. (2002). Ion-beam induced chemical and structural modification in polymers. *Surface and Coatings Technology*, 158-159**,** pp. 108-113.

54. HAMA, Y., HAMANAKA, K., MATSUMOTO, H., TAKANO, I. T., KUDOH, H., SUGIMOTO, M. AND SEGUCHI, T. (1996). The distribution profile of the chemical structural changes in ion-irradiated polyolefins. *Radiation Physics and Chemistry*, 148, pp. 549-554.

55. HAMA, Y., OKA, T., KUDOH, H., SUGIMOTO, M. AND SEGUCHI, T. (2003). Irradiation effects in polymers by heavy ions: The distribution of

the chemical structure transformation in polymers. *Nuclear Instruments and Methods in Physics Research B,* 208**,** pp. 123-132.

56. HELLBORG, R. WHITLOW, H. J., ZHANG, Y. (2009). Ion Beams in Nanoscience and Technology. pp. 1-439.

57. JEON, D. H., LEE, K. H. AND PARK, H. J. (2004). The effects of irradiation on physicochemical characteristics of PET packaging film. *Radiation Physics and Chemistry,* 71. pp. 1059–1064.

58. JORGESEN, G., AND SCHISSEL, P. (1985). Effective Antireflection coatings of transparent polymeric materials by gas phase surface fluorination. *Solar Energy Materials,* 12**,** pp. 491-500.

59. JUNG, C.-H., CHO, H-W., HWANG, I-T., CHOI, J-H., NHO, Y-C., SHIN, J-S., AND CHANG, K-H. (2012). The effects of energetic ion irradiation on metal-to-polymer adhesion. *Radiation Physics and Chemistry,* 81**,** pp. 919-922.

60. KARACAN, I. AND BENLI, H. (2011). An X-ray diffraction study for isotactic polypropylene fibres produced with take-up speeds of 2500-4250 M/mins. *Tekstil ve Konfeksiyon,* 3. pp. 201-211.

61. KANE, M. C. (2008). Permeability, solubility, and interaction of hydrogen in polymers- An assessment of materials for hydrogen transport. *Washington Savannah River Company*. pp.1-19

62. KASHIWABARA, H., SHIMADA, S. AND HORI, Y. (1991). Free radicals and crosslinking in irradiated polyethylene. *Radiation Physics and Chemistry,* 37**,** pp. 43-46.

63. KITAMURA, A., KOBAYASHI, T., MESGURO, T., SUZUKI, A., AND TERAI, T. (2009). The mechanism of protrusion formation on PTFE surface by ion-beam irradiation. *Surface & Coatings Technology,* 203 pp. 2406–2409

64. KORMUNDA, M., HOMOLA, T., MATOUSEK, J., KOVACIK, D., CERNAK, M. AND PAVLIK, J. (2012). Surface analysis of poly (ethylene naphthalate) (PEN) films treated at atmospheric pressure using diffuse coplanar surface barrier discharge in air and in nitrogen. *Polymer Degradation and Stability,* 97**,** pp. 547-553.

65. KOROS, W. J., AND FLEMING, G. K. (1993). Membrane-based gas separation. *Journal of Membrane Science,* 83**,** pp. 1-80.

66. KRIMM, S. (1960). Infrared spectra of high polymers. *Fcrtschr Hochopolym Forsch Bd,* 2. pp. 51-172.

67. KUDO, H., SUDO, S., OKA, T., HAMA, Y., OSHIMA, A., WASHIO, M. and MURAKAMI, T. (2009). Ion-beam irradiation effects on polyimide UV–vis and infrared spectroscopic study. *Radiation Physics and Chemistry,* 78**,** pp. 1067-1070.

68. KULSHRESTHA, V., AWASTHI, K., ACHARYA, N. K., SINGH, M., AVASTHI, D. K., AND VIJAY, Y. K. (2006). Gas and ion transport through a track-etched large-area polymer film. *Desalination,* 195**,** pp. 273-280.

69. LEE, E. H. (1999). Ion-beam modification of polymeric materials-fundamental principles and applications. *Nuclear Instruments and Methods in Physics Research B,* 151**,** pp. 29-41.

70. LI, Y., LU, Q., QIAN, X., ZHU, Z. AND YIN, Y. (2004). Preparation of surface bound silver nanoparticles on polyimide by surface modification method and its application on electroless metal deposition. *Applied Surface Science,* 233**,** pp. 299-306.

71. LIN, H., WAGNER, E. V., FREEMAN, B. D., TOY, L. G. AND GUPTA, R. P. (2006). Plasticization-enhanced hydrogen purification using polymeric membranes. *Science,* 311**,** pp. 639-642.

72. LOW, B. T., WIDJOJO, N. AND CHUNG, T. S (2010). Polyimide/Polyethersulfone dual-layer hollow fibre membranes for hydrogen enrichment. *Industrial Engineering Chemical Research,* 49**,** pp. 8778-8786.

73. LU, G. Q., DINIZ DA COSTA, J. C., DUKE, M., GIESSLER, S., SOCOLOW, R., WILLIAMS, R. H., KREUTZ, T. (2007). Inorganic membranes for hydrogen production and purification: A critical review and perspective. *Journal of Colloid and Interface Science*, 314. pp. 589–603.

74. MARIN, N. AND SERRUYS, Y. (1995). Diffusion of metals deposited on a polyimide film (Kapton) under and out of irradiation. *Nuclear Instruments and Methods in Physics Research B,* 105**,** pp. 175-180.

75. MARK, E. J. 2007. *Physical properties of polymers handbook,* Springer.

76. MATHAKARI, N. L., JADHAV, V. S., KANJILAL, D., BHORASKAR, V. N. and DHOLE, S. D. (2009). Surface and structural changes in polyimide by 100 MeV Ag^{7+} ion irradiation. *Surface and Coatings Technology*, 203**,** pp. 2620-2624.

77. MATTEUCCI, S., YAMPOLSKII, Y., FREEMAN, B. D. AND PINNAU, I. (2006). Transport of gases and vapours in glassy and rubbery polymers. *Materials science of Membranes for Gas and Vapour Separation*. pp. 1-47.

78. MIKE CHUNG (2002). Functionalization of Polyolefins. An Elsevier science imprint. Academic press. pp. 1-289

79. MOLARES, M. E. T. (2001). Fabrication and characterisation of copper nanowires electrochemically deposited in etched ion-track membranes. *PhD Thesis* Heidelberg, University of Heidelberg.

80. MISHRA, R., TRIPATHY, S. P., DWIVEDI, K. K., KHATHING, D. T., GHOSH, S., MULLER, M. AND FINK, D. (2003). Spectroscopic and thermal studies of electron irradiated polyimide. *Radiation Measurement*, 36**,** pp. 621-624.

81. MULLER, M. (1996). Basic principles of membrane technology. Second edition.

82. MURRAY, K. A., KENNEDY, J. E., MCEVOY, B., VRAIN, O., RYAN, D., COWMAN, R., AND HIGGINBOTHAMA, C. L. (2013). Characterisation of the Surface and Structural Properties of Gamma Ray and Electron Beam Irradiated Low Density Polyethylene

83. NAGEL, C., SCHMIDTKE, E., GUNTHER-SCHADE, K., HOFMANN, D., FRITSCH, D., STRUNSKUS, T. AND FAUPEL, F. (2000). Free volume distribution in glassy polymers membranes: Comparison between molecular modelling and experiments. *Macromolecules,* 33**,** pp. 2242-2248.

84. PANDIYARAJ, N. A., SELVARAJAN, V., DESHMUKH, R. R. AND GAO, C. (2009). Adhesive properties of polypropylene (PP) and polyethylene terephthalate (PET) film surfaces treated by DC glow discharge plasma. *Vacuum,* 83**,** pp. 332-339.

85. PARK, S. C., YOON, S. S. and NAM, J. D. (2008). Surface characteristics and adhesive strengths of metal on O_2 ion beam treated polyimide substrate. *Thin Solid Films,* 516**,** pp. 3028-3035.

86. PEEK, G. J., KILLER, H. M., REEVES, R., SOSNOWSKI, W., AND FIRMIN, R. (2002). Early Experience with a Polymethyl Pentene Oxygenator for Adult Extracorporeal Life Support. *ASAIO***,** pp. 480-482.

87. PERRY, J. D., NAGAI, K. AND KOROS, W. J. (2006). Polymer membranes for hydrogen separations. *Material Research Bulletin,* 31**,** pp. 745-749.

88. POWELL, C. E., AND QIAO, G. G. (2006). Polymeric CO_2/N_2 gas separation membranes for the capture of carbon dioxide from power plant flue gases. *Journal of Membrane Science,* 279**,** pp. 1-49.

89. QUAMARA, J. K., GARG, M. AND PRABHAVATHI, T. (2004). Effect of high-energy heavy ion irradiation on dielectric relaxation behaviour of kapton-H polyimide. *Thin Solid Films,* 449**,** pp. 242-247.

90. QURESHI, A., SINGH, N. L., RAKSHIT, A. K., SINGH, F. AND AVASTHI, D. K. (2007). Swift heavy ion induced modification in polyimide films. *Surface & Coatings Technology*, 201**,** pp. 8308-8311.

91. RAVANCHI, M. T., KAGHAZCHI, T. AND KAGARI, A. (2009). Application of membrane separation processes in petrochemical industry: A review. *Desalination*, 235**,** pp. 199-244.

92. RAHARJOA, R. D., LEE, H. J., FREEMAN, B. D., SAKAGUCHI, T., AND B, TOSHIO MASUDA, B. T. (2005). Pure gas and vapor permeation properties of poly[1-phenyl-2-[p-(trimethylsilyl) phenyl]acetylene] (PTMSDPA) and its desilylated analog, poly [diphenylacetylene] (PDPA). *Polymer*, 46, pp. 6316-6324.

93. RIVATON, A. AND ARNOLD, J. (2008). Structural modifications of polymers under the impact of fast neutrons. *Polymer Degradation and Stability*, 93**,** pp. 1864-1868.

94. ROBESON, L. M. (2008). The upper bound revisited. *Journal of Membrane Science*, 320**,** pp. 390-400.

95. ROBESON, L. M., BURGOYEN, W. F., LANGSAM, M., SAVOCA, A. C. AND TIEN, C. F. (1994). High performance polymers for membrane separation. *Polymer*, 35.

96. SAMUEL, E. J. J. AND MOHAN, S. (2004). FTIR and FT Raman spectra and analysis of poly (4-methyl-1-pentene). *Spectrochimica Acta Part A*, 60. pp. 19–24.

97. SASUGA, T., KAWANISHI, S., NISHI, M., SEGUCHI, T AND KOHNO, I. (1991).Effects of Ion irradiation on the mechanical properties of several polymers. *Radiation Physics and Chemistry,* 37**,** pp. 135-140.

98. SEGUCHI, T., KUDOH, H., SUGIMOTO, M. AND HAMA, Y. (1999) Ion beam irradiation effect on polymers. LET dependence on the chemical reactions and change of mechanical properties. *Nuclear Instruments and Methods in Physics Research B,* 151**,** pp. 154-160.

99. SHTANKO, N. I., KABANOV, V. YA., APEL, P.Y., YOSHIDA, M. AND VILENSKII, A. I. (2000). Preparation of permeability-controlled track membranes on the basis of 'smart' polymers. *Journal of Membrane Science,* 179**,** 155

100. SINGH, V., SINGH, T., CHANDRA, A., S.K. BANDYOPADHYAY S. K., SEN, P., WITTE, K., SCHERER, U. W. AND SRIVASTAVA, A. (2006). Swift heavy ion induced modification in PET: Structural and thermal properties. *Nuclear Instruments and Methods in Physics Research B,* 244. Pp. 243-247.

101. SIPERKO, L. M. AND THOMAS, R. R. (1989). Chemical and physical modification of fluoropolymer surfaces for adhesion enhancement: A review. *Journal of Adhesion Science Technology,* 3. pp. 157-173.

102. SINGH, R., SAMRA, K. S., KUMAR, R., AND SINGH, L. (2008). Microstructural modifications in swift ion irradiated PET. *Radiation Physics and Chemistry,* 77, pp. 575-580.

103. SPOHR, R. (1990). Ion tracks of microtechnology principles and applications. pp. 1-282.

104. STANNETT, V. (1978). The transport of gases in synthetic polymeric membranes: An historic perspective. *Journal of Membrane Science,* 3**,** pp. 97-115.

105. STECKENREITER, T., BALANZAT, E., FUESS, H., TRAUTMANN, C. (1997). Chemical modifications of PET induced by swift heavy ions. *Nuclear Instruments and Methods in Physics Research B,* 131. pp. 159-166.

106. STEPHANS, L. E., MYLES, A. AND THOMAS, R. R. (2000). Kinetics of alkaline hydrolysis of a polyimide. *Langmuir,* 16**,** pp. 4706-4710.

107. TORRES, N., ROBIN, J. J. AND BOUTEVIN, B. (2000). Study of thermal and mechanical properties of virgin and recycled poly (ethylene terephthalate) before and after injection molding. *European Polymer Journal,* 36. pp. 2075-2080.

108. THORNTON, A. W., NAIRN, K. M., HILL, A. J. AND HILL, J. M. (2009). New relation between diffusion and free volume: I. Predicting gas diffusion. *Journal of Membrane Science,* 338. pp. 29–37.

109. TJONG, S. C. (2006). Structural and mechanical properties of polymer nanocomposites. *Materials Science and Engineering R,* 53. pp. 73–197.

110. TRAUTMANN, C., BOUFFARD, S. AND SPOHR, R. (1996). Etching threshold for ion tracks in polyimide. *Nuclear Instruments and Methods in Physics Research B,* 116**,** pp. 429-433.

111. ULBRICHT, M. (2006). Advanced functional polymers. *Polymer,* 47. pp. 2217-2262.VERDIANZ, T., SIMBURGER, H. and LISKA, R. (2006a). Surface modification of imide containing polymers I: Catalytic groups. *European Polymer Journal,* 42**,** pp. 638-654.

112. VERDIANZ, T., SIMBURGER, H. and LISKA, R. (2006b). Surface modification of imide containing polymers II: Co-reactive groups. *European Polymer Journal,* 42**,** pp. 869-882.

113. WIJMANS, J. G. and BAKER, R.W. (1995). The solution-diffusion model: A review. *Journal of Membrane Science.* 107, pp. 1-21

114. WOHL, C. J., BELCHER, M. A., GHOSE, S. and CONNELL, J. W. (2010). Modification of the surface properties of polyimide films using polyhedral Oligomeric Silsesquioxane deposition and oxygen plasma exposure. *Applied Surface Science,* 255**,** pp. 8135-8144.

115. YOSHIDA, M., TAMADA, M., ASANO, M., OMICHI, H., KUBOTA, H., KATAKAI, R., SPOHR, R. AND VETTER, J. (1993). Stimulus-responsive trackpores. *Radiation Effects. Defects Solids,* 126. pp. 409–412.

116. YOSHIDA, M., ASANO, M., OMICHI, H., SPOHR, R. AND KATAKAI, R., (1997). Substrate-specific functional membranes based on etched ion tracks. *Radiation Measurements,* 28. pp. 799–810.

117. ZAPOROJTCHENKO, V., ZEKONYTE, J., ERICHSEN, J. and FAUPEL, F. (2003). Etching rate and structural modification of polymer films during low energy ion irradiation. *Nuclear Instruments and Methods in Physics Research B,* 208**,** pp. 155-160.